

## TABLE OF CONTENTS

DECLARATION BY CANDIDATE.....	iii
ACKNOWLEDGEMENTS.....	iv
SUMMARY.....	vi
TABLE OF CONTENTS .....	ix
GLOSSARY OF ABBREVIATIONS.....	xi
1. Introduction .....	1
2. Literature study .....	4
2.1. Multidrug resistant (MDR) cancer and circumvention thereof.....	4
2.2. Combination chemotherapy .....	6
2.3. Riminophenazines .....	7
2.3.1. Background .....	7
2.3.2. Clofazimine: Antineoplastic and Chemosensitizing potential .....	8
2.3.3. Tetramethylpiperidine (TMP)-substituted Riminophenazines .....	10
2.3.4. Pharmacodynamics: Anticancer multi-mechanism .....	11
2.4. Refinements in the pharmacokinetic usage of anticancer drugs .....	12
2.4.1. Loco-regional chemotherapy.....	12
2.4.2. The Enhanced Permeability and Retention (EPR) effect.....	14
2.4.3. Lipiodol Ultra-Fluid.....	15
2.4.4. Intelligent formulations: Nanoparticulate drug delivery systems .....	17
2.5. Pre-clinical development of anticancer drug products: Regulatory perspectives ....	21
3. Target product profile, critical path and pre-clinical development plan.....	25
4. Riminophenazine procurement, purification and authentication.....	30
4.1. Materials.....	30
4.2. Authentication of Riminophenazine purity and integrity.....	30
5. <i>In vitro</i> antiproliferative bioassays.....	38
5.1. Introduction.....	38
5.2. Materials.....	40
5.3. Methodology.....	43
5.3.1. Cell culture preparation and <i>in vitro</i> antiproliferative assays.....	43
5.3.2. Fixed molar ratio drug combination studies.....	44
5.3.3. Assessment of additional ABC transporter inhibition.....	47
5.3.4. Neoplastic specificity .....	48
5.3.5. Ethical considerations.....	48
5.4. Results .....	49
5.4.1. COLO 320DM neoplastic cell cultures .....	49
5.4.2. HCT-15 neoplastic cell cultures .....	54
5.4.3. ASH-3 cell line .....	56
5.5. Discussion and conclusion .....	57
6. Development of novel Nanoparticulate Drug Delivery Systems (NDDS).....	60
6.1. Introduction.....	60
6.2. Materials.....	66
6.3. Methodology.....	67
6.3.1. Development of Riminocelles™ .....	67
6.3.2. Development of RiminoPLUS™ Imaging .....	71
6.4. Results .....	77

6.4.1. Riminocelles .....	77
6.4.2. RiminoPLUS Imaging.....	86
6.5. Discussion and conclusion .....	90
7. <i>In vivo</i> models of experimental toxicity and oncology .....	94
7.1. Introduction.....	94
7.2. Materials.....	97
7.3. Methodology.....	98
7.3.1. Pilot safety and acute <i>in vivo</i> toxicokinetic assessment of Riminocelles.....	98
7.3.2. Toxicity marker profiling.....	99
7.3.3. Efficacy assessment .....	99
7.3.4. Ethical considerations and committee approval .....	103
7.3.5. Statistical analysis .....	104
7.4. Results .....	104
7.4.1. Acute toxicokinetics .....	104
7.4.2. GLP repeat dose toxicity.....	107
7.4.3. Efficacy assessment.....	109
7.5. Discussion and conclusion .....	114
8. Development and application of an optimised and validated LC-MS/MS method .....	117
8.1. Introduction.....	117
8.2. Materials.....	118
8.3. Methodology.....	119
8.3.1. Stock solutions, calibration standards, quality control and recovery samples	119
8.3.2. Sample preparation .....	120
8.3.3. Chromatographic conditions .....	121
8.3.4. Mass spectrometric conditions.....	121
8.3.5. Validation procedures .....	122
8.3.6. Application in pharmacokinetic study .....	123
8.4. Results and discussion.....	124
8.4.1. Chromatography and Mass spectrometry .....	124
8.4.2. Assay validation parameters.....	126
8.4.3. Method application.....	133
8.5. Conclusion.....	136
9. Final discussion and conclusions .....	137
References.....	146
Appendix A. AUCC approval letters.....	160
Appendix B. Review of Riminophenazine QSAR.....	162
Appendix C. Pharmacokinetic and tissue distribution study schedule.....	164

## GLOSSARY OF ABBREVIATIONS

ABC	ATP-binding cassette
ALT	Alanine aminotransferase
ANOVA	Analysis of variance
API	Active pharmaceutical ingredient
AST	Aspartate aminotransferase
ATCC	American tissue culture collection
ATP	Adenosine triphosphate
AUCC	Animal use and care committee
B663	Clofazimine
BCRP	Breast cancer resistant protein
BSA	Bovine serum albumin
$\text{CDCl}_3$	Deuterated chloroform
CE	Collision energy
$\text{CHCl}_3$	Chloroform
CI	Combination index
CMC	Critical micelle concentration
cP	Centipoise
CRL	Charles River Laboratory
CSIR	Council for Scientific and Industrial Research
CT	Computed tomography
CV	Coefficient of Variation
CXP	Collision-cell exit potential
$\text{D}_2\text{O}$	Deuterium oxide
DLS	Dynamic light scattering
DMEM	Dulbecco's Modified Eagle's Medium
DMSO	Dimethyl Sulphoxide
DP	Declustering potential
DTX	Docetaxel
EDTA	Ethylenediaminetetraacetic acid
EMA	European agency for the evaluation of medicinal products
EO	Ethylene oxide

EP	Entrance potential
EPR	Enhanced permeability and retention
ESI	Electrospray ionization
ETOP	Etoposide
<i>fa</i>	Fraction affect level
FCS	Fetal calf serum
FDA	Food and drug administration (USA)
FRDC	Fixed-ratio drug combination
GGT	Gamma-glutamyl transpeptidase
GLP	Good laboratory practise
GMP	Good manufacturing practise
HBSS	Hank's Balanced Salt Solution
HEPA	High efficiency particulate air
HCC	Hepatocellular carcinoma
HCO <sub>2</sub> H	Formic acid
HLB	Hydrophilic-Lipophilic Balance
HNSTD	Highest non-severely toxic dose
HTS	High throughput screening
IC	Inhibitory Concentration
IS	Internal Standard
IV	Intravenous
JCRB	Japanese Collection of Research Bioresources
LC-MS	Liquid Chromatography tandem Mass Spectrometry
LD	Lethal Dose
LOQ	Limit of quantification
MAB	Monoclonal Antibody
MCC	Medicines Control Council (South Africa)
MDR	Multi-drug resistance
ME	Matrix effect
MeCN	Acetonitrile
MeOH	Methanol
MHLW	Ministry of Health, Labour and Welfare (Japan)
MPS	Mononuclear phagocyte system
MRC	Medical Research Council

MRM	Multiple reaction monitoring
MRP	Multidrug Resistance Associated Protein
MtBE	Methyl <i>tert</i> butyl ether
MTD	Maximum tolerated dose
MTT	3-(4,5-dimethylthiazol-2-yl)-2,5-diphenyltetrazolium bromide
NCI	National Cancer Institute
NDDS	Nanoparticulate Drug Delivery System
nm	Nanometre
NMR	Nuclear Magnetic Resonance spectroscopy
PC	Phosphatidylcholine
PdI	Polydispersity index
PEG	Polyethylene glycol
Pgp	P-glycoprotein
PLA <sub>2</sub>	Phospholipase A <sub>2</sub>
PTFE	Polytetrafluoroethylene
PTX	Paclitaxel
PVP	Polyvinylpyrrolidone
QC	Quality control
QSAR	Quantitative structure activity relationships
R&D	Research and Development
R <sub>f</sub>	Retention / retardation factor
RPMI	Roswell Park Memorial Institute Medium
SC	Standard chemotherapeutic
S <sub>mix</sub>	Surfactant mixture
SPE	Solid phase extraction
STD	Severely toxic dose
T <sub>d</sub>	Tumour-volume doubling time
TEM	Transmission Electron Microscopy
TMP	Tetramethylpiperidine
UPBRC	University of Pretoria Biomedical Research Centre
UV	Ultraviolet
VIN	Vinblastine
WHO	World Health Organisation

## 1. Introduction

Cancer, characterized by invasive growth of self-tissue with insensitivity to normal death signals, is a consequence of microevolution - multiple genetic mutations occurring over time to genes intricately involved with the control of cell proliferation. Each year, more than seven million deaths are attributed to malignant tumours. [1] Death ensues as a result of vital organ or system obliteration and/or as a consequence of opportunistic secondary infections (owing to a progressive weakening). [2] Present therapy is multimodal and includes surgical resection, radiotherapy, immunotherapy or chemotherapy. Localised modalities (by nature) have a limited scope of application once the disease has metastasized.

Chemotherapy is most often indicated in the setting of advanced or disseminated disease with an aim to palliate symptoms and prolong life. Numerous other therapeutic modalities may include chemotherapy as an adjuvant. The intent unfortunately, is only curative in limited instances such as acute leukaemia, some types of lymphomas and testicular cancer, accentuating the great need for the development of innovative therapeutic strategies and improved early detection technology.

Contemporary cancer chemotherapy is limited by dose-related systemic toxicity owing to inefficient cytotoxic discernment (specificity) for cancer cells. Differential cytotoxic specificity depends on: cellular characteristics (chemosensitivity) of different transformed and non-transformed cells; the pharmacodynamic actions of administered drug/s at various ratios and concentrations; the relative pharmacokinetic distribution into tumour tissue. Through dynamically and kinetically increasing (controlling by design) the cancer specificity of a pharmacological intervention it is hoped that the vision of a “magic-bullet” as first conceptualised by Paul Ehrlich one hundred years ago can be realised. [3]

Pharmacodynamic sensitivity for cancer cells specifically can be improved through utilization of target-designed drug products or through the use of chemotherapeutic combinations - most notably Fixed-Ratio Drug Combinations (FRDC) that have been optimized *in vitro* for maximal synergistic effect against cancer. A further

obstacle thwarting chemotherapy is the development through somatic evolution of multi-drug resistance (MDR) that renders the cancer cell population progressively more insensitive to the cytotoxic action of chemotherapeutics.

Pharmacokinetic specificity can be improved by loco-regional administration (provided there is significant first pass retention) or through the use of tumour targeting, Nanoparticulate Drug Delivery Systems (NDDS). NDDS are the enabling technology that allows favourable uptake and retention of cytotoxic drugs by disseminated tumours after intravenous administration, thus minimizing systemic exposure (toxicity), affording dose reduction and improving anticancer efficacy. [4]

Riminophenazines have demonstrated potent *in vitro* and *in vivo* antineoplastic activity against a broad range of drug resistant tumour cells. The Riminophenazine antiproliferative activity is multi-mechanistic, seemingly inferring resistance against intrinsic drug resistance. Furthermore, Riminophenazines have been shown *in vitro* to inhibit P-glycoprotein (Pgp), an energy-dependent transmembrane efflux pump that is largely responsible for acquired resistance. Riminophenazine drug products therefore possess huge therapeutic and commercial promise as they could speculatively be included within many chemotherapeutic regimes involving Pgp substrates. It is also hypothesized that Riminophenazines are capable of inhibiting the action of other ATP-binding cassette (ABC) transport proteins in addition to Pgp, thus further warranting the title “broad-spectrum resistance circumventor”.

The scope of this study was the pre-clinical development of Riminophenazines as resistance circumventing, anticancer agents. The pre-clinical studies planned and described were intended to provide data that could justify and support the conduct of clinical trials. This project was more than merely academic - efforts were focused on progressing towards human trials and ultimately an approved pharmaceutical product. As such, the development strategy (founded upon the target product profile) was devised with due consideration to appropriate international regulatory guidelines and to the available resources.

The research question serving to drive and focus this project was: does a synergistic FRDC (including a Riminophenazine and Pgp substrate) encapsulated within a tumour-targeting NDDS result in a significantly improved anticancer effect compared to the standard chemotherapeutic alone.



## 2. Literature study

### 2.1. Multidrug resistant (MDR) cancer and circumvention thereof

Nearly half of all patients with cancer suffer from malignancies that are intrinsically resistant to chemotherapeutics. Furthermore, the majority of the remaining half will acquire resistance during the course of their therapy. [5] MDR has been described as the “thorniest obstacle” in developing improved systemic therapies for disseminated cancer. [6] Resistance to various structurally and mechanistically unrelated chemotherapeutics characterizes the MDR phenotype.

Categorically, MDR is classically associated with the over-expression of ATP binding cassette (ABC) transmembrane efflux pumps, particularly P-glycoprotein (Pgp). Pgp is a 170 kDa transmembrane “permeability” glycoprotein. Among other ABC transporters, multidrug resistance associated protein (MRP) and breast cancer resistant protein (BCRP) are also of clinical relevance. [7] These transmembrane proteins are energy dependent pumps that can efficiently expel various structurally and mechanistically unrelated chemotherapeutics including Epipodophyllotoxins (etoposide), Taxanes (paclitaxel) and Vinca alkaloids (vinblastine) to the extracellular environment (Figure 2.1.) thereby maintaining intracellular concentrations below effective cytotoxic levels. [8] Increased expression of these multidrug resistance proteins is associated with a poor response to treatment and grave prognosis.

Numerous different compounds have been shown to inhibit the efflux activity of Pgp and other ABC transporters thus restoring sensitivity to cytotoxic agents. [9,10] Unfortunately, due in the main to toxicity and poor pharmacokinetic control (altered distribution and thus altered toxicity profile), no such agents (termed chemosensitizers) are yet clinically available. [11] Verapamil and cyclosporin A are two examples of first generation chemosensitizers. Second and third generation chemosensitizers were developed with the aim of achieving more specific Pgp inhibition and fewer systemic pharmacological effects. [7]

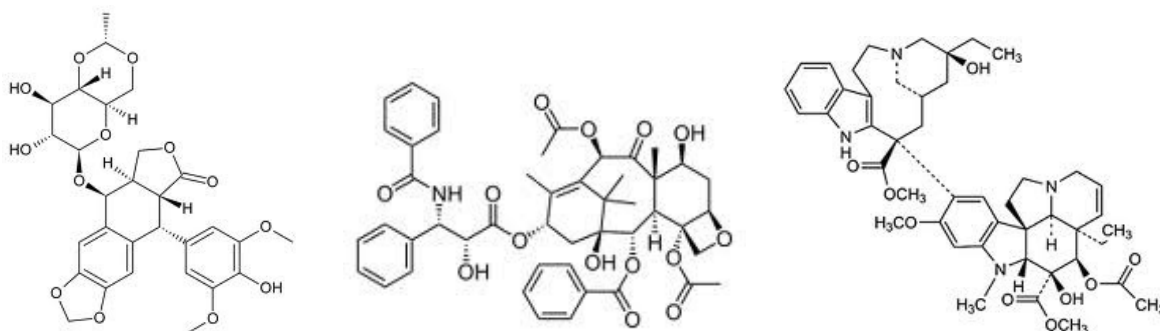


**Figure 2.1. Chemical structure of standard chemotherapeutic drugs (Pgp substrates)**  
From left to right: etoposide (ETOP), paclitaxel (PTX) and vinblastine (VIN)

Non-classical (non-transporter mediated) MDR involves evasion of cellular death through impairment of biochemical pathways controlling programmed cell death, as well as altered expression of enzymes responsible for intracellular detoxification and repair. Many of these alterations (e.g. inappropriate expression of oncogenes and loss of tumour suppressor gene function) are essential to neoplastic transformation itself. As the dynamics of these changes are complex and ill understood the contemporary strategy against MDR cancer involves the use of chemotherapeutic agents in combination. The rationale being that the MDR phenotype can be overcome (circumvented) through the action of multiple unrelated cytotoxic mechanisms acting in concert. [6]

In addition, non-cellular MDR resistance mechanisms may exist such as increased interstitial fluid pressure that negatively influences a cytotoxic drug's ability to penetrate deep into solid tumours rendering it ineffective and possibly toxic to healthy tissue. Clearly a targeted, selective approach employing synergistic drug combinations is called for to prevent and circumvent MDR.

## 2.2. Combination chemotherapy

Combination chemotherapy has been the mainstay of successful (curative) chemotherapy for the last 40 years, [12, 13] so much so, that it is now considered standard practice. [14] A strong correlation exists between the number of agents administered and successful cure rates. [15]

Combination chemotherapy regimens have predominately been developed empirically in late-stage clinical trials. Active single agents have typically been combined on the basis of minimizing the potential for overlapping toxicities (different organ toxicities) and possessing different (hopefully complementary), non-cross-resistant mechanisms of action. [16]

These poly-chemotherapy regimens offer the potential for increased efficacy (greater fractional affect), increased neoplastic specificity, decreased dosage (hence reduction in systemic toxicity) and a broader spectrum of activity against sub-populations present within a heterogeneous tumour cell population which in turn minimises the development of resistance. [12]

Clinically, the drugs are typically administered at their individual maximum tolerated doses. [14] This “more-is-better” approach ignores the possibility of subtle concentration and ratio dependent interactions capable of eliciting synergistic responses. [17, 18] Fixed-ratio drug combinations (FRDC) have recently been proposed as a more rational approach for the combination of drugs. Through *in vitro* optimisation, FRDC hold the promise of capturing maximal synergistic drug interactions thus reducing the total dose required to produce a particular fractional affect.

Were a synergistic FRDC to be administered intravenously in some arbitrary carrier solvent, the two drugs making up the FRDC would be distributed and eliminated independently of one another over time as a consequence of their inherent dissimilar pharmacokinetics. Consequently the optimized fixed-ratio would

not be maintained - moreover, there would not be an element of tumour specific drug delivery.

Ultimately, *in vivo* use of fixed drug ratio dependent synergistic pharmacodynamics is dependent upon the use of delivery systems that can maintain the optimised ratio after administration and selectively deliver the drug combination to the tumour site.

## 2.3. Riminophenazines

### 2.3.1. Background

The name “Riminophenazine” comes from the fact that “R” substitution has occurred at the imino region of the phenazine nucleus. [19]

Clofazimine [3-(4-chloroanilino)-10-(4-chlorophenyl)-2, 10-dihydro-2-(isopropylimino)-phenazine] with empirical formula  $C_{27}H_{22}Cl_2N_4$  (molecular weight of 473.14) (Figure 2.2.), otherwise known as B663 and marketed by Novartis under the trade name of Lamprene® is considered the prototype Riminophenazine. Clofazimine, has a characteristic deep red-orange colour that changes under different pH conditions. [20] B663 is very hydrophobic with a reported log *P* of 7.48. [21] B663 is a basic drug with a reported pKa value of 8.35. [21]

Clofazimine was originally described as a breakthrough in the treatment of tuberculosis. [22] Currently, clofazimine is primarily used in combination with rifampicin and dapsone for the treatment of *Mycobacterium leprae* (leprosy). [23] Clofazimine is also recommended in the treatment of *Mycobacterium avium* complex associated with AIDS. [24] B663 has broad activity against gram-positive organisms and has also been found to possess immunosuppressive and anti-inflammatory properties. [25] Furthermore, clofazimine is non-myelosuppressive, non-carcinogenic and non-teratogenic. Adverse effects include red-brown skin discoloration and reversible gastrointestinal toxicity. [20] Clofazimine has a safety record of more than 50 years in humans. Riminophenazines are attractive as drug

combination candidates because they have a long history of resistance circumventing actions in both cancer and mycobacterial models.

Clofazimine possesses an impressive multi-mechanistic anticancer action. The mandate driving this pre-clinical R&D project was to further develop (re-position) Riminophenazines as anticancer agents, so as to provide benefit to patients and a competitive advantage in the market by adding MDR circumventing value to standard chemotherapeutics regimes.

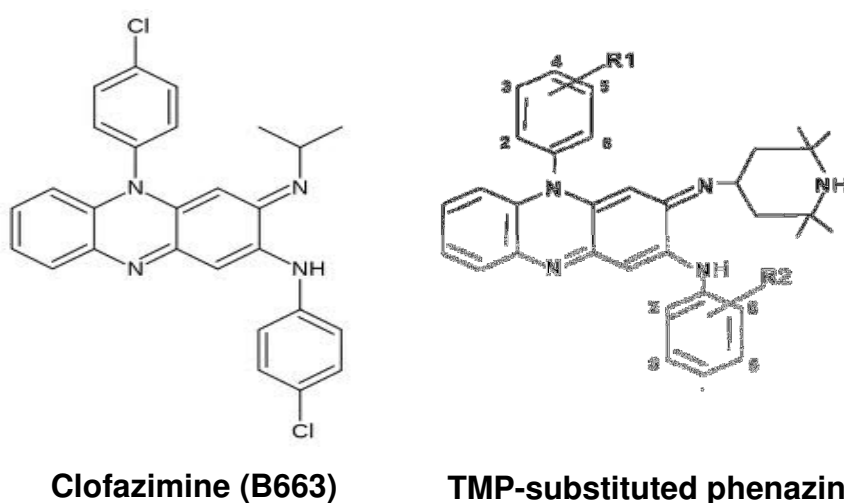


**Figure 2.2. Structure of Clofazimine and the lead Tetramethylpiperidine (TMP)-substituted Riminophenazine - B4125, where R<sub>1</sub> and R<sub>2</sub> are 2-Cl positional isomers**

### 2.3.2. Clofazimine: Antineoplastic and Chemosensitizing potential

*In vitro* studies conducted on B663 have served to highlight the ability of Riminophenazines to subvert both intrinsic (innate) and acquired, classical and non-classical MDR cancer thus justifying the label “broad-spectrum”:

Van Rensburg *et al.* [26] reported the *in vitro* cytotoxic activity of clofazimine to be comparable to that of methotrexate, bleomycin and cisplatin (standard chemotherapeutics) against a range of human neoplastic cell cultures including pharynx, cervical, bladder and hepatocellular carcinomas.

Van Rensburg *et al.* [27] showed clofazimine to uniformly inhibit (in contrast to vinblastine and etoposide, among others) the proliferation of various intrinsically resistant neoplastic cell lines at therapeutically relevant concentrations.

Van Rensburg *et al.* [28] demonstrated the chemosensitizing action of clofazimine using a P-glycoprotein (Pgp) expressing small cell lung cancer cell line (H69/LX4). Chemosensitivity was restored to a range of Pgp substrates when used in combination with non-toxic concentrations of clofazimine.

Myer and van Rensburg [29] using numerous sub-clones of an erythroleukaemia cell line expressing varying levels of Pgp, again demonstrated the ability of clofazimine to inhibit the efflux action of Pgp.

The anticancer potential of clofazimine has been investigated using several *in vivo* models of experimental oncology. These studies have served to demonstrate both the anticancer efficacy and safety of clofazimine:

Van Rensburg *et al.* [30] showed an oral dose of 30 mg/kg/day of clofazimine increased survival time and decreased tumour load in carcinogen induced rodent tumours models. Neither clinical signs of toxicity nor haematological toxicity was observed at 60 mg/kg/day.

Sri-Pathmanathan *et al.* [31] demonstrated significant reduction in the tumour load of drug resistant human (non-small cell) lung carcinoma xenografted subcutaneously into nude mice. After 22 days of treatment the tumours were approximately one-third the size of the control group. Moreover, neither mortality nor gross toxicity in terms of weight loss was observed at an approximate oral dose of 120 mg/kg using a diet supplemented with B663 (0.5% w/w).

Pourgholami *et al.* [32] using a rodent syngeneic (Novikoff), orthotopic hepatocellular carcinoma (HCC) model demonstrated regression of tumours after single administration of clofazimine solubilized in Lipiodol delivered via the intra hepatic artery.

Two clinical trials have been done to evaluate the anticancer activity of clofazimine against unresectable and metastatic HCC: Ruff *et al.* [33] reported an objective response rate of 10%, 43% disease stabilization for up to 20 months and an improved median survival time; Falkson and Falkson, [34] evaluated the combination of clofazimine (600 mg orally for 2 weeks followed by 400 mg daily thereafter) and doxorubicin and reported disease stabilization in 42% and a median survival time of 7 weeks. These results should be considered in the context that unresectable HCC is prognostically extremely poor and notoriously unresponsive to systemic chemotherapy. [35]

### **2.3.3. Tetramethylpiperidine (TMP)-substituted Riminophenazines**

Over the course of the last 40 years, hundreds of analogues have been synthesized allowing for extensive quantitative structure activity relationships (QSAR) to be performed. Modifications have focused on substitution in the imino nitrogen region of the molecule (at position 2 of the phenazine nucleus) along with varying halogenation profiles in the phenyl- and anilino-rings.

Tetramethylpiperidine substitution (Figure 2.2.) at the imino nitrogen position in comparison to the isopropyl group found in clofazimine has been shown *in vitro* to incur superior direct cytotoxicity against several intrinsically resistant neoplastic cell lines. [35] In addition they have been shown to possess greater chemosensitization activity using various Pgp expressing cell lines. [25, 37, 38]

These Riminophenazines thus possess the potential for inclusion in several chemotherapeutic regimes. B4125 has been identified from a review of the structure activity relationships (Appendix B) as possessing the best neoplastic-specific cytotoxicity.

#### 2.3.4. Pharmacodynamics: Anticancer multi-mechanism

As Riminophenazines possess a multi-mechanistic cytotoxic action, they are of use against non-classical MDR. They are thought to be active at the plasma membrane, the mitochondrial and the nuclear level.

The cytotoxic action at the level of the plasma membrane is attributed to enhancement of phospholipase A<sub>2</sub> (PLA<sub>2</sub>) activity. This in turn, leads to increased levels of lysophospholipids, which are potent detergents and membrane destabilizing agents. Lysophospholipids activate NADPH-oxidase leading to the production of cytotoxic oxidants by phagocytes. Furthermore the membrane associated enzyme Na<sup>+</sup>, K<sup>+</sup> ATPase is inactivated by lysophosphatidylcholine. This has significant antineoplastic consequences, as this enzyme is essential for cellular proliferation. Inhibition of this enzyme along with perturbations to the membrane lipid environment may be responsible for the observed inhibition of Pgp efflux activity. [25]

Riminophenazines have been shown [39] to act as artificial electron acceptors competing with cytochrome oxidase thus inhibiting energy-yielding reactions of the respiratory chain. This in turn is thought to inhibit down-stream energy requiring cellular processes including ABC pumps.

Morrison and Marley [21] demonstrated that Riminophenazines are capable of forming stable complexes with DNA through binding along guanine sequence regions associated with the minor groove resulting in loss of DNA template function.



## 2.4. Refinements in the pharmacokinetic usage of anticancer drugs

### 2.4.1. Loco-regional chemotherapy

Although systemic chemotherapy has proved effective in certain haematological malignancies (Acute myelogenous leukaemia) and a few solid tumours (notably testicular cancer), to date there is relatively poor efficacy against most systemic therapies (due to a lack of targeting) and the vast majority of disseminated cancers remain incurable.

Since Klopp *et al.* [40] first attempted intra-arterial chemotherapy in 1950 there has been a growing interest in delivering cytotoxic agents locally into the region of tumour growth via the artery supplying the region. The rationale being to expose the tumour to higher drug concentrations (above the maximum tolerated dose) thus producing a greater fractional tumour cell kill whilst limiting the side effects as systemic exposure is reduced. Regional delivery is thus an approach used to increase the exposure of cancer cells to drug/s beyond what can be achieved safely through systemic drug delivery. [41]

Regional chemotherapy can be divided into two categories: third space regional compartment therapy (e.g. cerebrospinal fluid space, peritoneal cavity, pleural space etc.) and intra-arterial infusion into an afferent artery feeding the tumour containing organ or body region.

Regional delivery of chemotherapeutics to tumours has a pharmacokinetic advantage over conventional systemic routes and offers significant benefit to patients. [42] Regional administration may increase exposure by 100-1000 fold compared to systemic administration. [43] The theoretical pharmacokinetic principles underlying the advantage offered by regional administration have been formally defined by Eckman *et al.* [44] This advantage is limited by how much drug is retained by the tumour after the "first pass" and for this reason the use of oil based vehicles as well as arterial occluding, embolizing agents of various forms

(e.g. starch microspheres) that act to prolong the transit time of the drugs within the tumour interstitium have great scope. [45]

The relative ease with which tumour blood supply can be accessed with high reproducibility and acceptable low complication rates is attributed to advances in surgical technique along with improved skills in interventional radiology, particularly the development steerable guide wires under fluoroscopic imaging guidance. Many of the smaller afferent arteries feeding prominent tumour types can now be routinely catheterized supra-selectively via percutaneous angiography using the Seldinger technique. [46] Isolated perfusion techniques, whereby artificial circuits are created removing the drug prior to entry into the systemic compartment, offer further benefit to the patient [46] all be it at the expense of time, money and added risk.

The application of regional chemotherapy has provided local remission in a number of tumour locations, including but not exclusive to brain, breast, head and neck and liver. As these studies have typically included patients with advanced, disseminated disease, the survival outcome has been determined by the extent and severity of metastatic disease. Viewed from such a point, other local treatment options - surgery and radiotherapy are considered more appropriate, less expensive and less toxic than regional chemotherapy.

Regional chemotherapy can be viewed as a local ablative technique paralleling surgery and radiation therapy but as it is based on molecular discernment, it holds the promise of greater specificity between cancerous and normal cells. [43] It must be remembered that ablation of disseminated disease is the real issue and the required outcome.

Advances in interventional radiology and the development of reliable, implantable drug delivery devices have made regional chemotherapy a rational endeavour to be combined (neo)-adjuvantly with other modalities to obtain greater therapeutic responses.

## 2.4.2. The Enhanced Permeability and Retention (EPR) effect

The enhanced permeability and retention effect (Figure 2.3.) of macromolecules and lipid-based particles is a general characteristic of viable and rapidly growing solid tumours. The increased vascular permeability underlying this effect is often considered the other side of the angiogenesis coin. [48] The EPR effect has been described both as the “gold standard” [48] and as the “royal gateway” in the design of new anticancer agents. [49]

Selective, passive targeting via the tumour vasculature is possible as result of extensive production of vascular permeability mediators including bradykinin, nitric oxide, vascular endothelial growth factor, peroxynitrite, prostaglandins and matrix metalloproteinases that promote angiogenesis or facilitate extravasation. Defective tumour vasculature that lack a continuous smooth muscle layer and contain gaps in endothelial cell-cell junctions further contribute towards permeability. This results in leakage of colloidal blood plasma components such as polymer conjugates and nanoassemblies (typically between 10 and 500 nm, dependent upon model) into the tumour tissue. [50]

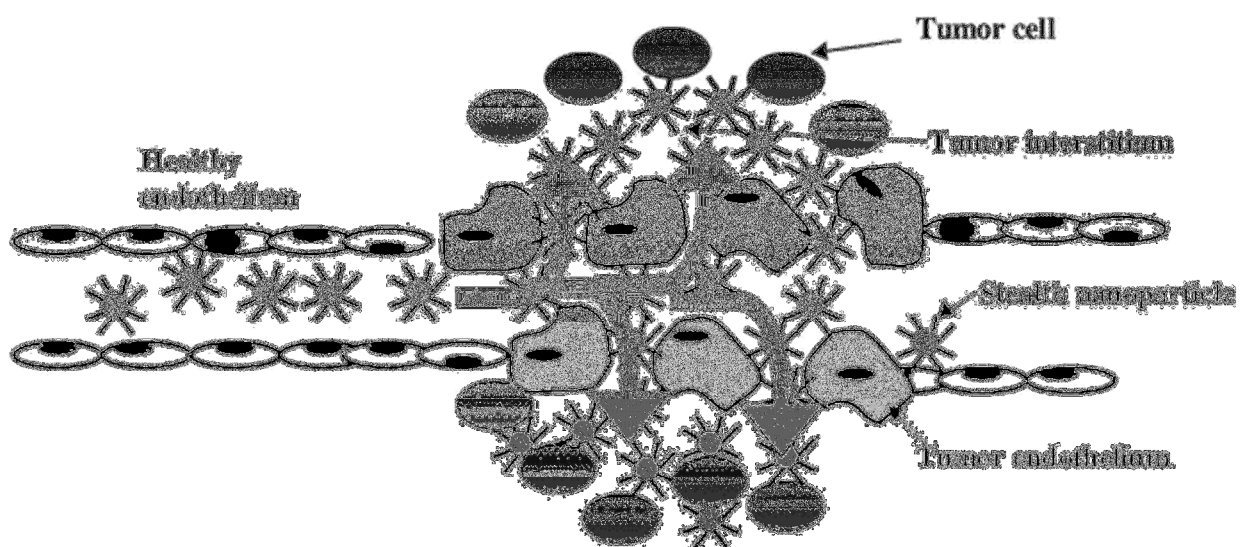


Figure 2.3. Depiction of the EPR effect displaying the leakage of nanoparticles through porous neoplastic endothelium. Modified from [47] (Used with permission)

Impaired lymphatic drainage and slow venous return ensure that colloidal drug carriers are retained within the tumour interstitium for long periods. Thus favourable distribution (akin to passive targeting) can be achieved which increases drug levels at the tumour site and reduces systemic exposure. [49]

The EPR effect and consequent passive targeting of colloidal drug carriers is dependent upon the molecular weight of the carrier being above the renal clearance threshold (>40 kDa) and very crucially that it possesses a lengthy plasma half live (>6 h). [48, 49] Passive accumulation of colloidal particles through exploitation of the EPR effect has been compared to the “magic bullet” concept put forward by Paul Ehrlich. [51]

It is well established that the ability of a NDDS to passively target tumours is dependent upon extended circulating properties and adequate particle size for optimal extravasation in the poorly formed tumour vasculature. A particle size of 50-200 nm is reported to be optimal. Colloidal particles smaller than 50 nm are thought to be eliminated by renal filtration or lost by non-specific extravasation into liver or bone marrow sinus endothelia. Particles larger than 200 nm may exceed the cut off size to traverse tumour vasculature. Splenic filtration may also rapidly clear such large particles. [52]

Kommareddy *et al.* [53] has stated that depending on the anatomical region and particular tissue model the pore size in discontinuous endothelium ranges from 100 -780 nm with a mean of approximately 400 nm.

### **2.4.3. Lipiodol Ultra-Fluid**

Lipiodol is an iodinated (480 mg iodine/ml) radio-opaque derivative of poppy seed oil, composed of ethyl esters of linoleic (73%), oleic (14%), palmitic (9%) and stearic acids (3%). [54] Lipiodol is used as a contrast agent in certain radiological investigations including lymphography, hysterosalpingography and sialography. [55]

Lipiodol has therapeutic potential as a targeting carrier of chemotherapeutics and / or radioisotopes. After intra-arterial injection into respective tumour feeder arteries, Lipiodol has been found through X-ray and CT imaging to remain selectively (for periods in excess of 2 months), within tumour tissue of the liver, lung, pancreas, gallbladder [56], bronchus, kidney [57], breast [58], bladder [59] and others. [60]

Lipiodol has been found to effectively solubilize clinically relevant concentrations of various drugs including: 5-fluorouracil, doxorubicin and mitomycin C [60], epirubicin [58] and paclitaxel. [62]

<sup>131</sup>I-Lipiodol has been developed as an internal radiation therapeutic agent [63] and is reputed to be capable of delivering an ablation dose of beta radiation resulting in high treatment response rates. [64]

Selective accumulation and prolonged retention after intra-arterial injection is attributed to first pass extraction (presumable due to the EPR effect). [48, 54] In addition, hepatoma cells have been shown to rapidly take up large quantities of Lipiodol through endocytosis and exhibit prolonged intracellular retention facilitating the activation of intracellular mechanisms of death induction. [65] This demonstrates that through intracellular trapping, Lipiodol and similar oily preparations may be an effective tool used to overcome high interstitial fluid (hydrostatic) pressure and serve as a reservoir of drugs for sustained release. As eluded to earlier, Lipiodol has been reported to offer a marked embolic effect thus effectively prolonging drug residence time within the tumour. [66]

As such, several benefits can be attained through implementation of such a targeted chemo-embolization strategy - notably, high cytotoxic specificity for cancer cells, prolonged action and imaging capabilities. However, as loco-regional administration is a requirement for such potent specificity, this approach is limited in the same way as surgery in that it is local and hence cannot find occult metastasis. The preparation needs to be distributed systemically and should passively accumulate or preferable actively target disseminated tumours.

So as to overcome the complications/limitations implicit in administration of an oil IV (pulmonary oil embolization), efforts have been made to encapsulate Lipiodol within nanostructures with controlled droplet size. Recently, Bae *et al.* [67] prepared and characterized a covalently cross-linked nanocapsule, consisting of an inner Lipiodol phase surrounded by a Pluronic (PEO-PPO-PEO)/ polyethylene (PEG) shell layer (corona). Paclitaxel was effectively solubilized within the inner Lipiodol phase.

Similarly, Ho Kong *et al.* [68] developed a Lipiodol encapsulated Pluronic (PEO-PPO-PEO)/PEG cross-linked nanocapsule. Results from this study suggest that such a nanoreservoir could efficiently deliver lipophilic therapeutic agents to cancerous tissue. In addition, owing to the high iodine concentration, the Lipiodol filled nanocapsule was shown to have effective X-ray attenuation properties. However, the cross-linked nature of the nanocapsule may impair effective release of drugs at the tumour site.

To the extent of the author's literature search, a Lipiodol loaded diacyl-lipid nanoemulsion has not been reported to date.

#### **2.4.4. Intelligent formulations: Nanoparticulate drug delivery systems**

Drugs are inanimate, exogenous chemical entities that have affinity for and intrinsic activity upon a receptor that can then elicit a biological response. The chemical structure of a drug dictates its pharmacological utility (both dynamic and kinetic). The physicochemical properties of a drug determines to a large extent, the ability of a drug to be adequately absorbed and distributed to the intended biophase. [69]

With the advent of combinatorial chemistry, computational *in silico* modelling, genomics and proteomics (supplying targets) there is an abundance of novel chemical entities that are emerging as drug candidates. Invariable *in vitro* assays are the means by which a particular target or suspected activity is determined (validated) using multi-well bioassays. As such, molecules with potent pharmacodynamics are discovered in high throughput screening (HTS) without



much consideration for their pharmacokinetic properties. Possessing impressive pharmacodynamics does not mean impressive pharmacokinetics.

Due to the ability to traverse membranes, the majority of the most potent anticancer agents discovered are hydrophobic in nature and are plagued by poor pharmacokinetic profiles, which requires higher doses for efficacy but also contributes towards toxicity and adverse effects. Many of these potent drugs are not easily formulated using conventional strategies. The lack of adequate aqueous solubility relative to the required therapeutic dose is the leading problem encountered for drugs intended for IV administration. [70] The formulation of new drugs has often been perceived as the bottleneck in the development of anticancer drugs. [71]

It is therefore not surprising that pharmaceutical companies often employ physicochemical screens and predictive software to eliminate compounds with undesirable physicochemical (implying pharmacokinetic) properties so as to decrease the attrition rate later in the pipeline thus reducing overall costs and speeding up the time to market of a new drug product. [72]

Formulation is an important and often underestimated aspect in the development of chemical entities as effective drug products. All drugs need to be formulated with excipients in a manner conducive to their intended route of administration. A solution must be found considering the particular physicochemical parameters of the drug and the therapeutic intent. As all living cells *in vivo* have a continuous blood supply in order to sustain life, the blood (circulatory system) presents a route by which targeting particulate (colloidal) drug products can be delivered. Parenteral dosage form excipients should serve as more than just a biocompatible vehicle for solubilising active compounds. There is an opportunity to impart “intelligence” through the use of a delivery system comprising functional excipients controlling distribution and release characteristics. [73]

In the past, the conventional means by which sparingly water-soluble drugs were formulated for parenteral administration included the use of low molecular weight

surfactants, pH adjustment, water miscible co-solvents and complexation. [72] Although effective at solubilising various drugs, these techniques suffer from several drawbacks including the risk of *in vivo* precipitation upon administration resulting in thrombophlebitis as well as causing allergic reactions. [74]

Recently, various nanoparticulate, colloidal drug carrier systems have been proposed as a solution to overcome poor solubility, low stability and toxicity issues. The advancement of polymer and material science has provided new opportunities for levels of pharmacokinetic intelligence to be added to dosage forms by design. There is currently much interest in the development of novel NDDS. Such new formulations may allow for the usable life of older drugs to be extended. [75]

High molecular weight surface active compounds (surfactants/amphiphiles) that possess both a hydrophilic and a hydrophobic portion in the same molecule are capable of forming a variety of assemblies at different weight percentages to service various administration (application) objectives.

The design of any cancer targeting drug delivery system should exploit at a minimum the EPR effect. The discovery that amphiphiles with hydrophilic polymeric domains (such as PEG and PVP) prevent opsonin binding through providing a steric barrier resulting in evasion of the mononuclear phagocyte system (MPS) has catapulted NDDS from vision to clinically reality. The term “stealth” has been used in contemporary literature to describe long circulating, immune evading, sterically stabilized/PEGylated nanoparticles. [76]

Over and above the EPR effect, there are several other tumour characteristics that can be exploited during drug product design. Active targeting through ligand and monoclonal antibody (MAb), e.g. Folate and 2C5 conjugation [77] to the PEG distal terminus have been shown to add further tumour selectivity. Active triggering mechanisms specifically at the tumour site add another dimension of focused drug delivery. Active triggering mechanisms are dependent on exploiting microenvironmental differences between normal and neoplastic cells and designing the nanoassembly to disassemble accordingly. Such triggering



mechanisms include enzymatic, ultrasonic, temperature and pH induced disassembly. [76]

A vast array of nanoparticulate structures have been assembled from various amphiphilic copolymers including but not exclusive to micelles, liposomes, nanospheres, nanocapsules, polymersomes, niosomes, solid lipid nanoparticles, nanoemulsions and microemulsions. This has led to much of the terminology been used interchangeable and at times erroneously. A recent review has attempted to more clearly classify the different nanoparticulate forms and clarify the terminology through an overview of the major features and factors that influence formation of the different structures. [78] This diversity in structure demonstrates the versatility of techniques to encapsulate compounds of different physicochemical properties within segregated compartments/cores of similar polarity for a variety of different applications.

Micelles are a binary system of water and amphiphile (surfactant) molecules. Micelles can be subdivided as either low molecular weight surfactant (detergent) or polymeric high molecular weight. [79] Polymeric amphiphiles possess lower Critical Micelle Concentration (CMC) values (the surfactant concentration above which micelles form) and are consequently more stable upon dilution. Mixed micellar systems with co-surfactant are common to aid either functionality or stability. Micelles have a hydrophobic core that lends itself to encapsulation of multiple lipophilic drugs. Encapsulation of drugs within the hydrophobic core of micelles by both thin film hydration and dialysis methods have been described [80]. The thin film hydration method is thought preferable in terms of optimisation of drug loading capacity.

## 2.5. Pre-clinical development of anticancer drug products: Regulatory perspectives

Pre-clinical development encompasses all the activities required (deemed necessary to ensure safety) before a new chemical entity can enter into human trials. The goal of pre-clinical studies is to provide accurate, reliable and timely data that will be used to justify the conduct of clinical trials in humans. It therefore follows that a drug development project must be undertaken with due consideration to appropriate regulatory guidelines.

These guidance documents are not intended to establish legally enforceable requirements, but rather reflect the current thinking of the respective agencies. The most scientifically sound and ethically correct approach for the particular “Target Product Profile” (TPP) under development should be adopted. Agent-directed, pre-clinical studies should be designed so as to support the conduct of clinical studies that may follow [81].

Pre-clinical modelling is aimed at saving time and resources. The principle outcome is to treat humans. Assumptions are made that pre-clinical data is predictive of activity in humans - therapeutic index (efficacy vs. toxicity). The value of any model is thus based on its ability to be predictive of clinical responses.

An internationally-harmonised document, ICH S9 [82], was recently released (29 October 2009) for final review (Step 4) by the respective regional agencies: USA - Food and Drug Administration (FDA); Europe - European Agency for the Evaluation of Medicinal Products (EMA); Japan - Ministry of Health, Labour and Welfare (MHLW) before adoption. It is important to realize that ICH S9 is intended to enhance and provide clarity [83] to the earlier guidelines implying DeGeorge *et al.* [84]; CPMP/SWP/997/96 [85] and Nakae *et al.* [86] representing the recommendations of the FDA, EMA and MHLW respectively. These documents are unique in that most guidelines, including those of the local (South African) regulatory authority - the Medicines Control Council (MCC), either explicitly or implicitly exclude cancer therapies from their recommendations. [87]

## **ICH S9**

The objectives of the ICH S9 document are to: Facilitate and accelerate the development of anticancer pharmaceuticals and to protect patients from unnecessary adverse effects.

Because malignant tumours are life threatening and because the death rate from these diseases is high and existing therapies have limited effectiveness, the pre-clinical evaluation of anticancer drug products is often abbreviated. Pre-clinical evaluations are conducted to: identify the pharmacological properties of a pharmaceutical; establish a safe initial dose level for the first human exposure and to understand the toxicological profile of a pharmaceutical.

The active pharmaceutical substance used in pre-clinical studies should be well characterized and should adequately represent the drug product (final dosage form) to be used in clinical trials. Concerning the required pharmacological studies, appropriate models should be selected based upon both the target and mechanism of action, but the pharmaceutical need not be studied using the same tumour types intended for clinical evaluation. These studies can serve to: provide non-clinical proof of principle; guide schedules and dose escalation schemes; provide information for selection of test species; aid in start dose selection and selection of investigational biomarkers (where appropriate) and justify pharmaceutical combination.

An assessment of the pharmaceuticals effect on vital organ functions should be made as part of a general toxicology test. However, in the absence of specific risk these studies will not be called for to support clinical trials nor marketing.

The evaluation of limited pharmacokinetic parameters can facilitate dose selection, schedule evaluation and escalation schemes during first in human studies. As the toxicity of a drug can be greatly influenced by schedule (dosing regimen), an approximation of the clinical schedule should be evaluated using usually both rodent and non-rodents. The reversibility of any observed toxicity should be investigated. Reproductive toxicology, genotoxicity and carcinogenicity

studies are not considered essential to support clinical trials intended for the treatment of patients with advanced cancer.

One of the primary goals of pre-clinical testing is to identify a safe dose that is reasonably expected to have pharmacological effects. Common practice is to set the start dose at 1/10 of STD10 (severely toxic dose in 10% of animals) in rodents. If the non-rodent is thought to be a more appropriate animal model, then 1/6 of a highest non-severely toxic dose (HNSTD) is to be the start dose in humans.

In general, the highest dose or exposure tested pre-clinically does not limit the dose escalation or highest dose investigated in a clinical trial. In Phase 1 clinical trials, treatment can continue according to the patient's response. A new toxicology study is not called for to support continued treatment beyond the duration of the prior completed toxicology studies.

Concerning drug combinations, data should be available that supports the rationale prior to starting clinical trials. Concerning conjugated products the safety of the conjugated material is the primary concern - stability of the conjugate in the test species and human plasma should be provided. A complete evaluation of drug delivery systems is not warranted if the unencapsulated Active Pharmaceutical Ingredients (API) have been well characterized. [82]

ICH S9 is to be read in conjunction with other pertinent guidelines: Regulatory requirements for the pre-clinical (non-clinical) safety studies required to support the conduct of human clinical trials is addressed by the ICH M3R2 [88]. In ICH M3R2 it is stated that only 1 GLP toxicity test, either acute or chronic is required for progression to clinical studies. Repeat dose toxicity studies mimicking the proposed clinical schedule and route of administration in two species (1 being non-rodent) will generally support any clinical trial up to an equivalent duration.

Although not an official FDA guideline, DeGeorge *et al.* [84] was authored by senior FDA employees and has directed much of contemporary thinking. [81] The primary aims of safety studies have been highlighted as: determine a safe starting

dose for subsequent clinical trials that is both reasonably safe and allows for possible clinical benefit to patient; identify organs of toxicity and the reversibility thereof. The use of specialized delivery systems and chemosensitizers is further discussed and may necessitate additional pre-clinical evaluation beyond that of conventional cytotoxic drugs. The EMEA [85] advocates pre-clinical investigation of pharmacodynamic, kinetic and toxicological interactions of drug combination products before clinical trials.

### **3. Target product profile, critical path and pre-clinical development plan**

The target product profile (TPP) is a tool used extensively in the pharmaceutical industry for planning research and development (R&D) projects. [89] The TPP can be viewed as a statement of the key features and attributes of the product intended to be developed. Strategic drug development begins with the TPP that then helps delineate the pre-clinical and clinical studies (pathways) necessary to support that particular product profile. [90] TPP is used as a tool when communicating with agencies: as a means to help define the due regulatory requirements that then drives the pre-clinical development plan. Statement of the TPP must be realistic considering resources.

In this study the primary TPP directing development efforts were described (envisioned) as a tumour-targeting, nanoparticulate drug delivery system (NDDS) that has encapsulated a synergistic Fixed-Ratio Drug Combination (FRDC) of a standard chemotherapeutic (paclitaxel) and a Riminophenazine (that is thereby capable of circumventing MDR). The label of “broad-spectrum MDR circumventing anticancer agent” is suggested to describe Riminophenazines.

Within the development portfolio, two additional TPP stipulations were pursued: firstly, imaging capability (through Lipiodol encapsulation in a nanoemulsion) and secondly the development of novel amphiphiles (PVP conjugates) for Riminophenazine encapsulation through strategic alliance with the Institute of Polymer Science (Stellenbosch University).

A list of scientifically and ethically justifiable tests required to prove safety and efficacy for the particular product under development should ideally be outlined with due consideration to the appropriate regulatory guidelines and the regulatory (approval) status of the individual components (drugs and excipients) used in the formulation.

As this project had view (although not scope) to progress through to human trials and eventual commercialization, a holistic view (considering resources available and future development avenues) had to be taken and the practical steps chronologically ordered. The critical path (Figure 3.1.) describes the different steps and activities that must typically be completed at different time points within different focus areas prior to successful commercialization of a drug product. This study concerned the prototype design/discovery and pre-clinical development phases.

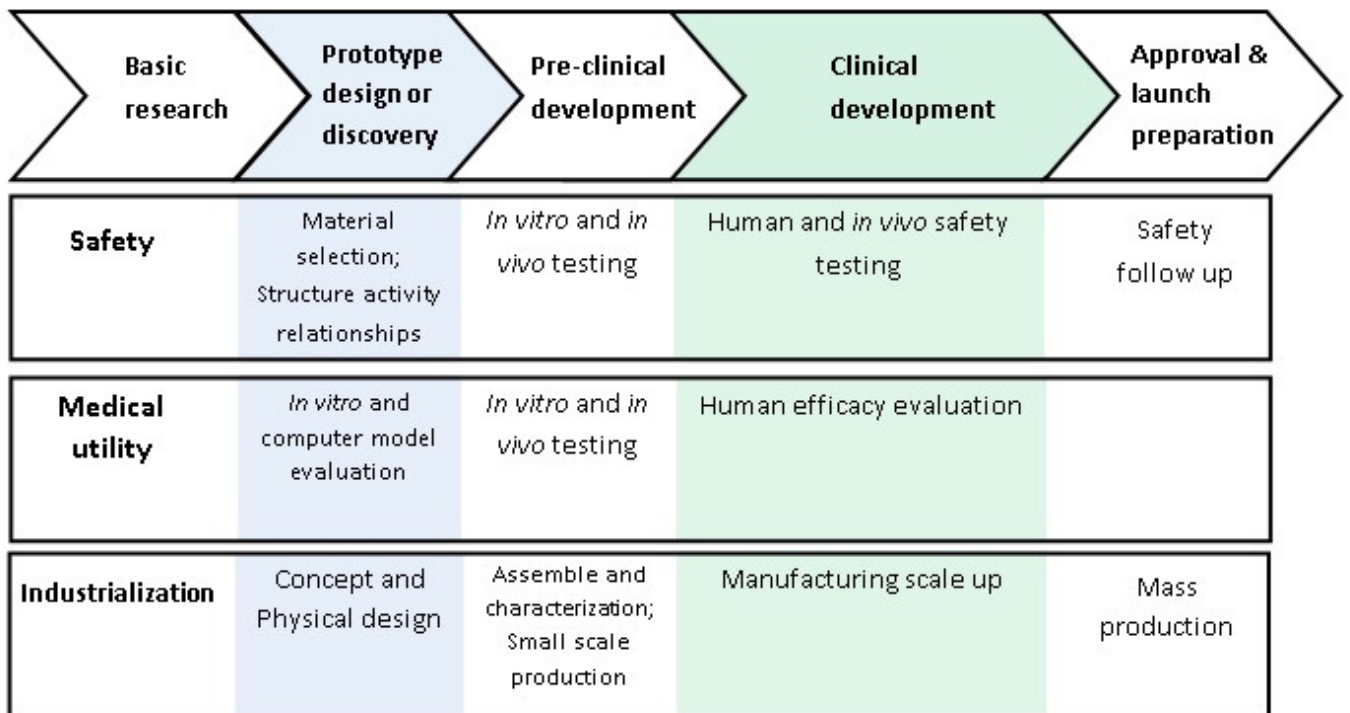


**Figure 3.1. A generalised schematic displaying the critical path outlining the different phases of development and the typical actions taken to successfully launch a pharmaceutical product. Adapted from Sadrieh and Miller [91]**

## ***Pre-clinical development plan of Riminocelles™***

### Stage I.

#### Aim:

- Determine the optimal synergistic FRDC *in vitro* using a Pgp expressing cell line.
- Assess the MDR-circumventing spectrum of Riminophenazines using different ABC expressing neoplastic cells.

#### Objectives:

- Procure authenticated experimental drugs.
- Purify lead Riminophenazines.
- Determine IC<sub>50</sub> values of the lead Riminophenazines and standard chemotherapeutics.
- Perform fixed molar ratio combination experiments - determine Combination Indexes (CI) and dose reduction afforded.

#### Checkpoint:

- Which drug combination possesses the most potential value?

### Stage II.

#### Aim:

- Assemble and characterize a marketable, passively tumour-targeting co-formulation of the lead standard chemotherapeutic and Riminophenazine.

#### Objectives:

- Characterize and optimize drug loading, particle size, zeta potential and drug retention (under sink conditions) of the developed system.



### Stage III.

#### Aim:

- Evaluate the pre-clinical *in vivo* safety and efficacy of the developed product in accordance with international regulatory guidelines.

#### Objectives:

- Assess acute toxicity parameters.
- Assess pharmacokinetic and organ accumulation parameters.
- Assess *in vivo* functioning of the developed drug delivery system.
- Evaluate efficacy using a relevant tumour model.
- Assess rodent repeat dose toxicity.

#### Check points:

- Is a 28-day repeat toxicity study in a non-rodent species warranted?
- Is further evidence of efficacy required?
- Phase II clinical trial?

## ***Pre-clinical development plan of RiminoPLUS™ imaging***

### **Aim:**

- Develop a nano-sized emulsion entrapping Lipiodol (contrast oil), suitable for parenteral administration.

### **Objectives:**

- Determine Riminophenazine solubility in Lipiodol.
- Create an excel sheet for simplified pre-calculated titration following the tie lines of a pseudoternary phase diagram.
- Characterise the formulation in terms of size using Dynamic Light Scattering (DLS).
- Evaluate the influence of co-surfactant ratio on size and stability.

## 4. Riminophenazine procurement, purification and authentication

### 4.1. Materials

#### Chemicals and reagents

##### *Riminophenazines*

Various batches (synthesised at various laboratories and at different times) of the possible lead Riminophenazines (B4112, B4121, B4125) were made available for investigation in this study. The various batches of interest were allocated unique identifier numbers that indicated their source of origin.

Methanol (MeOH), chloroform (CHCl<sub>3</sub>) and deuterated chloroform (CDCl<sub>3</sub>) were purchased from Merck (Darmstadt, Germany).

### 4.2. Authentication of Riminophenazine purity and integrity

To ensure integrity and validity throughout, it is prudent to authenticate and purify (if required) the investigational drugs prior to *in vitro* and *in vivo* investigations.

As a first step thin layer chromatograms (TLC) of all the different Riminophenazine batches of interest (Figure 4.1.) were run with an optimised mobile phase of Chloroform: Methanol (80:20) using normal phase plates (Alugram® SIL G/UV254, Macherey-Nagel). Qualitative visual comparisons were used to assess the impurity profile and conformity of the various Riminophenazine batches. Unfortunately, the precise date and site of synthesis for several of the stored batches were unavailable. Clofazimine (B663) was shown to be pure. However, several impurities were present for all the other available Tetramethylpiperidine (TMP) derivatives that necessitated purification prior to *in vitro* bioassays. Different batches of the same compound were shown to possess similar contamination profiles. Most of the major impurities (probably precursors or intermediates) were

seen to be more lipophilic and migrated further on a silica TLC plate than the compounds of interest.

After method development with using silica solid phase extraction (SPE) cartridges, normal phase preparative column chromatography was used to purify B4125.1. After preparing a silica (Silica gel 60, Merck, particle size 0.063-0.2 mm) slurry in  $\text{CHCl}_3$  and carefully filling the column (60 cm x 3 cm) ensuring the removal of air bubbles through gentle taping of the chromatography column glass wall, a small volume of concentrated drug (in  $\text{CHCl}_3$ ) was carefully loaded onto the surface of the column (that was protected from disturbance with non-adsorbent cotton wool). Elution of compounds was initiated with 100 ml of  $\text{CHCl}_3$ . Thereafter the % (v/v) of MeOH (in  $\text{CHCl}_3$ ) was increased 10% every 100-250 ml. Many fractions (based in part on visual observation) were collected and an aliquot of each fraction again run on TLC (Figure 4.2.) to assess purity.

Clean fractions were pooled, an aliquot dried, reconstituted in  $\text{CDCl}_3$  and sent to Dr. E. Palmer (Department of Chemistry, University of Pretoria) for  $^1\text{H}$  and  $^{13}\text{C}$  NMR analysis (Bruker Advance 500 MHz) to confirm compound authenticity (Figure 4.3).

To confirm compound purity, a preliminary HPLC method with a wide-polarity, gradient-elution scheme was developed on a C18 column (Figure 4.4 & 4.5). Elution was monitored in series by UV and MS detectors. Detection parameters were broad so as to detect the widest possible range of impurities. Direct infusion, Electrospray Ionization, Mass Spectrometry (ESI MS) was performed and confirmed drug structure through accurate mass and isotopic distribution (Figure 4.6.).

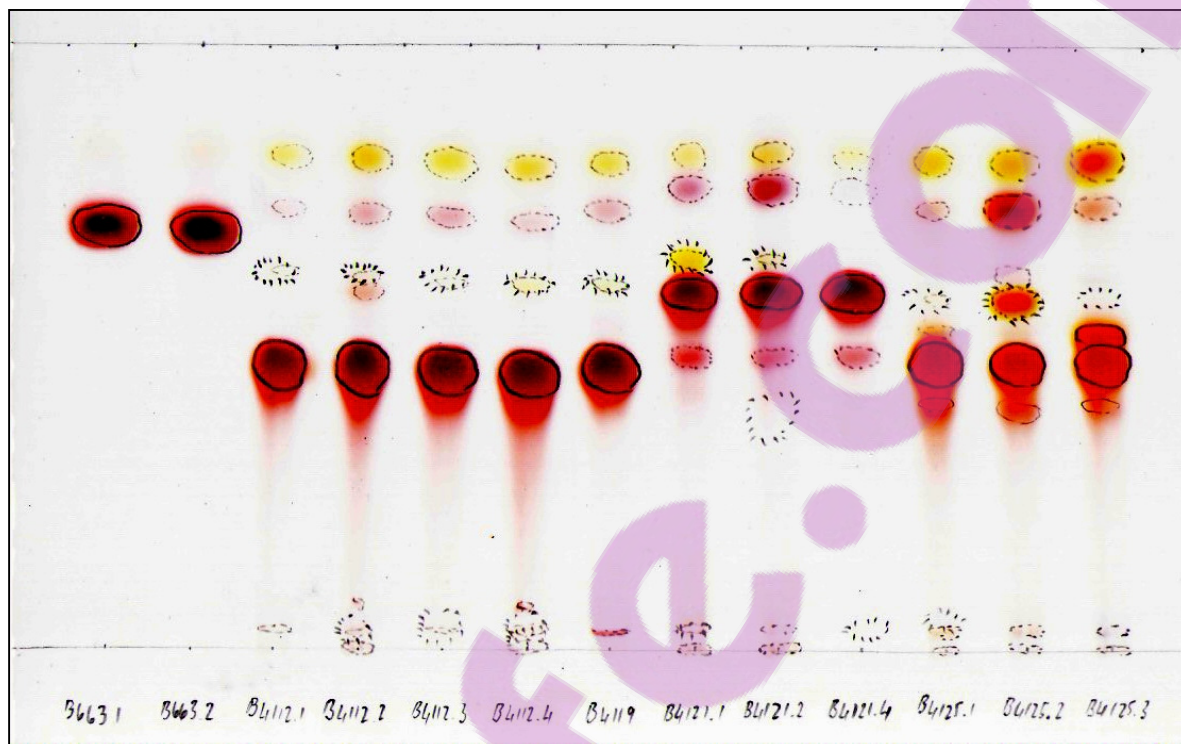


**Figure 4.1. TLC chromatogram of the various batches of synthesised TMP-substituted Riminophenazines showing the impurity profile**

**Batch 1. Origin unconfirmed but used in previous studies; Batch 2. Irish reference sample; Batch 3. Synthesised by Dr. Patricia Gitare (PET laboratories, Little Company of Mary Hospital) in late 2007; Batch 4. Stored at 2-8 °C for prolonged periods. The various batches are denoted with corresponding suffixes.**

**Developed using CHCl<sub>3</sub>: MeOH (80:20) on silica plates showed adequate resolution with the major compounds eluting at an R<sub>f</sub> of roughly 0.5. Visualised additionally under UV light - 254 (solid lines) and 360 nm (broken lines).**

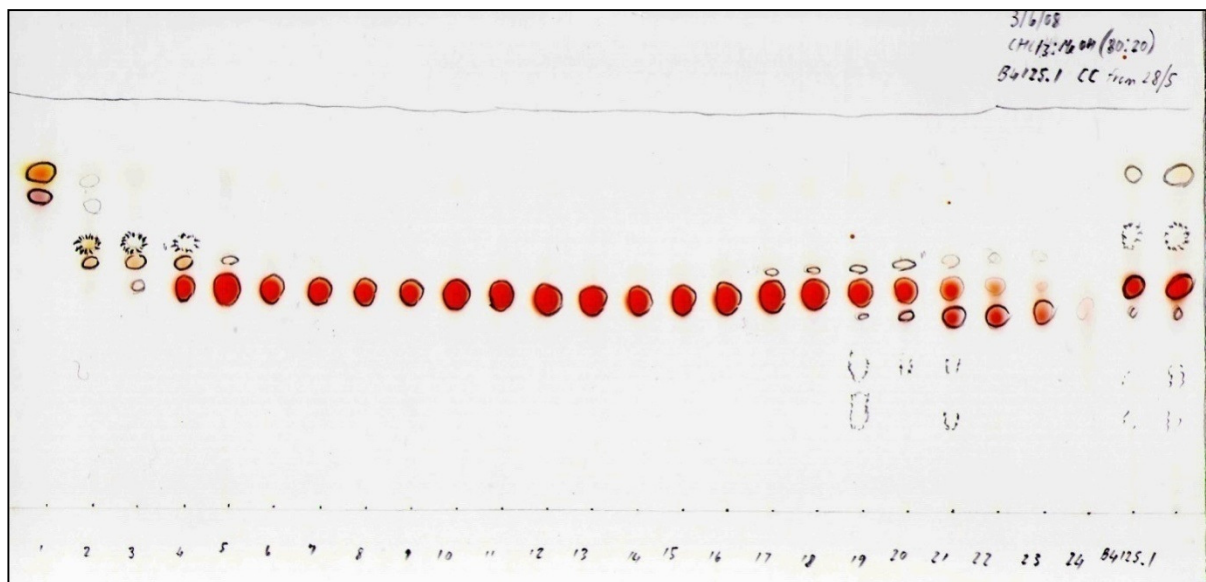


**Figure 4.2. TLC chromatogram of the fractions of B4125.1 attained through column chromatography**

**Developed using  $\text{CHCl}_3$ : MeOH (80:20). Visualised under UV light, 254 and 360 nm.**

**Twenty four fractions were collected. Fractions 6-16 were pooled and gravimetrically shown to represent 75.8% (w/w) of the original dry starting material**

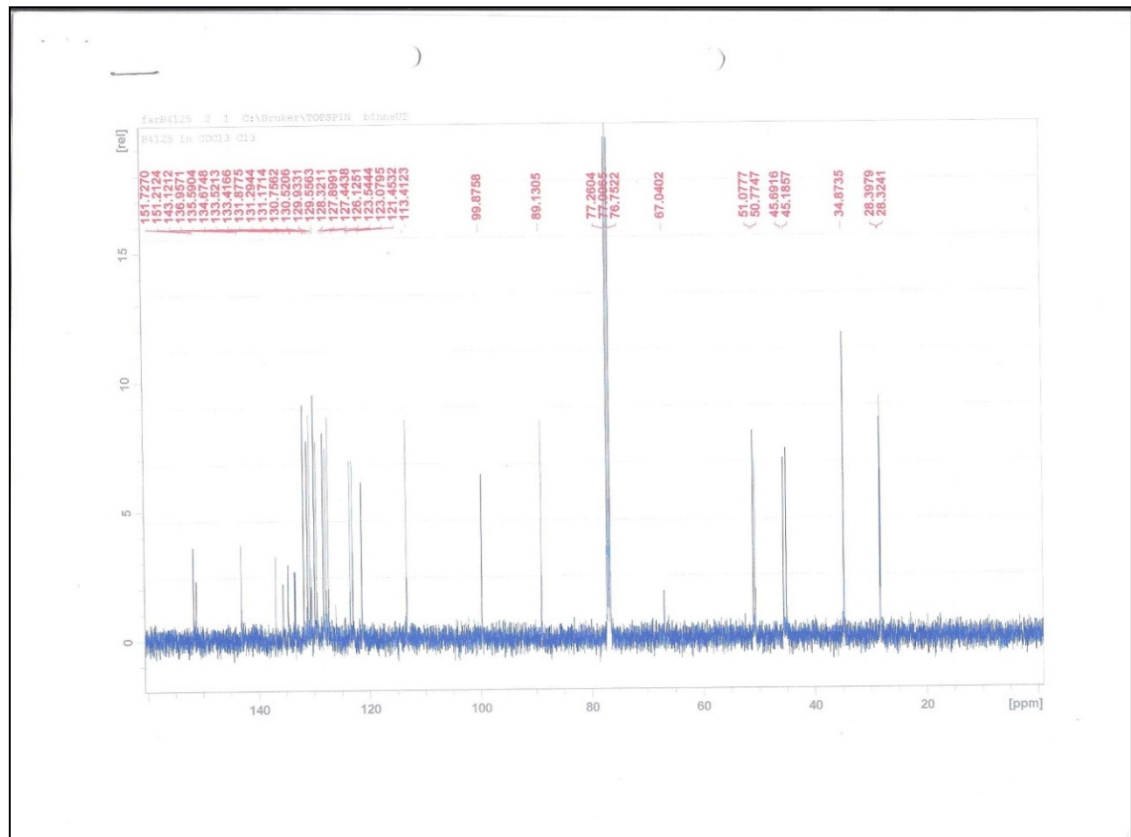
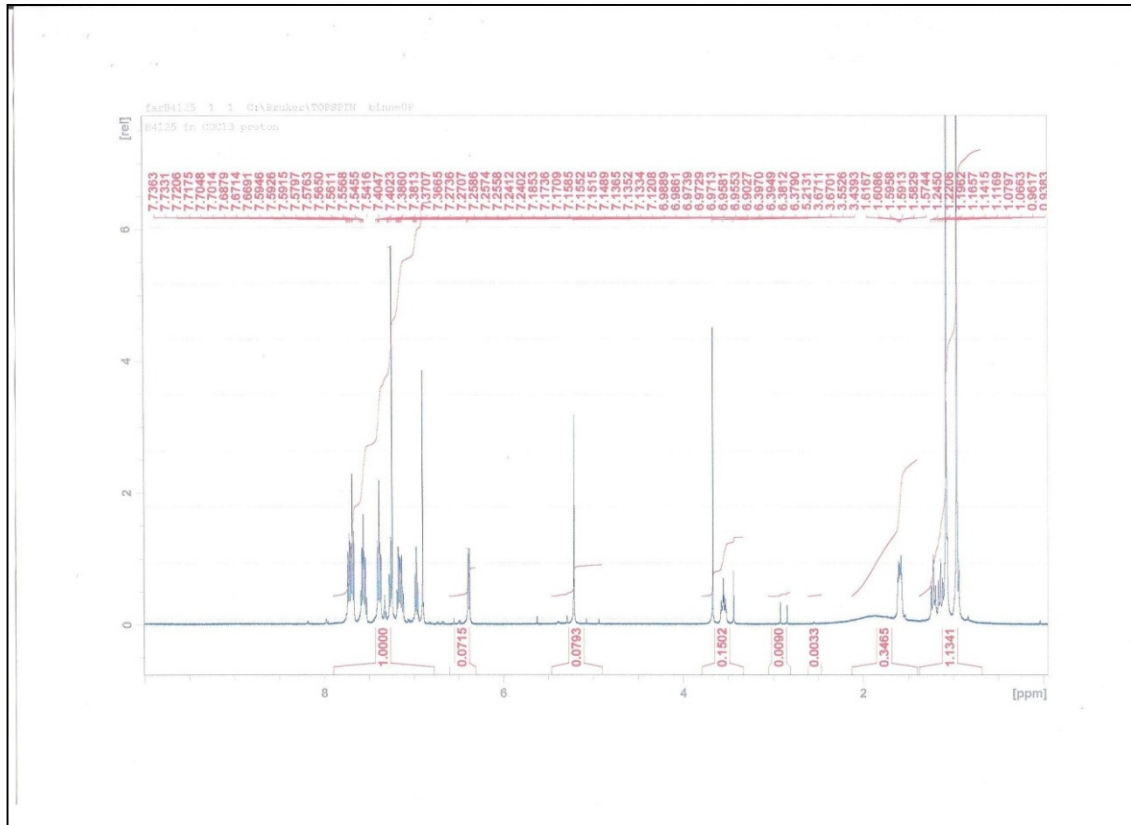
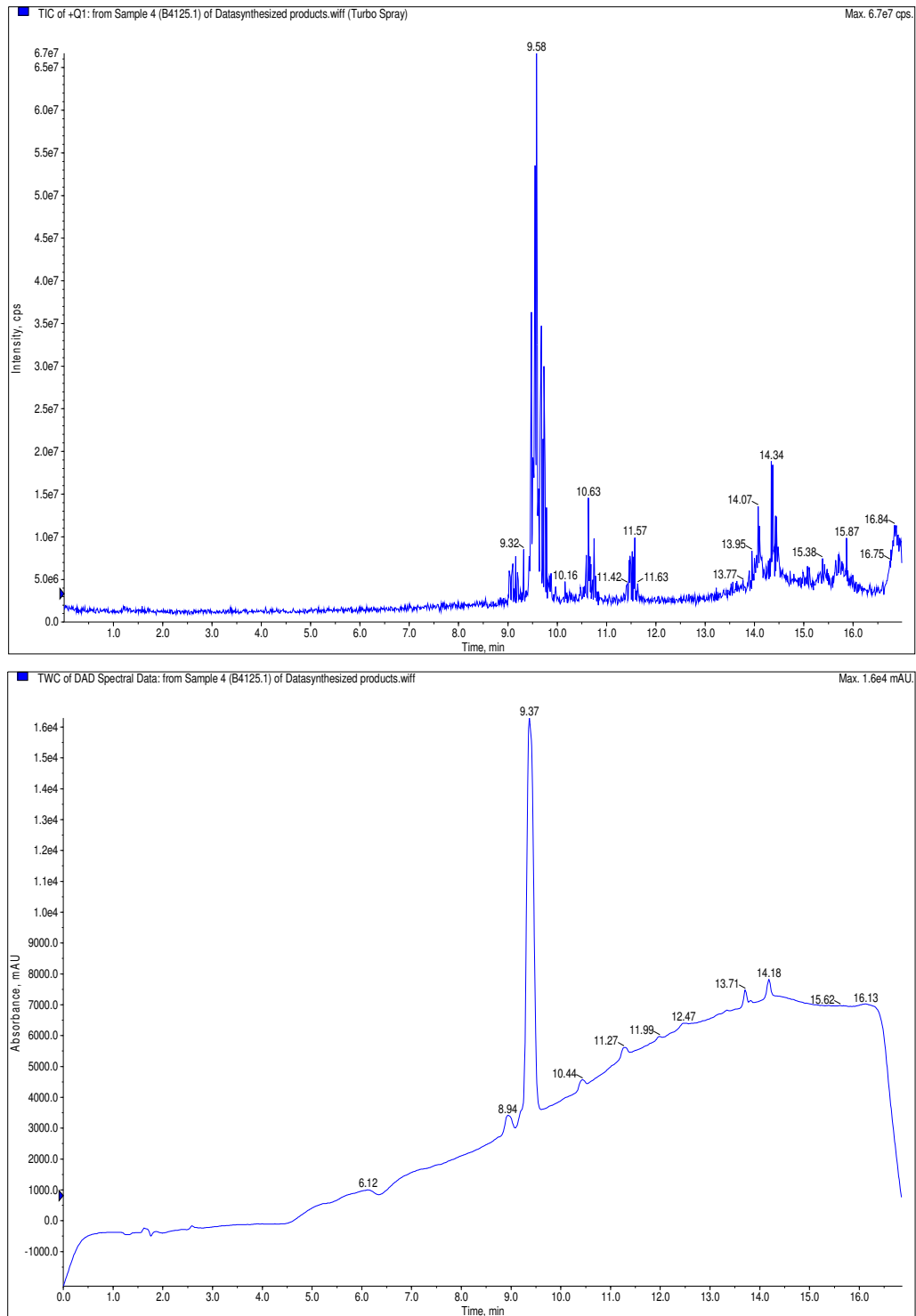


Figure 4.3.  $^1\text{H}$  (above) and  $^{13}\text{C}$  (below) NMR of B4125



**Figure 4.4. B4125.1 with minor impurities as shown through HPLC with MS (above) and UV (below) detection**

**Mobile phase: A, H<sub>2</sub>O (0.1% HCO<sub>2</sub>H); B, MeOH (0.1% HCO<sub>2</sub>H). Elution: time 0 min, 25% B; time 2 min, 25% B; time 12 min, 100% B; time 14 min, 100% B; 15 min, 25% B; 17 min, 25% B. 5 µl injection of a 10 µg/ml solution in 25% MeOH (0.1% HCO<sub>2</sub>H)**



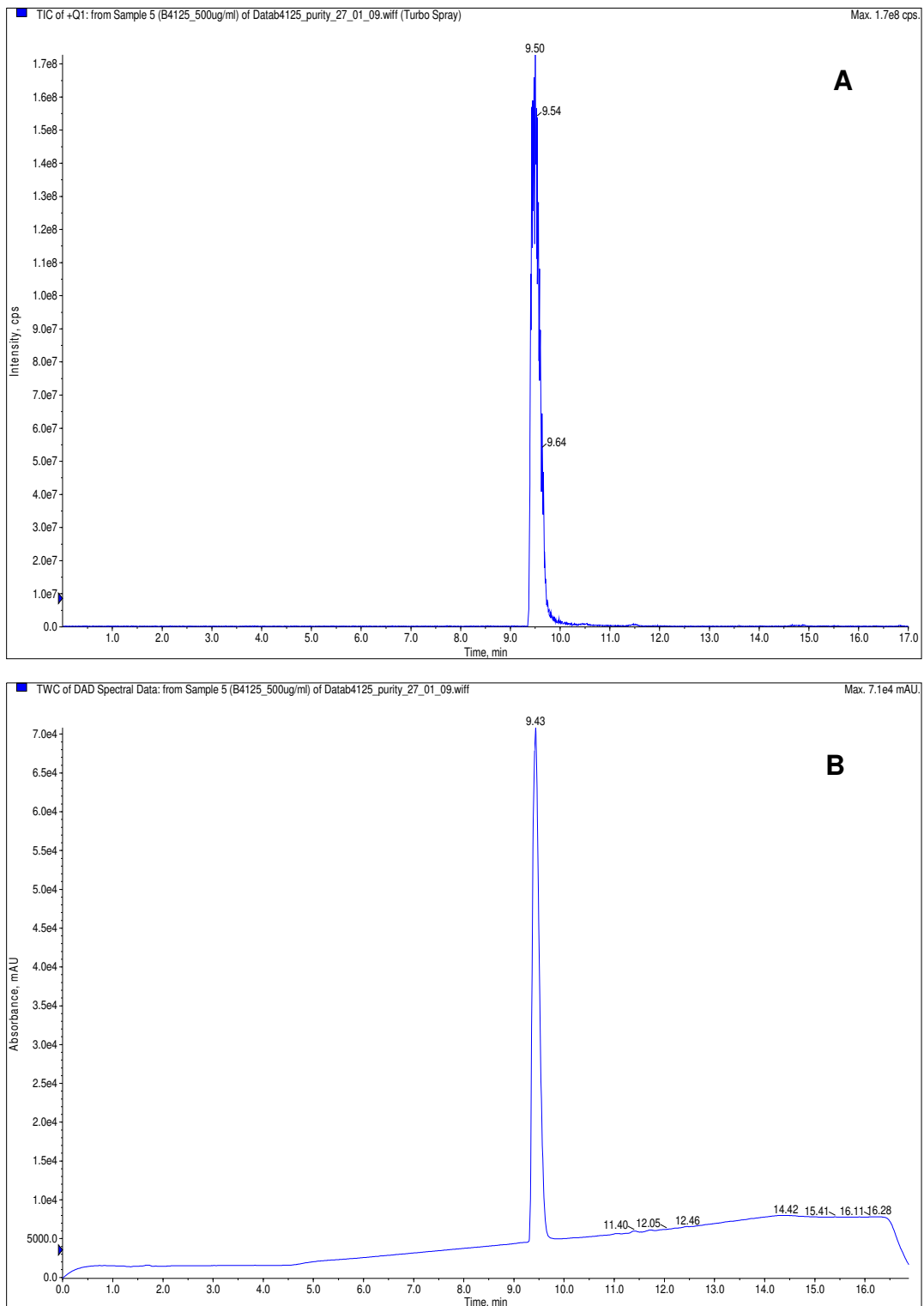


Figure 4.5. Purified B4125 after normal phase preparative column chromatography

**A: Total ion chromatogram (100-1200 m/z)**  
**B: Total wavelength chromatogram (UV 250-900 nm)**

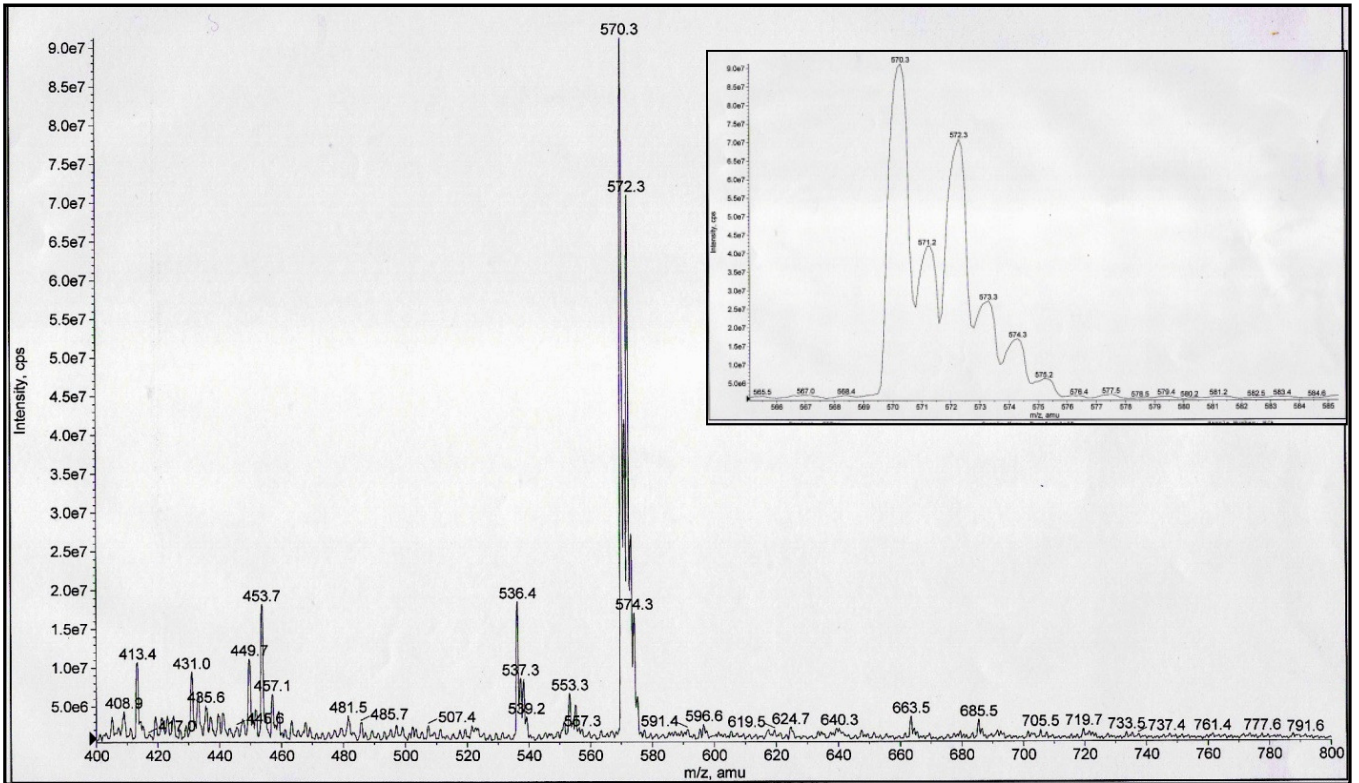


Figure 4.6. Direct infusion of B4125 into the ESI source displaying the expected mass to charge ratio 570.56 m/z and the inset showing the isotopic distribution of the 570.56 peak

## 5. *In vitro* antiproliferative bioassays

### 5.1. Introduction

So as to speed research, decrease development costs and improve therapeutic response, there is an increased interest in designing combination drug regimens rationally, early in the pre-clinical drug development stage. *In vitro* bioassays using 96 well plates is an effective way of screening various drug-drug combinations at specified ratios and various concentrations for cytotoxic activity against different cell cultures.

In contemporary scientific literature, synergy is best defined as greater than the expected additive activity of two or more drugs. Drug interactions (whether synergistic, additive or antagonistic) are dynamic and are dependent upon both the ratio of the drugs and on the dose level. [92] Distinguishing between synergistic, additive and antagonistic drugs combinations requires experimental designs and statistical analysis that require appreciable experimental time and effort. [93] Each individual fixed-ratio combination tested can be considered as a unique drug entity.

Many methods including fractional product analysis, isobologram methodology and surface response models have been put forward to evaluate drug interactions. The most popular analysis technique is the combination index method based on the median effect principle derived from the law of mass action. [94] Median effect analysis allows for the evaluation of drug combinations irrespective of whether the drugs exert their effect in the same pathway or through a completely different mechanism of action. [95] Such analysis is widely used as its application has been simplified by the availability of user-friendly software (CalcuSyn).

The Median-effect equation correlates dose and effect in the simplest form possible:

$$fa / fu = (D / D_m)^m$$

Where: D: dose of the drug;  $D_m$ : median effect dose signifying the potency (similar to  $IC_{50}$ );  $fa$ : the fraction affected by the dose;  $fu$ : the fraction unaffected;  $m$ : exponent signifying the sigmoidicity (shape) of the dose effect curve

As stated, synergy is defined as a more than the expected additive effect and antagonism as less than the expected additive effect. A combination index (CI) of 1 at a selected fractional affect ( $fa$ ) represents an additive effect (the combined effect of the drugs used separately, results in the same effect as if the drugs were used together at the equivalent doses), while a CI<1 represents synergism and a CI>1 represents antagonism.

A combination index (CI) at a particular fractional affect ( $fa$ ) can be obtained from:

$$CI = (D)_1 / (D_x)_1 + (D)_2 / (D_x)_2 + (D)_1(D)_2 / (D_x)_1(D_x)_2$$

Where:  $(D)_1$  and  $(D)_2$ : represent the dose of the drugs (in combination) eliciting a particular fractional affect and  $(D_x)_1$  and  $(D_x)_2$  are the doses of the drugs (used alone) that elicit the same fractional affect.

To perform such analysis: dose response curves are required for each of the respective drugs individually and dose response curves are required for each potential FRDC. In this study we elected to combine both B663 and the lead TMP derivative (B4125) with three standard chemotherapeutics (SC): etoposide, paclitaxel and vinblastine. These first-line SC were elected for combination with Riminophenazines for two reasons. Firstly on the basis that these cytotoxic drugs have been reported to be substrates of Pgp (often leading to clinical failure) and secondly that they possess different mechanisms of action and may therefore be used to derive mechanistic information.

Phenotypically stable (intrinsic) Pgp expressing, neoplastic cell cultures (COLO 320DM and HCT-15) were used to evaluate the antiproliferative effect of various fixed molar ratio drug combinations. The purpose of such investigations was to identify what specific ratios and of which drug combinations possess synergy against MDR neoplastic cell cultures.

Additionally, the hypothesis that Riminophenazines could be used as inhibitors of additional ABC transporters was evaluated. To this end, a MRP expressing cell line (ASH-3) was obtained.

## **5.2. Materials**

### Cell cultures

COLO 320DM (ATCC number: CCL-220) and HCT-15 (CCL-225), human colorectal carcinoma cell cultures were obtained from American Tissue Culture Collection (ATCC). Both these cultures were grown in Roswell Park Memorial Institute (RPMI) media with 10% Fetal calf serum (FCS).

ASH-3 (JCRB 1073), a human anaplastic thyroid carcinoma cells were purchased from the Japan Health Sciences Foundation (Health Science Research Resources Bank) and cultured in a 1:1 mixture of RPMI and Dulbecco's Modified Eagle's Medium (DMEM) with 10% FCS.

CalcuSyn ver.2.0 software for performing dose effect analysis was purchased from Biosoft (Cambridge, UK).

### Preparation of reagents

#### *Ammonium chloride solution*

Ammonium chloride solution was prepared by dissolving 8.3 g Ammonium chloride (NH<sub>4</sub>Cl), 1 g Sodium bicarbonate (NaHCO<sub>3</sub>), (both purchased from Merck, JHB,

SA) and 74 mg EDTA (Sigma Aldrich, JHB, SA) in 1000 ml of distilled water. The solution was filter sterilized using a 0.2  $\mu\text{m}$  syringe filter and refrigerated until use

#### *Cell counting fluid*

One millilitre of a 0.1% crystal violet solution and 2 ml glacial acetic acid was dissolved in 97 ml of distilled water. The solution was mixed well and refrigerated until used.

#### *Dulbecco's Modified Eagle's Medium (DMEM)*

DMEM powder (Sigma-Aldrich, JHB, SA) was dissolved in sterile water with the aid of a sterile stirrer. The pH of the solution was adjusted to 4 with 1 N HCl to ensure complete solubilisation. Thereafter 2 g of  $\text{NaHCO}_3$  was added to each litre of the medium. The pH was readjusted to 7.1 through the addition of either 1N HCl or 1 N NaOH. The medium was filter-sterilized through a 0.2  $\mu\text{m}$  filter and divided into 500 ml aliquots. Typically, 55 ml was removed from each 500 ml aliquot and the remaining solution was supplemented with 5 ml of a 1% penicillin/streptomycin solution and 50 ml sterile heat inactivated fetal calf serum (HI FCS). The medium was stored at 4°C until used.

#### *Heparin*

Thirty grams of Heparin (Sigma-Aldrich, JHB, SA) was dissolved into 90 ml of distilled water. The solution was filtered sterilized using a 0.2  $\mu\text{m}$  syringe filter and refrigerated until use.

#### *MTT solution*

A stock solution was prepared by dissolving 200 mg of 3-(4,5-dimethylthiazol-2-yl)-2,5-diphenyltetrazolium bromide (MTT), (Sigma-Aldrich, JHB, SA) in 40 ml PBS solution. After solubilising the light sensitive solution was filter sterilized using a 0.2  $\mu\text{m}$  syringe filter and stored (covered in tin foil) at 4°C until use.

### *Phosphate buffered saline (PBS)*

Using the manufacturers recommendations, 0.923 g of buffer powder (The Scientific Group, JHB, SA) was dissolved in 100 ml of deionised water. The pH was adjusted to 7.2.

### *Roswell Park Memorial Institute Medium (RPMI) 1640*

RPMI 1640 powder (Sigma-Aldrich, JHB, SA) was dissolved in sterile water with the aid of a sterile stirrer. The pH of the solution was adjusted to 4 with 1N HCl to ensure complete solubilisation. Thereafter 2 g of NaHCO<sub>3</sub> was added to each litre of the medium. The pH was readjusted to 7.1 through the addition of either 1N HCl or 1N NaOH. The medium was filter-sterilized through a 0.2 µm filter and divided into 500 ml aliquots. Typically, 55 ml was removed from the 500 ml aliquot and the remaining solution was supplemented with 5 ml of a 1% penicillin/ streptomycin solution and 50 ml sterile HI FCS. The medium was stored at 4°C until used.

### *Trypan blue*

A 0.2% w/v stock solution was made in PBS.

### *Standard Chemotherapeutics (SC):*

Paclitaxel (PTX), etoposide (ETOP), vinblastine (VIN) and doxorubicin (DOX) were purchased from Sigma Aldrich (St Louis, MO, USA).

Clofazimine was kindly supplied by Dr. J.F. O'Sullivan, Laboratories of the Medical Research Council of Ireland, Trinity College, Dublin, Republic of Ireland.

Water was 18 MΩ water produced from the municipal water supply after processing by an ELGA purification unit (ELGA, Wycombe, UK).



## 5.3. Methodology

### 5.3.1. Cell culture preparation and *in vitro* antiproliferative assays

All handling of cultures and experiments were conducted sterile within an ISO particle count certified High Efficiency Particulate Air (HEPA) filtered laminar flow cabinet.

Cultures of the respective cell lines were established using standard *in vitro* methods and the suppliers recommended media in 25 - 175 cm<sup>2</sup> plastic culture flasks (AEC-Amersham P/L, JHB, SA) to achieve the required cell numbers for each assay. Cultures were incubated at 37°C in a humidified atmosphere with 5% CO<sub>2</sub>. The cultures were regularly sub-cultured in order to maintain log phase growth.

On each day of experiment initiation, cells were harvested from their flasks using 0.25% (w/v) trypsin/EDTA with the aid of gentle agitation. Non-adherent COLO 320DM cells were simply decanted into 15 ml tubes and centrifuged at 350 *g* for 5 minutes at room temperature. The cell pellets were resuspended in 1 ml of complete medium and thoroughly aspirated. An aliquot (typically 50 µl) of the cell suspension was taken and added to 450 µl of a trypan blue solution before performing cell counts and assessing viability using a haemocytometer.

The remaining cell suspension was adjusted to a suitable volume using complete media to yield the final desired cells/ml concentration based on previously determined cell line specific seeding numbers for the duration of a particular assay. A volume of 100 µl of the adjusted cell suspension was seeded into 96 well tissue culture plates (Nunc). Cell seeding numbers were as follows: 500 cells/well for COLO 320DM cells, 2500 cells/well for HCT-15 cells and 10000 cells/well for ASH-3 cells. A further 80 µl of the specific complete medium was added to each well. Cultures were pre-incubated for a period of 1 hr for the COLO cell line and 24 h for the HCT and ASH cell line to allow the cells attach. Thereafter, 20 µl of each of the pre-prepared, 10 x concentration of the respective drug concentrations were



pipetted into each of the corresponding experimental wells to make up a total volume to 200  $\mu$ l thus producing a 1:10 dilution (in well) of the drug concentration. After an incubation period of 7 days for the COLO cell line or 3 days for the HCT and ASH cell lines, MTT cell enumeration assays were performed as follows:

*MTT assay (Methods of Mossmann [96] with modifications):*

This assay is based on the reduction of yellow MTT into purple formazan crystals by metabolically active cells. This assay was used to quantitate the percentage of viable cells compared to untreated controls.

A volume of 20  $\mu$ l of a 5 mg/ml MTT solution in PBS was added to each well. Plates were incubated for a further 3 - 4 hours in 5% CO<sub>2</sub> at 37°C. Plates were then centrifuged at 500 *g* for 10 minutes before the supernatants of each well were carefully removed without disturbing the pellet. Pellets were washed with 150  $\mu$ l PBS and again the plates were centrifuged at 500 *g* for 10 minutes. The supernatant was again carefully removed before drying the plate overnight. The next day 100  $\mu$ l of DMSO was added to each well. Plates were gently shaken on a model VRN-200 shaker for at least an hour before they were read spectrophotometrically using a microplate reader (Bio-Tek instruments, ELx 800 UV) at 570 nm, using 630 nm as a reference. The absorbance values were used to determine the relative percentage of viable cells compared to the untreated controls.

### **5.3.2. Fixed molar ratio drug combination studies**

*Experimental design and procedures: COLO 320DM*

The following stock solutions were made up in DMSO: Riminophenazines (B663 & B4125) - 2 mM; Etoposide - 4 mM; Paclitaxel - 1 mM; Vinblastine - 0.5 mM.

Drug combination studies were performed in a manner similar to that described in the CalcuSyn software manual. As a first step, IC<sub>50</sub> values were estimated for each

of the drugs alone against COLO neoplastic cell cultures using various concentrations of drug after 7 days exposure, determining cell survival relative to untreated controls then using GraphPad Prism version 4 to plot a response curve from which the individual drug  $IC_{50}$  values were estimated. ETOP, PTX and VIN were then combined with either Riminophenazine: B663 or B4125 at the following arbitrary fixed molar ratios: 10:1, 5:1, 2:1, 1:1, 1:2, 1:5, 1:10 and tested for drug response over an appropriate concentration range.

To accomplish this, the highest desired concentrations (in well), of a particular ratio for a particular combination (e.g. 0.2:0.4  $\mu$ M, PTX: B663, 1:2) was multiplied by 10 and by 2 to compensate for the 1:10 dilution in well and for mixing equivalent volumes of each of the drugs making up the FRDC. Appropriate volumes of working solutions for each of the respective FRDC were made up in complete medium from stock solutions. From these working solutions, 8 further calculated serial dilutions were made to cover an expected dose response range.

Experiments were performed in triplicate at each concentration level (Table 5.1.) Absorbance values obtained after performing MTT assays were normalised relative to vehicle treated control (0.5% DMSO). The final concentration of DMSO in any well was less than 0.5% (v/v) to avoid any contribution of DMSO towards cytotoxicity. Dose response curves were plotted as percentage of vehicle control using GraphPad and the  $IC_{50}$  values calculated. Data was appropriately transformed and captured into CalcuSyn software. Using the software, the curves were fitted to linear models using the median effect equation allowing for CI values as a measure of synergy to be simulated at any  $fa$  value using the combination index equation. The dose reduction afforded by the different fixed-ratio drug combinations was expressed as the percentage reduction in  $IC_{50}$  value of PTX alone.

**Table 5.1. Example of a 96 well plate lay out showing the final concentration (in well) of two drugs (PTX and B663) alone as well as two representative FRDC**

	B663		Paclitaxel		5	6	1:1 (PTX:B663)			1:2 (PTX: B663)		
	1	2	3	4			7	8	9	10	11	12
<b>A</b>	4 $\mu$ M	4 $\mu$ M	0.2 $\mu$ M	0.2 $\mu$ M	0.5% DMSO Controls		0.2 $\mu$ M PTX 0.2 $\mu$ M B663		0.2 $\mu$ M PTX 0.4 $\mu$ M B663			
<b>B</b>	2 $\mu$ M	2 $\mu$ M	0.15 $\mu$ M	0.15 $\mu$ M			0.15 $\mu$ M 0.15 $\mu$ M		0.15 $\mu$ M 0.3 $\mu$ M			
<b>C</b>	1.5 $\mu$ M	1.5 $\mu$ M	0.1 $\mu$ M	0.1 $\mu$ M			0.1 $\mu$ M 0.1 $\mu$ M		0.1 $\mu$ M 0.2 $\mu$ M			
<b>D</b>	1 $\mu$ M	1 $\mu$ M	0.075 $\mu$ M	0.075 $\mu$ M			0.075 $\mu$ M 0.075 $\mu$ M		0.075 $\mu$ M 0.15 $\mu$ M			
<b>E</b>	0.75 $\mu$ M	0.75 $\mu$ M	0.05 $\mu$ M	0.05 $\mu$ M			0.05 $\mu$ M 0.05 $\mu$ M		0.05 $\mu$ M 0.1 $\mu$ M			
<b>F</b>	0.5 $\mu$ M	0.5 $\mu$ M	0.025 $\mu$ M	0.025 $\mu$ M			0.025 $\mu$ M 0.025 $\mu$ M		0.025 $\mu$ M 0.05 $\mu$ M			
<b>G</b>	0.25 $\mu$ M	0.25 $\mu$ M	0.01 $\mu$ M	0.01 $\mu$ M			0.01 $\mu$ M 0.01 $\mu$ M		0.01 $\mu$ M 0.02 $\mu$ M			
<b>H</b>	0.1 $\mu$ M	0.1 $\mu$ M	0.005 $\mu$ M	0.005 $\mu$ M			0.005 $\mu$ M 0.005 $\mu$ M		0.005 $\mu$ M 0.01 $\mu$ M			

#### *Experimental design and procedures: HCT-15*

*In vitro* experimentation with HCT-15 cultures were used as a proof of concept prior to initiating expensive animal studies. The requirement to proceed further was that the IC<sub>50</sub> of the FRDC must be significantly lower than that of PTX alone.

FRDC samples: 1 mg/ml PTX and 2.77 mg/ml B663, i.e. 1.17 mM PTX and 5.85 mM B663 (1:5 molar ratio) were prepared in 100% DMSO. Stock solutions (2 mg/ml) of PTX (2.34 mM) and B663 (4.22 mM) were prepared separately in DMSO and shipped via DHL (in a low temperature “Solution 9” packaging) at 2 - 8°C to Charles River, Michigan, USA as a pilot to the *in vivo* efficacy studies that were to follow.

The individual drugs were diluted with complete media to make starting stock solutions of 4000 nM and 2000 nM for the B663 and PTX respectively. Solutions were serially diluted 1:3 in complete medium to produce a range of concentrations (0.2 - 4000 nM and 0.1 - 2000 nM respectively). An aliquot of 100 µl of each drug concentration was added to 100 µl of cell suspension thus producing a 1:2 dilution in well to obtain the final testing concentration range.

Similarly, the FRDC was diluted in complete media to make a starting stock solution of 2000 nM PTX and 10000 nM B663 in combination. After consecutive 1:3 serial dilutions, the final concentration range tested in the wells were 0.5 - 1000 nM PTX in combination with 0.25 - 5000 nM B663 thus maintaining the fixed molar ratio of 1:5.

### **5.3.3. Assessment of additional ABC transporter inhibition**

The hypothesis that Riminophenazines inhibit the action of ABC transporters in general was evaluated by Ms. M. Finberg under the supervision of D. Koot. The purpose of such investigations was to establish Riminophenazines as true broad-spectrum resistance circumventers thus increasing the potential scope of the use of this class of drug.

#### *Experimental design and procedures: ASH-3*

For preliminary investigation, the intrinsic MRP expressing cell cultures were seeded in 96 well plates (10000 cells/well) and incubated for 24 hrs before the addition of test drug/s.

A checkerboard design was used with a varying final (in well) concentration of doxorubicin (MRP substrate) generally ranging from 0.1 – 2 µg/ml either alone or in combination with three fixed non-toxic concentrations of B663. As such, non-fixed-ratio drug combination experiments were used to assess the chemosensitizing action of Riminophenazines in an *in vitro* MRP expression model.

#### **5.3.4. Neoplastic specificity**

Primary human lymphocytes were used in comparison with COLO 320DM cells as an indicator of the cytotoxic specificity for normal versus neoplastic cells allowing for a specificity index to be calculated.

##### *Experimental design and procedures: Lymphocyte isolation and bioassay*

Lymphocytes were isolated from healthy human volunteers through the following procedure: 30 ml heparinized blood (0.1 ml heparin / 1 ml blood) was carefully loaded onto 15 ml Histopaque followed by centrifugation at 500 *g* for 25 min. The top plasma layer was removed and the lymphocyte /monocyte layer transferred to sterile 50 ml centrifuge tubes; the tubes were filled with RPMI 1640 medium and again centrifuged at 500 *g* for 15min; the supernatant was discarded and the tube again filled with RPMI media before centrifugation at 500 *g* for 10 min; After again discarding the supernatant, the tube was filled with sterile, cold ammonium chloride and placed on ice for 10 min before once more centrifuging at 500 *g* for 10 min, discarding the supernatant, washing the pellet with RPMI and finally re-suspending the cells in 1 ml of RPMI supplemented with 10 % FCS.

The isolated lymphocyte concentration was determined using a haemocytometer and appropriately diluted with full media so as to attain a final seeding concentration of 20000 cells per well. After pre-incubation for a period of 1 hr, 20  $\mu$ l of various concentrations of each of the drugs (B663, B4125, ETOP, PTX and VIN) were added so as to span the expected dose response range. As was for the COLO 320DM neoplastic cell cultures, 20  $\mu$ l of an appropriate DMSO percentage was added to all control wells upon which results could be normalized. Cultures were incubated in 5% CO<sub>2</sub> at 37 °C for 3 days before MTT assays were conducted.

#### **5.3.5. Ethical considerations**

Research ethics committee approval for the use of primary human lymphocytes was obtained (Project number 164/02 of the Research Ethics Committee of the Faculty of Health Sciences, University of Pretoria).

## 5.4. Results

### 5.4.1. COLO 320DM neoplastic cell cultures

Dose response curves (Figure 5.1.) were produced for each drug alone as well as for selected fixed molar ratio combinations (10:1, 5:1, 2:1, 1:1, 1:2, 1:5, 1:10) of either B663 or B4125 with ETOP, PTX or VIN. IC<sub>50</sub> values were estimated from triplicate experiments using Graph Pad software for all of the drugs alone (Table 5.2). As a measure of neoplastic specificity the drugs were also screened against primary human lymphocytes. Specificity (normal/neoplastic) indexes of 1.26, 1.99, 0.62, 1.2 and 4.71 were calculated for B663, B4125, ETOP, PTX and VIN respectively.

CalcuSyn software was used to perform median effect analysis and generate CI index for actual and simulated *fa* values. The linear correlation coefficient, *r*, of the respective median effect plots was found to be greater than 0.90 for all drug combinations tested suggesting good fitting to the model.

The extent of drug interaction (CI) was expressed at a nominal fraction affect (*fa*) level of 0.5 (Table 5.3.). CI values below 1, denoting synergy were found for all tested drug ratios of both Riminophenazines with VIN. Synergy tended to increase as the relative proportion of VIN increased. Concerning Riminophenazine combinations with ETOP, it is apparent that the highest degree of synergy is present at the highest proportion of Riminophenazine and that this positive interaction steadily decreases, finally resulting in antagonism at high ETOP content ratios. A similar dynamic interaction was observed for Riminophenazine combinations with PTX.

The greatest synergy was observed for PTX:B663 (1:10) with an impressive CI of 0.19 which is qualified as strong synergism in the CalcuSyn software manual. This synergy is superior to that obtained for B4125 in spite of B4125 gaining a ~40% improvement in the IC<sub>50</sub> value. This could be attributed to greater inhibition of Pgp

as result of a mechanism separate to that inducing cell death or could simply be ascribed to the increased hydrophilicity of the TMP derivative.

At this stage of development (and with due consideration to the synergy results attained and the regulatory status of the compounds), the world's best-selling anticancer drug to date - Paclitaxel (PTX), was elected as the lead SC for development in a resistance-circumventing, synergistic combination with the already approved Riminophenazine, Clofazimine (B663).

CI values for PTX:B663 ratios with a greater proportion of B663 were found to be synergistic ( $CI < 1$ ) at all simulated  $f_a$  levels (0.1 - 0.9). The trend is for synergy to be greater at lower  $f_a$  levels (Figure 5.2).

This observed synergy is responsible for the large % reduction in the  $IC_{50}$  value of PTX (Figure 5.3.). An increasing dose response was observed with increasing B663 levels. The  $IC_{50}$  value was reduced 69% from 44.2 nM (for PTX alone) to 13.5 nM when used in a FRDC of 1:5 with B663. This must be taken in the context that the  $IC_{50}$  value of B663 is  $>1000$  nM clearly demonstrating that B663 is sensitizing the cultures to the action of PTX through inhibition of efflux pumps and is not necessarily having a direct antiproliferative effect at these concentrations

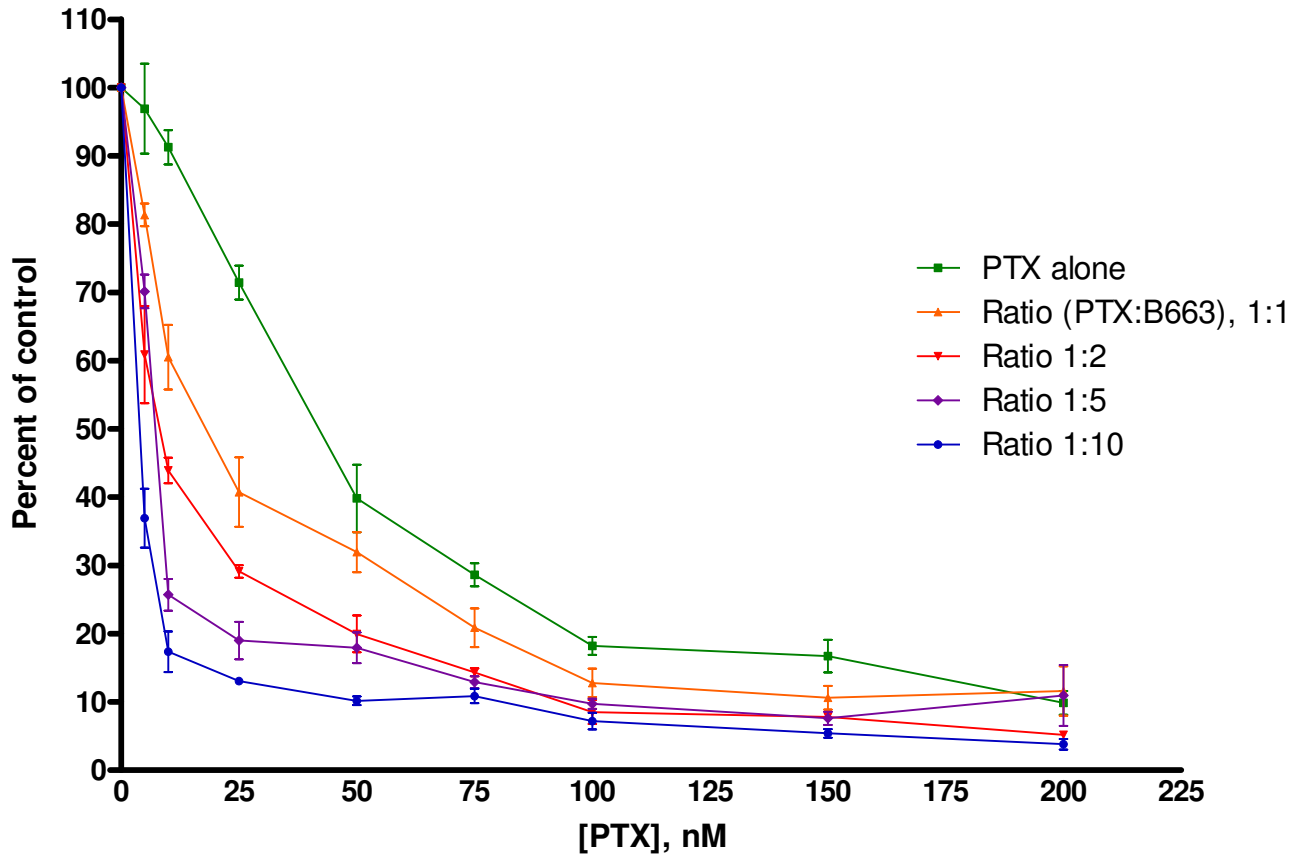


Figure 5.1. The antiproliferative effect of selected fixed ratio drug combinations (FRDC) of PTX and B663 against the COLO320DM cell cultures





**Table 5.2. Mean IC<sub>50</sub> values (nM) of all the tested drugs against COLO neoplastic cell cultures and PHA stimulated primary human lymphocytes**

	<b>B663</b>	<b>B4125</b>	<b>ETOP</b>	<b>PTX</b>	<b>VIN</b>
<b>COLO 320DM</b>	1353	800	1370	44	7
<b>Normal Lymphocytes</b>	1700	1594	850	53	33

**Table 5.3. Summary of the Combination Index (CI) attained for various fixed ratio drug combinations (FRDC) of Standard Chemotherapeutic (SC) with either of the lead Riminophenazines at a selected simulated *fa* of 0.5**

<b>CI index values at <i>fa</i> 0.5</b>						
<b>Molar ratio (SC: Rimino)</b>	<b>B663</b>			<b>B4125</b>		
	<b>Etop</b>	<b>PTX</b>	<b>Vin</b>	<b>Etop</b>	<b>PTX</b>	<b>Vin</b>
<b>10:1</b>	1.04	1.63	0.53	1.37	1.68	0.59
<b>5:1</b>	0.94	1.32	0.72	1.37	1.19	0.53
<b>2:1</b>	0.79	1.2	0.75	1.14	1.34	0.77
<b>1:1</b>	0.54	0.76	0.95	0.86	2.24	0.77
<b>1:2</b>	0.54	0.43	0.89	0.56	0.75	0.91
<b>1:5</b>	0.65	0.39	0.95	0.67	0.58	0.83
<b>1:10</b>	0.66	0.19	0.91	0.61	0.47	0.86

 Synergism (CI<1)  
 Antagonism (CI>1)

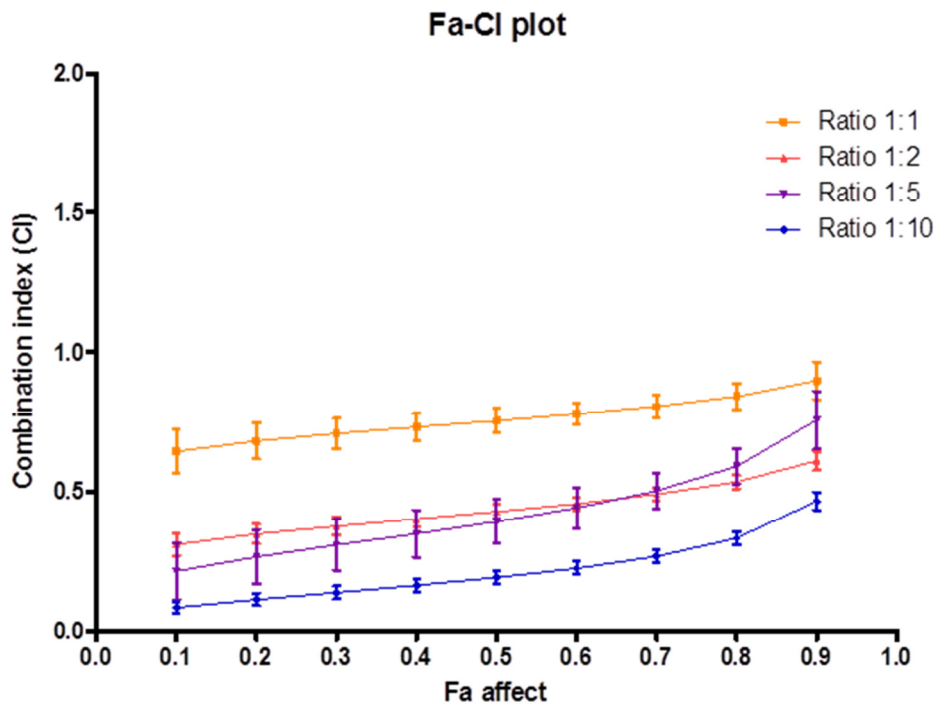


Figure 5.2. Simulated CI index values for selected FRDC of PTX and B663 as a function of the fraction affected (*fa*)

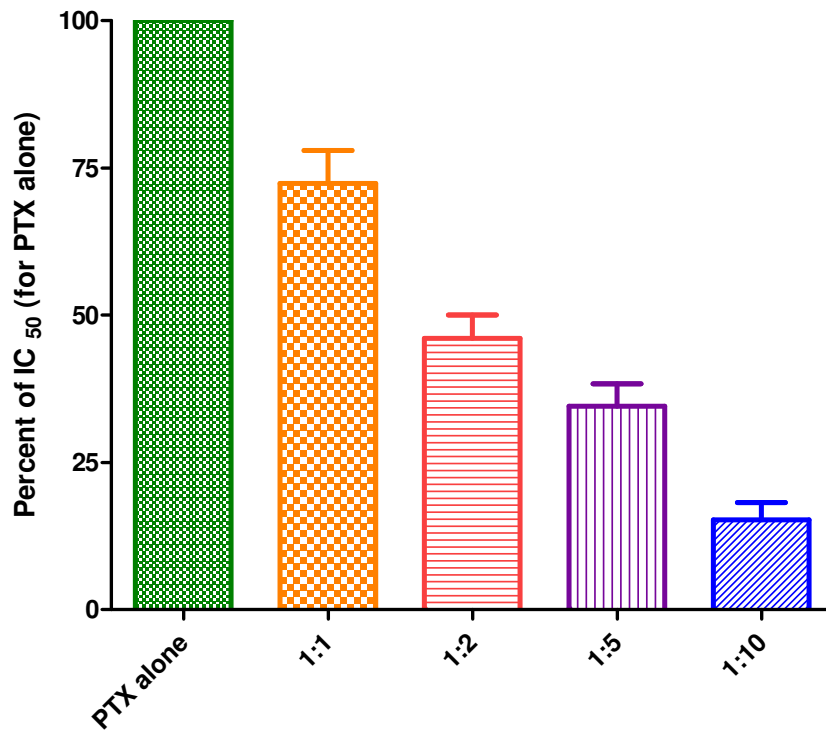


Figure 5.3. Normalised change in the IC<sub>50</sub> of PTX against COLO 320DM cultures when used in fixed ratio combinations with B663

### 5.4.2. HCT-15 neoplastic cell cultures

For strategic and practical reasons, *in vitro* experiments on the drug resistant HCT-15 neoplastic cell cultures were outsourced to Charles River prior to initiating expensive *in vivo* efficacy studies using implanted HCT-15 cells as a proof that the FRDC does indeed offer antiproliferative benefit. Dose response curves against HCT-15 cells in culture (Figure 5.4.) were produced for PTX alone and for a FRDC of PTX: B663 (1:5) as this was the achieved encapsulation ratio in the NDDS (Chapter 6) used in the *in vivo* study. Similar to the cytotoxicity results observed for COLO 320DM cell cultures, the FRDC showed a large reduction (Figure 5.5) in the dose required to inhibit cell proliferation by 50% ( $IC_{50}$ ) compared to the cells treated with PTX (alone).

The  $IC_{50}$  value was reduced by 72%, from 123 nM for PTX alone to 34.5 nM for the FRDC with B663 (Table 5.4). The  $IC_{50}$  of B663 was found to be >2000 nM. This illustrates that HCT-15 cultures are less sensitive (more resistant) than COLO 320DM cells and many other intrinsically resistant tumours (Appendix B). It is evident that a clear chemosensitizing affect is seen at concentrations of B663 that are not directly cytotoxic.

As part of Charles River's standard assay procedure, cisplatin was used as an intra-assay quality control confirming validity of the assay compared to previous experiments. The relatively high  $IC_{50}$  value for cisplatin demonstrates the highly resistant nature of these HCT-15 cells for numerous drugs through diverse mechanisms.

**Table 5.4. Mean  $IC_{50}$  value (nM) of various drugs against HCT-15 neoplastic cell cultures**

	<b>B663</b>	<b>PTX</b>	<b>FRDC (PTX:B663, 1:5)</b>	<b>Cisplatin</b>
<b>HCT-15</b>	>2000	123	34.5	10600

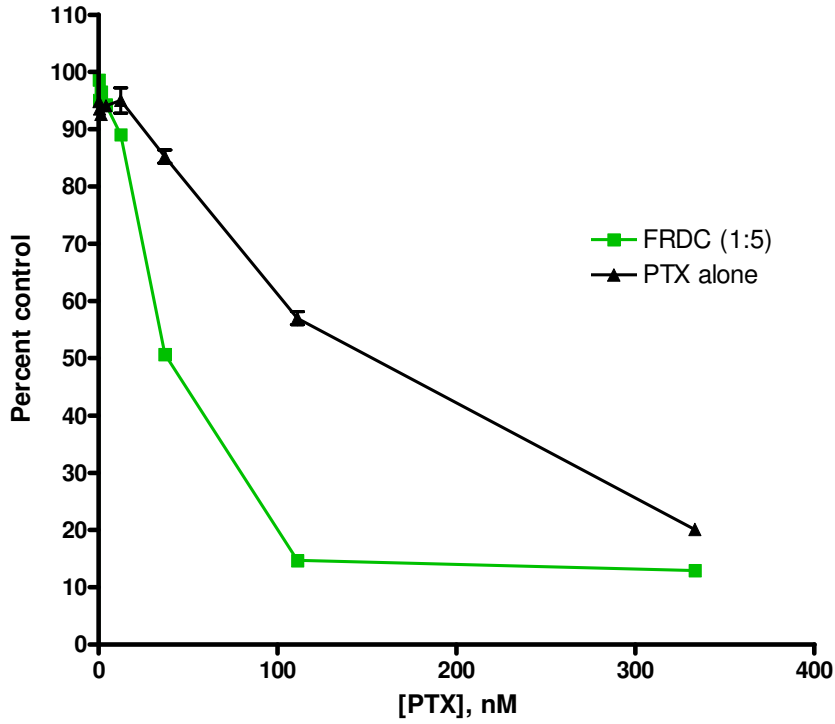


Figure 5.4. Dose response curves for PTX (alone) and the FRDC (PTX:B663, 1:5) against HCT-15 neoplastic cultures

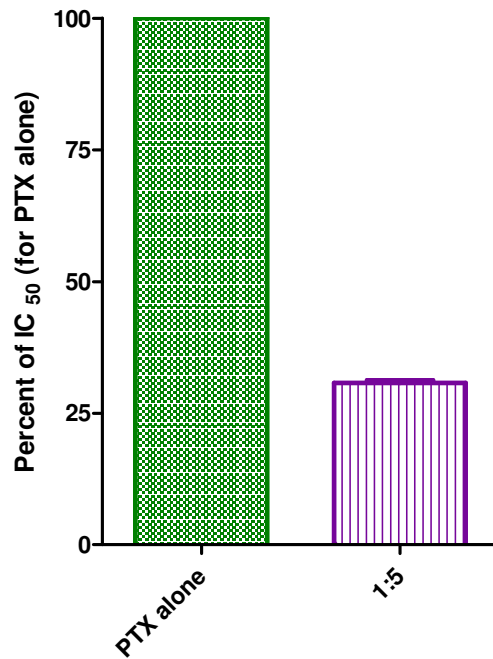


Figure 5.5. Normalised change in IC<sub>50</sub> value of PTX against HCT-15 cultures when used in a fixed ratio combination with B663

### 5.4.3. ASH-3 cell line

The MRP expressing ASH-3 cell line was used to assess the ability of three non-cytotoxic concentrations of B663 to potentiate the antiproliferative effect of DOX in a checkerboard manner. The antiproliferative effect of Doxorubicin was shown to increase as the constant dose (non-fixed ratio) of B663 increased (Figure 5.6.). This is strongly indicative that Riminophenazines are inhibiting the efflux action of the MRP pump.

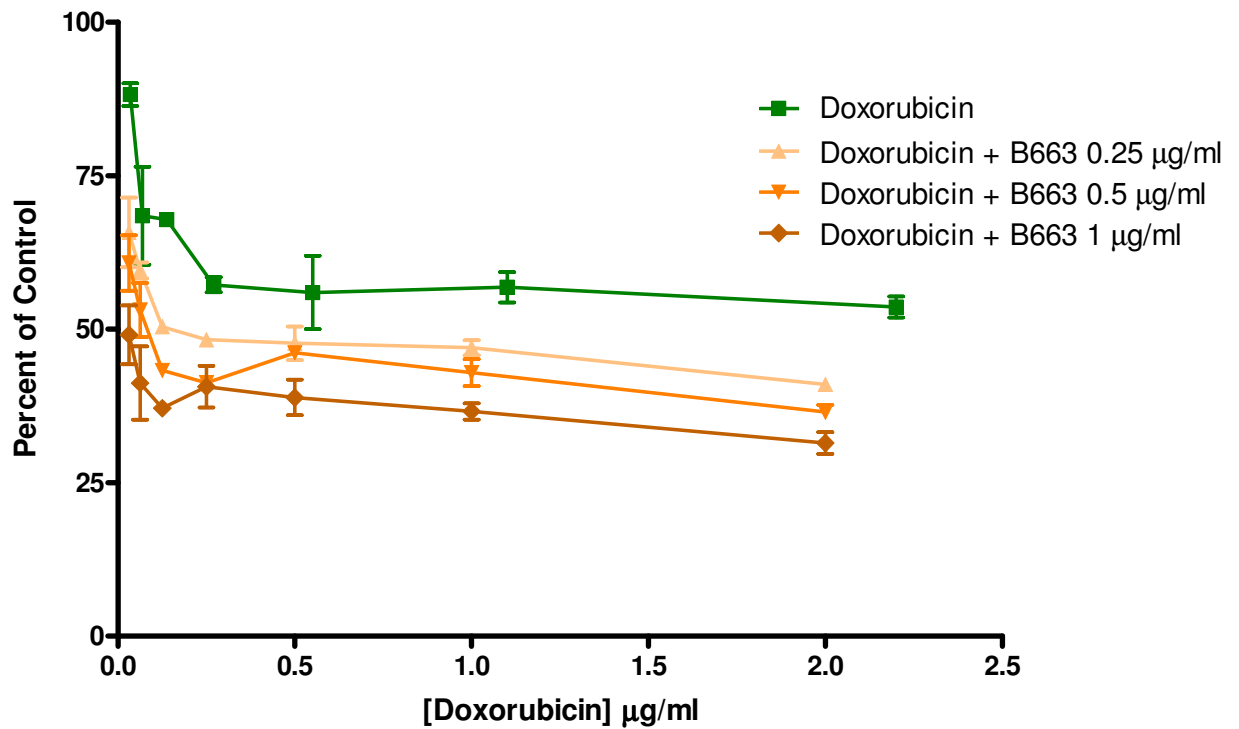


Figure 5.6. The antiproliferative effect of doxorubicin with and without various constant concentrations of B663 against ASH-3 cell cultures

## 5.5. Discussion and conclusion

For good reason, the evaluation of potential anticancer drugs begins with *in vitro* bioassays prior to pre-clinical animal and finally clinical human studies. This allows the cytotoxicity of various new chemical and biological entities as well as novel combinations thereof to be investigated quickly in a controlled manner at various concentrations against several different cell types and critically assessed thereby justifying the expense of studies that are to follow. *In vitro* bioassays have the advantage of requiring minimal amounts of drug substance and are unaffected by pharmacokinetic effects - this is however, a reductionist point of view and does not consider the effect of the body (absorption, distribution, metabolism and excretion) on the drug/s.

With the advent of programmable liquid handlers, automated high throughput screening (HTS) is facilitated and a huge opportunity exists to screen innumerable drug combinations *in vitro* quickly. This scale of screening is not ethically acceptable, nor rational using *in vivo* models because of the large number of animals required to obtain a statistically valid result and the enormity of possible combinations. [97] Nevertheless, *in vivo* assays employing a whole organism are always required to substantiate findings prior to human trials and to investigate pharmacokinetics, dose ranging as well as to identify organ accumulation and possible adverse effects. Furthermore, the functionality of the dosage form (formulation) needs to be evaluated *in vivo*. Synergistic drug combinations are both ratio and dose level dependent and therefore need to be controlled both spatially and temporally to achieve the best possible interaction.

In this study, for the first time it has been demonstrated that Riminophenazines act synergistically ( $CI < 1$ ) in combination with etoposide, paclitaxel and vinblastine against Pgp expressing COLO 320DM neoplastic cell cultures. It is therefore reasonable to expect that B663 or B4125 could be used (with benefit) within chemotherapeutic regimes involving these Pgp substrates. After considering the potential clinical value, the results of the initial experiments, the physicochemical characteristics and particularly the wide spectrum of use, PTX was selected as the

combination partner for the already registered B663. This combination was further evaluated in an additional neoplastic cell culture and ultimately co-formulated within a NDDS (Stage II) in preparation for *in vivo* investigations (Stage III).

Importantly, synergy affords a reduction in the dose required to produce a particular fractional effect. The elected FRDC of 1:5 (PTX:B663) produced roughly a 70% reduction in the IC<sub>50</sub> value compared to PTX alone in both of the tested colon carcinoma cell lines, each displaying different levels of drug resistance. This strongly attests to the inhibition of Pgp by B663 increasing the intracellular (active) concentration of PTX making PTX far more efficacious. Over and above the direct antineoplastic effect (at higher Riminophenazine concentrations), there is clearly therapeutic benefit to be gained in terms of PTX dose reduction afforded and therefore reduced drug related adverse effects.

In all three neoplastic cell cultures tested, the synergistic effect was shown to be dose dependent for B663 and observed at concentrations at which little to no direct cytotoxic effect was detectable when used alone. The distinction between potentiation through chemosensitization and true synergy through both drugs possessing a direct effect can however be debated. Regardless of the distinction (which would require a statement of the concentration used), true quantifiable synergistic interactions (defined as greater than additive activity regardless of what model) were attained through the well-established combination index methods of Chou. [94]

Based on IC<sub>50</sub> values observed for the tested drugs, PTX is roughly 30 fold more cytotoxic than B663 regardless of the cell line used. This implies that a ratio near 1:30 (PTX:B663) would be required before the expected direct cytotoxic action of B663 could be observed over and above the chemosensitizing effect. This has practical bearing in terms of the encapsulation efficacy required within delivery systems, especially when considering the limitations of IV dosing volumes and infusion rates in small animals. This is not to say that these concentrations (of B663) are not clinically achievable particularly if administered independently via the oral route.

Results obtained using the MRP expressing ASH-3 cell line strengthens the case for the use of Rimonophenazines as broad-spectrum resistance circumventers and supports their use against MRP and possible all ATP dependent transmembrane efflux pumps. This indirect way of testing drug efflux inhibition should however be supplemented by additional quantitative assays determining the concentration of the an ABC transporter substrate intra- and extracellularly in the presence and absence of Rimonophenazines so as to confirm these findings.

Numerous other resistant neoplastic cell types with diverse resistance mechanisms and different sensitivities to Rimonophenazines should be investigated in addition to those described in Appendix B. Unfortunately, neoplastic cell cultures with well understood and well reported resistance mechanisms are not readily commercially available. Induction of acquired resistance in-house through clonal selection is laborious and does not necessarily achieve a stable phenotypic (efflux pump) expression. For this reason, future work might do well to explore the use of *ex vivo* patient explants that will truly represent the extent of natural diversity of the disease. Links to personalising a specific FRDC through HTS to a particular patient's cancer phenotype could rationally be pursued. An innovative means whereby this personalised (tailored) approach could be evaluated and the processes optimised is through the use of cancer burdened domesticated animals that will more accurately represent the natural resistance diversity of cancer.



## 6. Development of novel Nanoparticulate Drug Delivery Systems (NDDS)

### 6.1. Introduction

To focus on cancer where blatantly cytotoxic drugs with small if any therapeutic margins are classically employed, the issue of specific pharmacokinetic distribution to tumourous tissue is of paramount importance to increase efficacy and decrease systemic toxicity. The great need for novel innovative NDDS is highlighted by the knowledge that many treatment failures are attributed to inadequate drug delivery alone, regardless of the actual effectiveness of the drugs. [98] The use of intelligent delivery systems is imperative to realize the full potential of chemotherapy. DeGeorge *et al.* [84] has identified several advantages afforded by drug delivery systems, including: targeting to tumour; minimization of systemic toxic effects; prolongation of therapeutic drug concentrations; practical administration of highly hydrophobic drugs and membrane transport of highly hydrophilic drugs into the tumour cells.

Of importance is that NDDS can passively or actively compensate for pharmacokinetic profiles that are not conducive to effective therapy. Through the ability to dictate pharmacokinetics and reliant upon stable co-encapsulation of drug combinations, NDDS embody the enabling technology that allows ratio-dependent synergistic FRDC identified *in vitro* to be translated into *in vivo* applications. [99] FRDC consisting of more than two drugs or in combination with biological agents is conceivable.

The ultimate success of any novel NDDS is dependent upon various dynamic factors (many unforeseeable). In truth, these delivery systems are often assembled empirically via convention through identification of what ratio of drug and amphiphile combine well to produce nanoparticles of the desired characteristics (encapsulation efficacy, size and zeta potential) and not through full pre-determined thermodynamic understanding. Drug encapsulation efficacy is

inextricably dependent upon the drugs (structure), the type of amphiphile used and their respective ratios. [80]

The choice of copolymer structure or mixture of amphiphiles used considering the HLB may well need to be reviewed in order to accommodate the concentration of a particular drug/s (drug-excipient compatibility) in aqueous solution. Additional considerations for choice of amphiphile include drug encapsulation efficacy, the attained particle size, zeta potential (electrostatic stability), toxicity as well as the cost and regulatory status.

In this study, a diversified portfolio of NDDS was investigated to increase the probability of success. With due consideration to the stated TPP (Chapter 3) and available resources, the portfolio of NDDS under development included:

#### A) *Riminocelles*<sup>TM</sup>

The primary aim of this stage of development was to develop and characterise a passively tumour targeting NDDS that co-encapsulates a synergistic FRDC of PTX and B663 (identified in Chapter 5) at clinically relevant concentrations. Knowing that both PTX and B663 are highly lipophilic, the simplest choice for co-formulation was a micelle with a hydrophobic core.

In terms of composition, Riminocelles can be described as a binary mixed lipopolymeric micellar system (Figure 6.1.) assembled from a mixture ( $S_{mix}$ ) of the commercially available amphiphiles, DSPE PEG 2000 (Figure 6.2.) and phosphatidylcholine (Figure 6.3.) as the co-surfactant.

Advantageously, such PEGylated diacyl lipids are known to self-assemble at very low critical micellar concentration (CMC) values making them very useful for prolonged systemic circulation - a requirement for successful passive tumour targeting via the EPR effect. [100] Importantly, a low CMC value is required to ensure that the assembled system can sustain the dilution encountered upon IV administration. Lipopolymeric micelles constructed from PEGylated diacyl lipids are

thought to possess superior stability compared to conventional polymeric micelles owing to greater hydrophobic interactions due to the presence of two highly lipophilic fatty acyl chains. [101] Furthermore these amphiphiles are non-toxic and are internationally approved by regulatory bodies for parenteral administration. [102]

As reviewed by Torchilin in 2005 [103] numerous studies have described the assembly and encapsulation of various drugs within micelles constructed from DSPE PEG 2000. Strangely and despite several authors [77, 100, 104, 105, 106] having described the encapsulation of PTX within such micelles (as will be discussed in greater detail), to date there have been no reports concerning *in vivo* efficacy evaluations of PTX loaded DSPE PEG 2000 micelles - In fact, to the extent of the authors literature review, only Tang *et al.* [107] has reported any *in vivo* anticancer efficacy data using DSPE PEG 2000 micelles, in that case loaded with doxorubicin.

However, the *in vivo* passive targeting qualities (longevity within circulation) have been long known and were thought to be well established by Lukyanov *et al* [108] who reported that radio-labelled, drug-free DSPE PEG 2000 micelles possess long-circulating properties (plasma half-life of 2 hours) and to preferably accumulate in tumours compared to muscle. Similarly, Lukyanov *et al.* [109] reported on the increased tumour accumulation by drug-free immuno-micelles (MAb conjugated distally to PEG on the surface of the micelles).

Phosphatidylcholine as a co-surfactant in various proportions has been described as a successful means to increase the encapsulation efficacy of PTX within mixed lipopolymeric micelles. [77, 102, 104] Krishnadas *et al.* [104] identified a molar ratio of 10:1 (DSPE PEG:PC) as the optimal mixed micellar state. The general consensus is that the increased solubility of PTX within mixed (PC) micelles is as result of the higher hydrophobic content as a consequence of two long diacyl chains, [110] although this does not consider the influence of the charged head portion.

Amphiphiles are added to a mixture to reduce the interfacial tension, promoting assembly through hydrophobic interactions and to provide stability through electrostatic and/or steric repulsive forces. Commonly, a surfactant mixture ( $S_{mix}$ ) is used that allows additional steric flexibility, enabling conformational rearrangements and the formation of spherical droplets preferably as opposed to various liquid crystalline and mesomorphic phases. [111]

In this study, the thin film hydration method was used to encapsulate PTX and B663 within the hydrophobic core of lipopolymeric micelles. The formulation strategy included optimising both the drug: drug ratio as well as the  $Drug_{total}: S_{mix}$  ratio prior to optimising the amphiphile wt. %, represented as the  $[S_{mix}]$  in mg/ml required within the binary system with water to successfully solubilise  $>1$  mg/ml PTX.

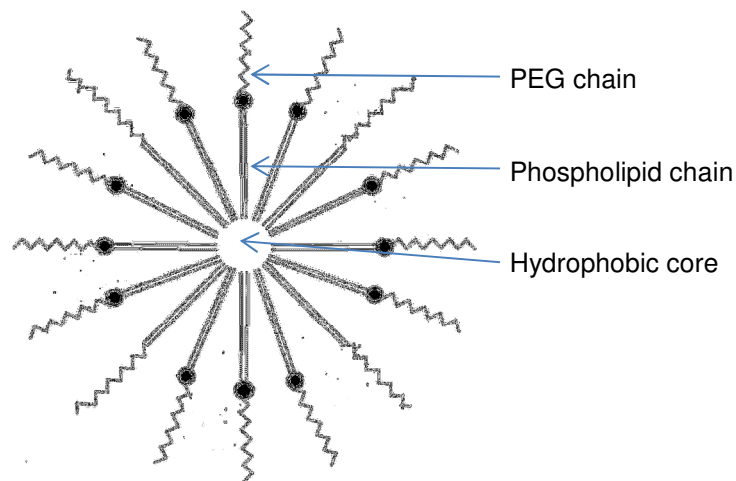


Figure 6.1. Depiction of a lipopolymeric micelle

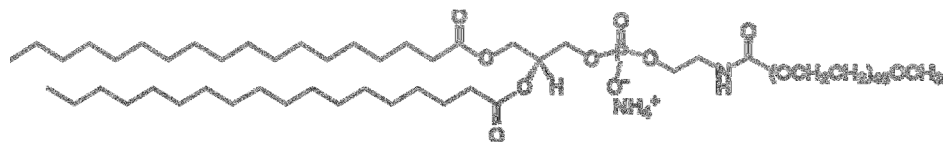


Figure 6.2. Chemical structure of DSPE-PEG 2000

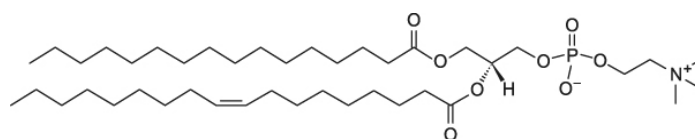


Figure 6.3. Chemical structure of a typical phosphatidylcholine

### *B. RiminoPLUS™ imaging*

A further aim of this study was to explore the development of a multifunctional (theranostic) NDDS for use in diagnosis and treatment. Efforts were directed towards encapsulating Lipiodol (an oil based contrast agent) within a nano-sized, oil-in-water (o/w) emulsion suitable for IV administration that could be used as both an imaging agent and as a carrier of multiple drugs. The RiminoPLUS imaging system is a pseudoternary system ( $S_{mix}$ , oil and water) composed of DSPE PEG 2000, phosphatidylcholine, Lipiodol and water.

Emulsions are semi-stable mixtures of two immiscible liquids with one phase being dispersed as droplets within the other continuous phase. Emulsions are (pseudo)ternary systems consisting of oil, water and surfactant acting as the interfacial stabilizing film. Various possible assemblies can arise from mixing different ratios of  $S_{mix}$ , oil and water. [112] Such systems can be mapped through the use of phase diagrams.

In literature a distinction has been made between nanoemulsions and microemulsions both of which are nano-sized and appear translucent [113] (optically isotropic) as result of the particle size being smaller than the wavelength of visible light (below 200 nm). [111] Microemulsions are thermodynamically stable and form spontaneously, whereas nanoemulsions (also referred to as miniemulsions or sub-micron emulsions) are kinetically metastable and generally require considerable energy input for their preparation. [113-117] Kinetically stable nanoemulsions that possess adequate electrostatic and steric stability (interfacial affinity interactions) [118] have been described as approaching thermodynamic stability. [116]

Emulsification methods can be categorized as either low energy or high energy emulsification. Low energy emulsification techniques make use of inherent chemical potential of the components to spontaneously form emulsions as result of phase transitions (inversion from w/o to o/w) produced through changing the systems composition at constant temperature or through altering the temperature

at constant composition - the so called phase inversion temperature method. [119] The preparation method in terms of the order of adding phases (water added to oil phase or vice versa) can influence the final properties of the emulsion obtained. [114] Spontaneous emulsification is dependent upon favourable physicochemical interactions between the specific oil and surfactant components used. [116]

High energy emulsification techniques require the input of external energy for formation. Commonly ultrasonication, high-shear mixing or high pressure homogenisation is used to achieve sub-micron sized emulsions. Importantly, high energy emulsification methods allows for a greater variety in composition as the free energy inherent within a particular system is not required to promote formation [119].

An emulsion for intravenous administration by definition must be stable and maintain particle size upon the dilution encountered after IV injection. For this reason, non-equilibrium (metastable) nanoemulsions which unlike microemulsions can be diluted without change in droplet size are considered preferable. [111, 113, 118, 120]

In this study, the emulsification strategy initially employed the aqueous titration method affording visual observations of phase transitions, consistency and possible spontaneous emulsification (as evidenced by optical isotropy) whilst titrating along various Oil:  $S_{mix}$  ratios / “tie-lines” represented in a ternary phase diagram (Figure 6.4.). After dilution to 90% water (w/w) all mixtures (respective Oil:  $S_{mix}$  ratios) were ultrasonicated and again visually observed for optical isotropy before conducting thermodynamic stability assessments and size determinations of single phase dispersions only.

The intent was not to exhaustively classify the various conformations (micro and nanostructural characteristics) produced at various component compositions within the ternary phase diagram but rather to quickly and efficiently identify a nano-sized emulsion suitable for parenteral administration. In such a stream-lined approach, special interest was paid only to the water-rich region (in which parenterally

suitable, nanoemulsion formulations are deemed feasible). Following a resource sparing strategy, PTX as the combination drug partner for B663 was not included in these initial experiments.

### *C. PVP-PVAc polymeric micelles*

PVP (Polyvinylpyrrolidone) is a cyclic amine based water-soluble polymer with characteristics similar to PEG. [102, 121] It can be used to impart stealth properties in circulation through immune evasion. Through a strategic alliance with Stellenbosch University, Polymer Science Institute, Ms. N. Bailly developed a B663 loaded PVP-PVAc polymeric micelles under the supervision of Prof. B. Klumperman. The novel amphiphiles synthesized have great potential for further development.

## **6.2. Materials**

### *Chemicals and reagents*

For the pilot study a 1 g sample of LIPOID PE 18:0/18:0-PEG 2000 (1, 2-distearoyl - *sn*- glycerol- 3- phosphatidylethanolamine - *N* - [ methoxy (polyethylene glycol) - 2000] - DSPE PEG 2000), (Figure 6.2.) and 50 g sample of LIPOID S 75-3 Phosphatidylcholine, (Figure 6.3.) were generously provided by Lipoid GmbH (Ludwigshafen, Germany).

Lipiodol® Ultra-Fluid (Guerbet, France) was purchased from Axiam Radiopharmaceuticals (JHB, SA) and stored in the dark at room temperature.

HEPES (4-(2-Hydroxyethyl) piperazine-1-ethanesulfonic acid) and Sodium salicylate were purchased from Sigma Aldrich and freshly prepared as solutions in water before successive experiments.



## 6.3. Methodology

### 6.3.1. Development of Riminocelles™

*Assembly procedures:*

Stock solutions of DSPE PEG 2000 and PC were typically prepared to 100 mg/ml and 10 mg/ml respectively in  $\text{CHCl}_3$ . PTX and B663 stock solution were made up to 0.5 mg/ml in MeOH. Stock solutions were stored in air tight glassware at  $-20^\circ\text{C}$ .

In pilot studies, a checkerboard layout using 96 well plates were used to establish the optimal formulation. B663:PTX (w/w) ratios of 1:0, 5:1, 10:1, as well as Drug<sub>total</sub>: S<sub>mix</sub> (w/w) ratios of 1:5, 1:10, 1:20, 1:50 were investigated for the optimal composition. The S<sub>mix</sub> (DSPE PEG 2000: PC) ratio was kept constant at 97:3 (w/w).

To do this practically and simply, the S<sub>mix</sub> weight used for each of the mixtures was kept constant. A S<sub>mix</sub> weight of 5 mg was the minimum scale required in order to produce sufficient volume (>1.5 ml) of the desired S<sub>mix</sub> concentration permitting syringe filtration and servicing subsequent characterization procedures.

Calculated volumes of drug stock solutions were added to individual pre-weighed Büchi flasks to produce each of the desired ratios (Table 6.1.). The solvents were evaporated off under reduced pressure at temperatures below  $40^\circ\text{C}$  using a rotary evaporator. The dried films were desiccated overnight and subsequently weighed to ensure mass balance. Thereafter all of the thin films were hydrated with 1.728 ml of 10 mM HEPES with the aid of a water bath sonicator (Branson) to produce a final DSPE PEG 2000 (MM 2806 g/mol) concentration of 1 mM. Finally the dispersions were syringe filtered using a Minisart® SRP (25 mm), 0.2  $\mu\text{m}$  PTFE membrane (EO sterilized) filter to remove unencapsulated drug. In further small scale (sparing expensive PTX) experiments, centrifugation as opposed to filtration was used as an effective means of removing unencapsulated drug.



**Table 6.1. Workflow detailing the actual weights of each component used in the pilot study producing the desired ratios**

B663:PTX (w/w)	Drug <sub>total</sub> : S <sub>mix</sub> (w/w)	B663 (µg)	PTX (µg)	DSPE (µg)	PC (µg)
1:0	1:50	100	0	4850.0	150.0
	1:20	250	0	4850.0	150.0
	1:10	500	0	4850.0	150.0
	1:5	1000	0	4850.0	150.0
5:1	1:50	83.3	16.7	4850.0	150.0
	1:20	208.3	41.7	4850.0	150.0
	1:10	416.7	83.3	4850.0	150.0
	1:5	833.3	166.7	4850.0	150.0
10:1	1:50	90.9	9.1	4850.0	150.0
	1:20	227.3	22.7	4850.0	150.0
	1:10	454.5	45.5	4850.0	150.0
	1:5	909.1	90.9	4850.0	150.0

*Characterisation procedures:*

### Drug encapsulation

After assembly and filtration of the various NDDS, a 20 µl aliquot was taken, diluted into linear dynamic range of the instrument with MeOH, transferred to vials and quantified using the optimised and validated LC-MS/MS method (Chapter 8). Both encapsulation efficacy and the percentage of drug weight in the system were determined via the respective calculations:

$$\% \text{ Encapsulation} = \text{drug encapsulated} / \text{drug loaded (w/w)} \times 100$$

$$\text{Drug loading index} = \text{total drug encapsulated} / (\text{amphiphile} + \text{total drug encapsulated}) \times 100$$

After preliminary characterization and establishment of the optimal formula, the effect of  $S_{\text{mix}}$  concentration (within the binary system with water) on the encapsulation efficacy of the two drugs was assessed thus identifying the lowest amphiphile concentration required to effectively solubilize PTX at clinically relevant concentrations (>1 mg/ml). Encapsulation efficacy was assessed at final  $S_{\text{mix}}$  concentrations of 5, 10, 20 and 40 mg/ml.

### Size and Zeta potential

Various formulations were assessed through dynamic light scattering (DLS) / photon correlation spectroscopy and laser Doppler electrophoresis using a folded capillary cell - DTS1060 (Malvern Instruments) to determine the hydrodynamic diameter and the zeta potential respectively using a Zetasizer Nano ZS (Malvern Instruments). Typically 3 independent measurements of 60 seconds or longer were performed per sample to establish measurement repeatability. Dependent on drug loading, typically 50 µl aliquots were diluted further with 0.2 µm filtered, deionised water (typically 2 ml) to ensure that the scattering properties of the sample achieved a suitable intensity as indicated by the average sample count rate.

The following settings were used: Material - PEG polymer; Refractive index (RI) - 1.5; Dispersant - H<sub>2</sub>O; Dispersant RI - 1.330; Viscosity (cP) - 0.8872; Measurement temperature - 25 °C.

### Transmission Electron Microscopy (TEM)

After optimisation of the formulation in terms of drug encapsulation, particle size and zeta potential, the lead formulation was assessed by TEM using a Phillips 301 Multipurpose, 100 kV TEM, equipped with a eucentric goniometer stage and a heating holder. TEM was performed at the Microscopy and Microanalysis Laboratory (University of Pretoria). Briefly, an aliquot of the 1 mg/ml PTX Riminocelle solution was diluted 1:100 in water and a drop placed on a carbon film coated on a copper grid before drying at room temperature and subsequent observation.

### CMC determination

Experimentally CMC values are determined by plotting a selected physicochemical property that changes upon micellization (e.g. UV absorption, fluorescence emission, electrical conductivity, viscosity, surface tension etc.) as a function of amphiphile concentration. An abrupt change in the response slope represents self-association and thus indicates the CMC value. Determination of CMC values can thus be ambiguous and dependent upon how sensitive the measured property is to micelle formation. [122]

A UV spectrophotometric method employing the inherent dye quality of Riminophenazines was used to estimate the CMC value:

From CHCl<sub>3</sub> stock solutions, a fixed weight (typically 50 µg) of B663 was mixed with various weights (0.0004 – 0.4 mg/ml) of S<sub>mix</sub> in clean glass test tubes. Solvents were evaporated off under vacuum using a Centrivap at <40 °C and subsequently reconstituted in 10 mM HEPES to a constant volume (typically 4 ml) thereby obtaining a range of S<sub>mix</sub> concentrations ranging from 0.1 µg/ml – 100

µg/ml. Each tube was centrifuged, thoroughly vortex mixed and sonicated in a water bath (185 watts at 42 kHz for 10 min) before centrifugation at 10 000 *g* for 10 min at 20°C. Thereafter 200 µl aliquots of each colloidal dispersion were transferred to a 96 well plate and the absorbance values read at a wavelength of 450 nm (reference 630 nm).

#### *In vitro* release profile under sink conditions

As the water solubility of both PTX and B663 is very poor, the use of a hydrotropic agent, sodium salicylate as described by Cho *et al.* [123] was used to maintain adequate sink conditions.

A volume of 100 µl of Riminocelles solution ready for injection (1 mg/ml PTX, 2.5 mg/ml B663) was diluted in 2 ml HEPES and introduced into a dialysis membrane bag (MWCO=6000-8000 Da). The bag was sealed and the experiment was initiated by placing the bag in 100 ml of 1 M sodium salicylate. The release medium was stirred at a constant speed with a magnetic stirrer. At predetermined time intervals of 10 min, 30 min, 1 h, 3 h and 6 h, 0.5 ml samples were withdrawn and replaced with fresh medium so as to assess the stability of the micelles after dilution (mimicking *in vivo* administration). After sample clean-up using SPE to remove the ionization interfering hydrotrope, the validated LC-MS/MS method as described in Chapter 8 was used to quantitate the different drug concentrations in the dialysate to calculate the percentage of each drug released from the micelle formulation.

### **6.3.2. Development of RiminoPLUS™ Imaging**

#### *Drug solubility in Lipiodol*

As a first step, the solubility of B663 and B4125 in Lipiodol was determined. From literature, it is known that the solubility of PTX in Lipiodol is approximately 10 mg/ml. [62]

UV spectrophotometry (Perkin Elmer, Lambda 25, UV/Vis Spectrometry) was used to determine the maximum solubility of the two lead Riminophenazines (B4125 and B663) in Lipiodol. One millilitre of Lipiodol oil was saturated with an excess of the respective Riminophenazine powders in clean microreaction vials. Each of the mixtures were thoroughly vortex mixed and ultrasonicated in a water bath for 10 min before being centrifuged at 15 000 *g* for 20 min at 10°C to remove any unsolubilised material. Complete removal of unsolubilised compound was confirmed by the absence of any drug crystals when an aliquot was viewed under a light microscope at high magnification (400X). Thereafter, triplicate 20 µl aliquots were removed and diluted with MeOH into the linear range of the assay. Linear calibration lines with correlation coefficients of 0.999 were produced for each of the Riminophenazines in MeOH over a range of 1.5-50 µg/ml using a characteristic absorbance wavelength ( $\lambda_{\text{max}}$ ) of 460 nm.

#### *Aqueous titration method*

In the past, the optimal composition/formulation of nano-sized emulsions has been determined rather arbitrarily without adequate control for the influence of composition variables (the ratio of different materials that are mixed). Systematic studies utilising ternary phase diagrams to 'map' the various possible aggregated structures (polymorphism) that can form at various component ratios, as the water content (wt. %) increases, is a convenient means of identifying optimal chemical formulation with minimal expense of material resources and time. Advantageously this method allows for the identification of both spontaneously forming microemulsions and nanoemulsion formed after the input of ultrasonic energy at a pre-specified water content measured as weight percent (wt. %).

As a first step, the density of Lipiodol was calculated gravimetrically by three independent weight determinations of a known volume at ambient room temperature to be on average 1.242 g/ml.

Concentrated stock solutions of DSPE PEG 2000 and PC were typically prepared to 100 mg/ml and 10 mg/ml respectively in CHCl<sub>3</sub>.

For preliminary studies conducted on a minimum scale, a fine syringe (Series II, SGE Scientific) was used to aliquot 10  $\mu\text{l}$  of B663 saturated Lipiodol (corresponding to 12.42 mg) into each of 9 tubes. At this scale, with the weight of Lipiodol being constant, the calculated total weight of  $S_{\text{mix}}$  required to represent 9 tie lines (i.e. Lipiodol:  $S_{\text{mix}}$  ratios) is roughly 240 mg.

So as to assess the influence of co-surfactant, the following  $S_{\text{mix}}$  (DSPE PEG 2000: PC) ratios: 97:3, 94:6 and 91:9 (w/w) were evaluated. Calculated volumes of each of the three  $S_{\text{mix}}$  stock solutions were added to each of the 9 tubes to represent the following Lipiodol:  $S_{\text{mix}}$  ratios: 0.9:0.1; 0.8:0.2; 0.7:0.3; 0.6:0.4; 0.5:0.5; 0.4:0.6; 0.3:0.7; 0.2:0.8 and 0.9:0.1 (w/w). Dependent upon the scale of the specific experiment, the  $\text{CHCl}_3$  was evaporated off using either a Centrivap (typically) or a rotary evaporator at  $<40^\circ\text{C}$ .

To each specific Lipiodol:  $S_{\text{mix}}$  ratio, calculated volumes of water were slowly added in 10% increments along the tie lines represented in Figure 6.4. The specified volume of water to be added to each specific tube so as to progress along the designated tie lines (Lipiodol:  $S_{\text{mix}}$  ratio) was calculated using a simple Excel spreadsheet. Examples of the output is shown in Table 6.2. for the Lipiodol:  $S_{\text{mix}}$  ratios of 0.9:0.1 and 0.8:0.2.

After each incremental addition of water the respective mixtures were thoroughly vortex mixed. The mixtures were allowed to settle, visually observed and brief qualitative notes made concerning consistency (number of distinct phases, translucency or presence of precipitate).

At 90% wt. water each of the mixtures were ultrasonicated (Biologics, Inc. Model 3000) with a power output of  $\sim 150$  watts at 20 kHz for 5 min (50% pulse - to ensure that the samples did not overheat) using a stepped titanium micro tip (3.81 mm diameter). The samples were observed through the clear door of the sound abating chamber for distinctive translucency changes (optical isotropy) indicating the formation of nanoemulsions. Formulations that were observed to visually phase change from cloudy to translucent after the input of ultrasonic energy were

aliquoted and subjected to multiple freeze-thaw cycles followed by centrifugation at 15 000 *g* for 20 min to assess the colloidal (thermodynamic) stability of the system. Metastable homogenous dispersions (nanoemulsions) were stored in the fridge at 2 - 8°C and were visually observed daily for phase separation. On a weekly basis samples were further diluted to 99 wt. % water, immediately centrifuged and visually observed for phase separation or precipitate formation. Thereafter, samples were filter sterilized through 0.2 µm syringe filters (as would be required prior to IV administration) and sized via DLS.

As no spontaneous emulsification (indicating microemulsion formation) was seen to occur as titration progressed from water-in-oil (W/O) to oil-in-water (O/W), it was concluded that phase inversion was not a prerequisite in the formation of nano-sized emulsions using the materials tested in this study. Therefore, the direct emulsification method whereby the dispersed phase (oil with  $S_{mix}$ ) is added to the continuous phase (water) under intensive mixing followed by ultrasonication was successfully used in scaled up production using the identified optimal Oil:  $S_{mix}$  ratio to produce metastable nanoemulsions.

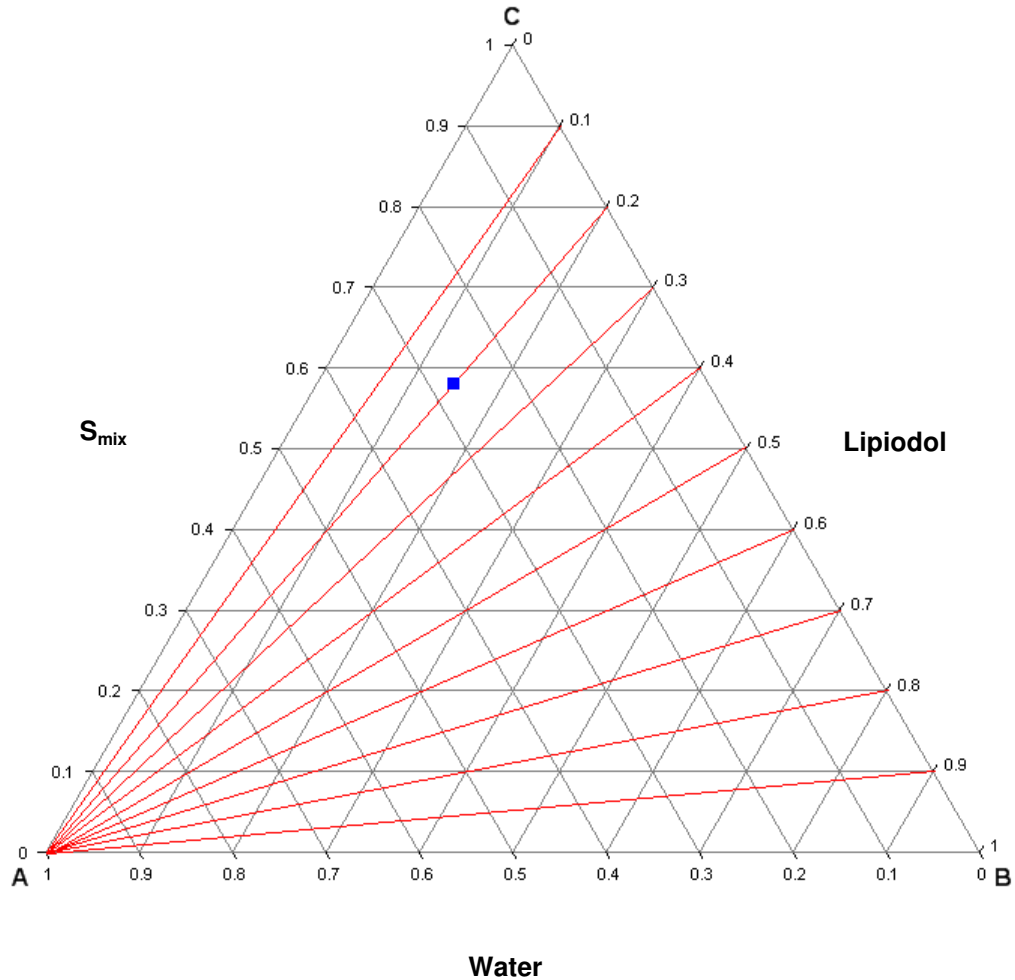


**Figure 6.4. Pseudoquaternary phase diagram showing the respective tie / dilution lines (Red), along which titrations were made. A - Water; B - Lipiodol; C - S<sub>mix</sub>**

**In a ternary phase diagram all the components (Lipiodol, S<sub>mix</sub> and Water) add up to 100% of the weight. Titration begins in the upper right side of the triangle with 9 fixed Lipiodol: S<sub>mix</sub> ratios. Water is slowly added in calculated proportions so as to titrate along the indicated tie lines.**

**The blue dot in the ternary phase diagram corresponds to a composition (w/w) of: Water - 27%, Lipiodol - 15%, S<sub>mix</sub> - 58%**



**Table 6.2. Example calculations (Excel outputs) for dilution along two tie lines (Oil:  $S_{mix}$ , 0.9: 0.1 and 0.8: 0.2)**

0.9 : 0.1 (Lipiodol : $S_{mix}$ )							
Oil		$S_{mix}$		Water			Total wt. of system
wt. %	wt. (mg) <sup>a</sup>	wt. %	wt. (mg)	wt. %	Add $\mu$ l	Cumulative wt. (mg)	
0.900	12.420	0.100	1.380	0.000	0.000	0.000	13.800
0.810	12.420	0.090	1.380	0.100	1.533	1.533	15.333
0.720	12.420	0.080	1.380	0.200	1.917	3.450	17.250
0.630	12.420	0.070	1.380	0.300	2.464	5.914	19.714
0.540	12.420	0.060	1.380	0.400	3.286	9.200	23.000
0.450	12.420	0.050	1.380	0.500	4.600	13.800	27.600
0.360	12.420	0.040	1.380	0.600	6.900	20.700	34.500
0.270	12.420	0.030	1.380	0.700	11.500	32.200	46.000
0.180	12.420	0.020	1.380	0.800	23.000	55.200	69.000
0.090	12.420	0.010	1.380	0.900	69.000	124.200	138.000
0.045	12.420	0.005	1.380	0.950	138.000	262.200	276.000
0.018	12.420	0.002	1.380	0.980	414.000	676.200	690.000
0.009	12.420	0.001	1.380	0.990	690.000	1366.200	1380.000

0.8 : 0.2 (Lipiodol : $S_{mix}$ )							
Oil		$S_{mix}$		Water			Total wt. of system
wt. %	wt. (mg) <sup>a</sup>	wt. %	wt. (mg)	wt. %	Add $\mu$ l	Cumulative wt. (mg)	
0.800	12.42	0.20	3.11	0.00	0.00	0.00	15.53
0.720	12.42	0.1800	3.11	0.10	1.73	1.73	17.25
0.640	12.42	0.1600	3.11	0.20	2.16	3.88	19.41
0.560	12.42	0.1400	3.11	0.30	2.77	6.65	22.18
0.480	12.42	0.1200	3.11	0.40	3.70	10.35	25.88
0.400	12.42	0.1000	3.11	0.50	5.18	15.53	31.05
0.320	12.42	0.0800	3.11	0.60	7.76	23.29	38.81
0.240	12.42	0.0600	3.11	0.70	12.94	36.23	51.75
0.160	12.42	0.0400	3.11	0.80	25.88	62.10	77.63
0.080	12.42	0.0200	3.11	0.90	77.63	139.73	155.25
0.040	12.42	0.0100	3.11	0.95	155.25	294.98	310.50
0.016	12.42	0.0040	3.11	0.98	465.75	760.72	776.25
0.008	12.42	0.0020	3.11	0.99	776.25	1536.98	1552.51

<sup>a</sup> 10  $\mu$ l Lipiodol = 12.42 mg

## 6.4. Results

### 6.4.1. Riminocelles

The approach adopted was to first establish the optimal composition with respect to the relative concentrations of the different compounds to be included in the formulation and thereafter to assess the influence of amphiphile concentration on the solubilisation of the drugs considering the minimum concentration requirements and practical (injection volume and infusion time) restrictions when using small animal models.

The thin film hydration method was found to be a simple and effective way to co-encapsulate the FRDC (PTX and B663) within lipopolymeric micelles (Figure 6.5.). After hydration of the various dried films, syringe based filtration using 0.2  $\mu\text{m}$  filter cartridges was found to effectively remove any insoluble and thus unencapsulated drug. After quantitation of the respective drug concentrations using LC-MS/MS, the percentage drug encapsulation and the drug loading index were calculated for the various formulations prepared. In addition, the particle size and size distribution as well as the zeta potential were determined for each formulation (Table 6.3).

Due to imperfect encapsulation, final drug ratios different to that which had been loaded were attained. The drug loading index that considered the encapsulation of both drugs simultaneously in one expression revealed three samples to possess a total drug wt. above 10% of the mass of the formulation.

Concerning DLS, the attenuator was generally automatically set to 7 which compensated for high scattering samples while maintaining the count rate within acceptable limits. The mean count rate ranged between 290.4 - 407 kcps. In Table 6.3, the results of cumulants analysis are given as: mean size (Z-average/cumulants mean) of the particles based on signal intensity and Polydispersity index (PDI), which is a dimensionless measure of the extent of the particle size distribution.

All prepared formulations gave particles with bimodal distribution (Figure 6.6.) and were therefore not comparable to other sizing techniques. [124] The first population that accounted for a varied % (intensity) ranged from a particle diameter of 12.37-17.06 d.nm and is consistent with the size range reported by numerous authors for PEGylated phospholipid micelles. [100, 101, 102, 104, 108, 125, 126, 127, 128] The second population that generally accounted for a higher % (intensity) ranged from 124-185.5 d.nm (Table 6.4.). The bimodal distribution is consistent with that reported by others. [128, 129] It should however be stated that this phenomenon is difficult to interpret and could possibly be an artefact of the DLS technique. [130] Population % (intensities) and particulate size were seen to vary in a composition-dependent (drug: surfactant ratio) manner.

All the pilot formulations had a negative surface charge with zeta potentials ranging from -7.1 to -35.1 mV. As the zeta potential of particles in suspension will determine whether the particles within a dispersion will tend to aggregate or not, it is often used as an aid to predict the stability of colloidal systems. The greater the charge (whether positive or negative), the greater is the stability. The zeta potentials obtained are consistent with Wang *et al.* [131] who reported a zeta potential of -25 mV for empty DSPE PEG micelles.

After consideration of the various measured parameters taken together, the formulation adopted for further investigation was a drug (PTX) to drug (B663) loading ratio (w/w) of 1:5 and a total drug to amphiphile loading ratio (w/w) of 1:5. Further characterization studies were only carried out on this lead formulation:

Due to lipid polymorphism, the mean percentage encapsulation for the two respective drugs varied as a function of system composition (amphiphile concentration in water). Encapsulation efficacies for the respective drugs (using the optimised loading ratios) were therefore determined as a function of increasing  $S_{mix}$  concentration - The encapsulation of PTX was shown to increase linearly as a function of  $S_{mix}$  concentration (Figure 6.7.), consistent with previously reported results [77, 100, 104] and [110] who prepared bile salt/PC mixed micelles.

In contrast, the encapsulation efficiency of B663 steadily declined as the amphiphile concentration was increased. This has a direct effect on the final drug: drug (w/w) ratio achieved. Ultrasonication was shown to have no effect on drug encapsulation efficacy. The minimum  $S_{mix}$  concentration required to solubilize >1 mg/ml PTX was found to be 35 mg/ml. The drug encapsulation efficacies at this amphiphile concentration are shown in Figure 6.8. The slight variability of encapsulation was used as an advantage. Repeat preparations produced a range of drug concentrations that when mixed together in calculated proportions could be used to ensure that a precise final PTX:B663 (1:2.5, w/w) concentration is attained.

Morphological characteristics of the final formulation were examined using TEM. TEM revealed well-dispersed, electron dense, micellular particles in the size range of 200 nm (Figure 6.9.). The individual micelles were shown to have a spherical shape and to be of narrow size distribution. The slightly larger particle size suggested by TEM over DLS may be attributed to difference in the physical property that is actually measured (e.g. hydrodynamic diffusion versus the projected area). It is important to understand that no particle sizing technique is inherently more correct as they are dependent upon various parameters. [132] Discrepancies are often observed in the particle size distribution obtained and for this reason it is recommended that particle size analysis be performed using more than one technique. [119]



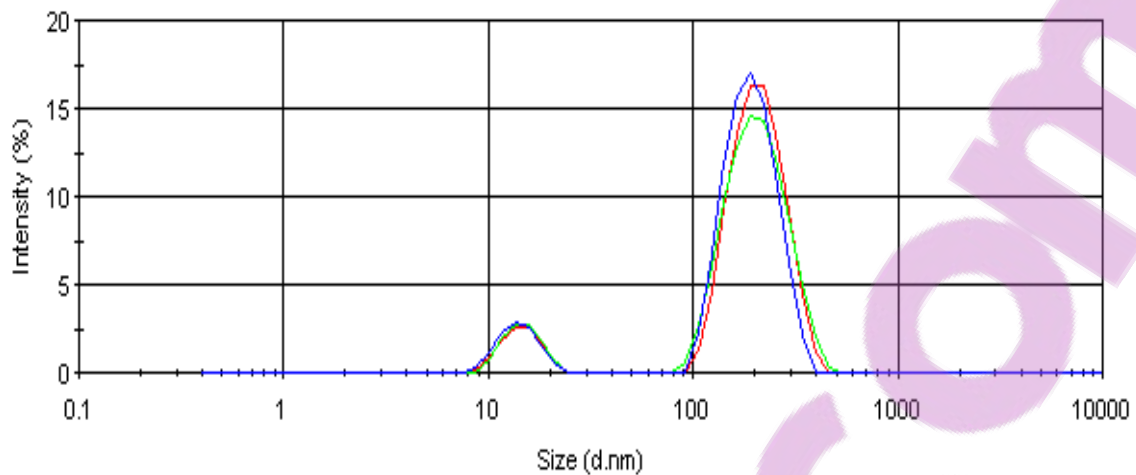
**Figure 6.5. Photograph of diluted Riminocelles**  
The distinctive red colour is evidence that (non-water-soluble) B663 has been solubilised in an aqueous dispersant through encapsulation within micelles.

Table 6.3. Characterisation of various mixed lipopolymeric pilot formulations at a DSPE PEG 2000 concentration of 1 mM in 10 mM HEPES

<b>B663: PTX ratio (w/w)</b>	<b>1:0</b>				<b>5:1</b>				<b>10:1</b>			
<b>Drug<sub>total</sub>: S<sub>mix</sub> ratio (w/w)</b>	<b>1:50</b>	<b>1:20</b>	<b>1:10</b>	<b>1:5</b>	<b>1:50</b>	<b>1:20</b>	<b>1:10</b>	<b>1:5</b>	<b>1:50</b>	<b>1:20</b>	<b>1:10</b>	<b>1:5</b>
<b>B663 % encapsulation</b>	87.6	92.8	87.6	77.2	87.0	97.0	98.9	92.1	93.5	100.0	89.5	86.1
<b>PTX % encapsulation</b>	<i>Not applicable</i>				65.7	59.4	67.5	74.0	58.2	82.7	55.9	70.7
<b>[B663] µg/ml</b>	50.7	134.3	253.5	447.0	42.0	117.0	238.5	444.0	49.2	132.8	235.5	453.0
<b>[PTX] µg/ml</b>	<i>Not applicable</i>				6.3	14.3	32.6	71.4	3.1	10.9	14.7	37.2
<b>Final drug ratio</b>	1:0	1:0	1:0	1:0	6.6:1	8.2:1	7.3:1	6.2:1	15.9:1	12.2:1	16:1	12.2:1
<b>Drug loading index</b>	1.72	4.43	8.06	13.38	1.64	4.34	8.57	15.12	1.77	4.73	7.96	14.49
<b>Z-Average Size (d.nm)</b>	175.0	32.2	105.6	37.4	184.9	164.0	95.1	137.6	134.8	117.8	120.6	95.8
<b>Pdl</b>	0.22	0.64	0.18	0.14	0.23	0.25	0.25	0.18	0.22	0.20	0.25	0.17
<b>Zeta potential (mV)</b>	-29	-25.6	-31.7	-7.1	-28.5	-31.1	-35.1	-20.6	-31.7	-18.3	-31.9	-10.3

**% Encapsulation = drug encapsulated / drug loaded (w/w) x 100**

**Drug loading index = total drug encapsulated / (amphiphile + total drug encapsulated) (w/w) x 100**



**Figure 6.6. Z-average size (hydrodynamic diameter) distribution by intensity demonstrating the bimodal distribution of Riminocelles as determined by Dynamic light Scattering**

**Table 6.4. Bimodal size distributions of the various pilot formulations at a DSPE PEG concentration of 1 mM in 10 mM HEPES**

<b>B663:PTX</b>	<b>Drug: S<sub>mix</sub></b>	<b>Population 1 (d.nm)</b>	<b>% (Intensity)</b>	<b>Population 2 (d.nm)</b>	<b>% (Intensity)</b>
<b>(w/w)</b>	<b>(w/w)</b>				
<b>1:0</b>	<b>1:50</b>	12.7	35.1	124.0	64.9
	<b>1:20</b>	13.7	42.6	158.6	53.3*
	<b>1:10</b>	14.7	55.7	150.4	44.3
	<b>1:5</b>	17.1	78.5	148.5	20.1*
<b>5:1</b>	<b>1:50</b>	12.5	20.6	134.1	79.4
	<b>1:20</b>	12.4	22.6	155.2	77.4
	<b>1:10</b>	14.7	46.0	163.6	54.0
	<b>1:5</b>	15.8	59.8	138.2	40.2
<b>10:1</b>	<b>1:50</b>	13.7	29.7	138.3	70.3
	<b>1:20</b>	15.7	43.5	167.7	56.5
	<b>1:10</b>	14.9	40.5	185.5	59.5
	<b>1:5</b>	16.9	66.2	157.1	33.8

\* Third population >4000 d.nm (suspected dust particles)

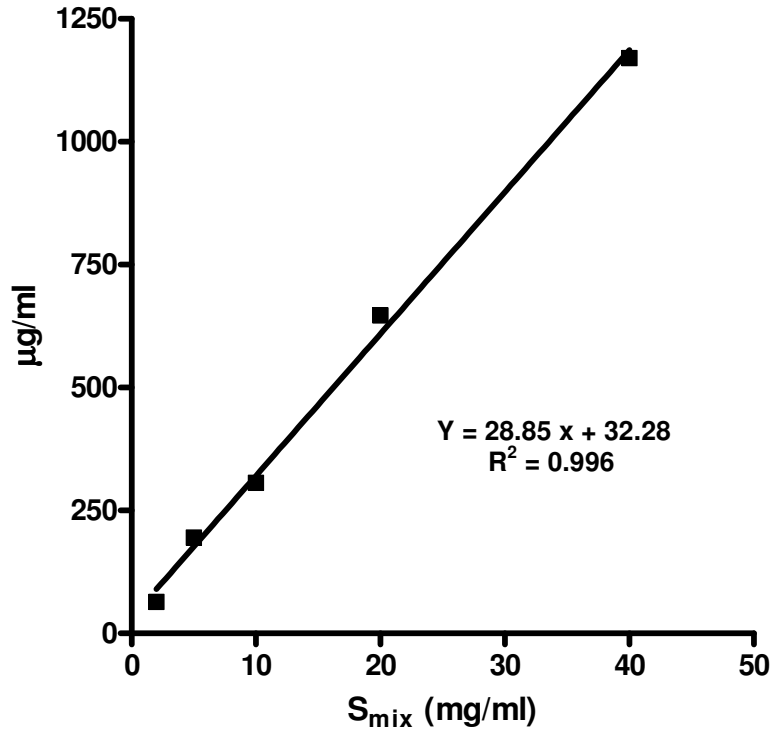


Figure 6.7. Encapsulation of PTX within mixed lipopolymeric micelles as a function of  $S_{mix}$  concentration

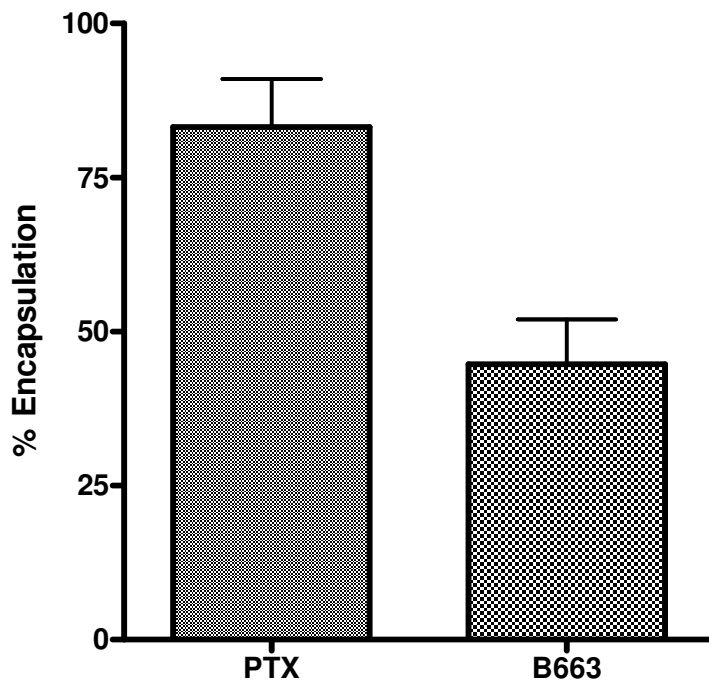


Figure 6.8. Percent encapsulation of PTX and B663 within Riminocelles at a  $S_{mix}$  concentration of 35 mg/ml as determined by LC-MS/MS



The inherent dye quality of Riminophenazines was effectively used to determine the CMC value of the  $S_{mix}$  using a UV spectrophotometric method (Figure 6.10.). Using the molecular mass for DSPE PEG 2000 of 2806 g/mole an estimated CMC value of  $0.178 \times 10^{-5}$  M was obtained. The CMC of micelles formed from DPSE PEG 2000 has been reported as approximately  $1.1 \times 10^{-5}$  M as determined using the pyrene assay method. [106, 108] Although it is ill advised to compare CMC values obtained through different techniques, it is not surprising to have attained lowered (improved) CMC values as the incorporation of PC adds to the hydrophobic driving force behind micellization. It was expected that Riminocelles prepared ready for injection can endure greater than 1:7000 dilution in water before micelle dissociation occurs.

*In vitro* drug release studies were performed under sink conditions simulated through the use of sodium salicylate in the release media (Figure 6.11.). Both drugs were shown to be well retained within the particle. PTX was slowly released over the first hour increasing to approximately 40% PTX release after 6 hours. B663 was steadily released over the 6 hour sampling period to approximately 10% cumulative release. These relative losses support the maintenance of a synergistic ratio between the two drugs.

Drug loaded mixed lipopolymeric micelles demonstrated high integrity after storage for up to 6 months at 4°C as determined through thermodynamic (centrifugation) tests. No precipitate was observed indicating that the drugs were stably encapsulated. The stability under the recommended storage condition was further attested to independently in a GLP accredited laboratory prior to IV administration in the efficacy study (Chapter 7).

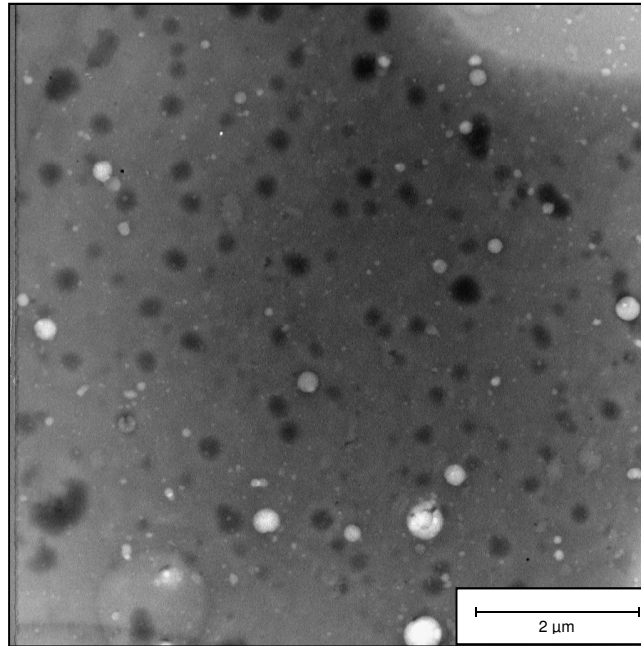


Figure 6.9. TEM image of Riminoelles

Dark spots correspond to the lipopolymeric micelles diffracting the electron beam.

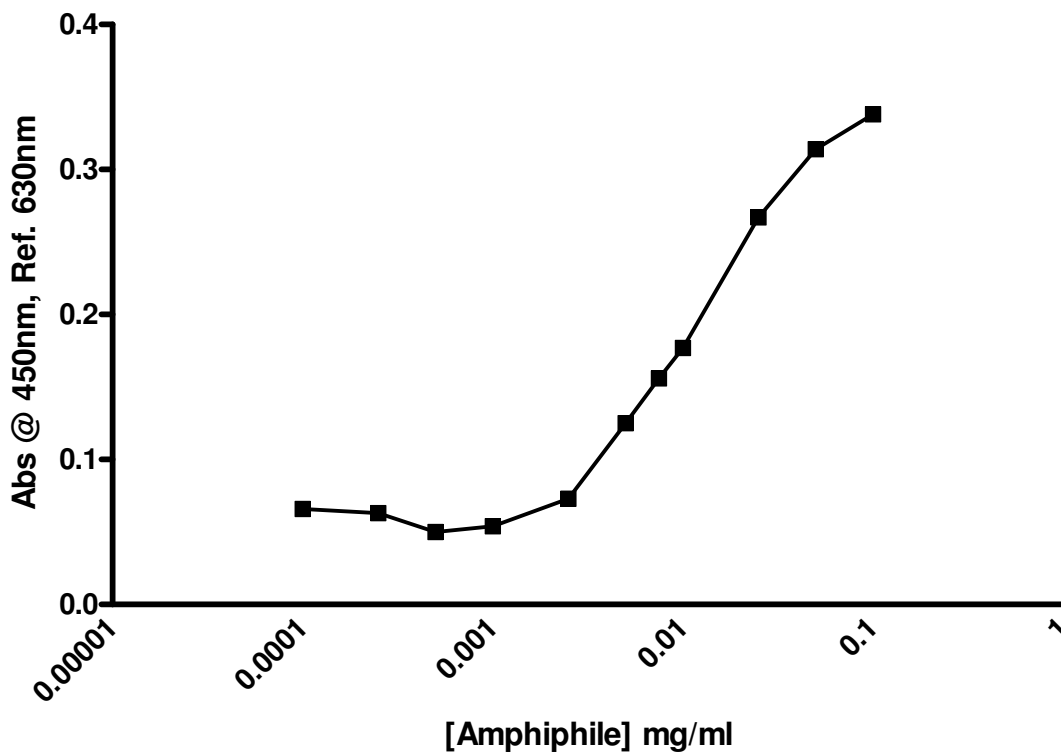


Figure 6.10. Determination of the critical micellar concentration (CMC) of the  $S_{mix}$  using the dye micellization method. Semi-log graph representing the approximate CMC value of Riminoelles.

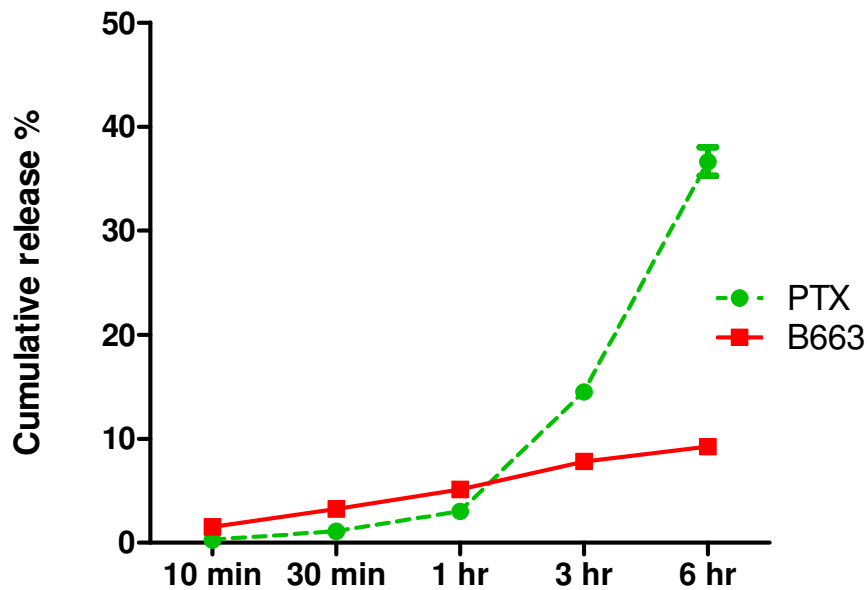


Figure 6.11. Typical release profiles of PTX and B663 from Riminocelles in 1 M sodium salicylate at ambient room temperature

#### 6.4.2. RiminoPLUS Imaging

After a 200 fold dilution of drug saturated Lipiodol using pure MeOH, the solubility of B663 and B4125 in Lipiodol was measured using a calibrated UV spectrophotometric method and found to be roughly 7 mg/ml and 4 mg/ml respectively.

An efficient stream-lined approach was adopted with the intent of quickly formulating a Lipiodol-core, nano-sized emulsion satisfying the requirements for a ready to inject IV solution. Although phase inversion naturally occurred from W/O to O/W as aqueous titration proceeded, no spontaneous nanoemulsification was observed as evidenced by optical isotropy. Nor could spontaneous emulsification be achieved in pilot experiments for any of the compositions through repeated heating to in excess of 90 °C followed by rapid cooling in ice water (phase inversion temperature method). Although various different associated structures (lipid

polymorphisms) were assumed to form during transition, so as not to detract away from the study's aim, the nature of these intermediate phases were not investigated and merely qualitatively visually observed.

Prior to ultrasonication, all ternary systems (oil, surfactant, water mixtures) appeared opaque to different degrees (Figure 6.12.); colloidal dispersions were centrifuged to assess the degree of homogeneity and complete solubility. Pellets of different colours and quantities were observed for different compositions demonstrating the heterogeneity of the various mixture systems.

After ultrasonication at 90% water (w/w) all mixtures were again visually inspected. Several compositions notably the Lipiodol:  $S_{mix}$  ratios of 6:4, 5:5 and 4:6 appeared optically isotropic after ultrasonication (Figure 6.13.). These single phase translucent compositions were subjected to three repeated freeze-thaw cycles followed by centrifugation. The Lipiodol:  $S_{mix}$  ratio of 4:6 appeared to be thermodynamically stable as no pellet was evident after prolonged centrifugation.

A reproducible monodisperse population with a Z-average size of 101.2-105.1 d.nm and a Pdl of <0.22 for the Lipiodol:  $S_{mix}$  ratio of 4:6 was attained (Figure 6.14.A.). Nanoemulsions produced with varying proportions of PC as a co-surfactant were shown not to influence the particle size nor stability (Figure 6.14. B & C). This dispersion was shown to maintain particle size for 7 days when stored at 2-8 °C despite possessing approximately zero electrophoretic mobility (zeta potential). Neither freeze thaw cycle nor ultracentrifugation produced phase separation for a period of approximately 2 weeks, after which degradation through Ostwald ripening and/or coalescence was evident that could be mitigated through re-sonication. Filtration of the dispersion through 0.2  $\mu$ m syringe filters did not influence the particle size.



**Figure 6.12. Flattop scanned image of the 9 Lipiodol:  $S_{mix}$  ratios at 0.90% water, visually indicating the difference in consistency  
From right to left – 0.9:0.1 to 0.1:0.9 (Lipiodol:  $S_{mix}$ )**



**Figure 6.13. Photograph of RiminoPLUS demonstrating the homogeneity and optically isotropic nature (visual perspective) of the nanoemulsions (roughly 100 nm). The dispersion is being held horizontal.**

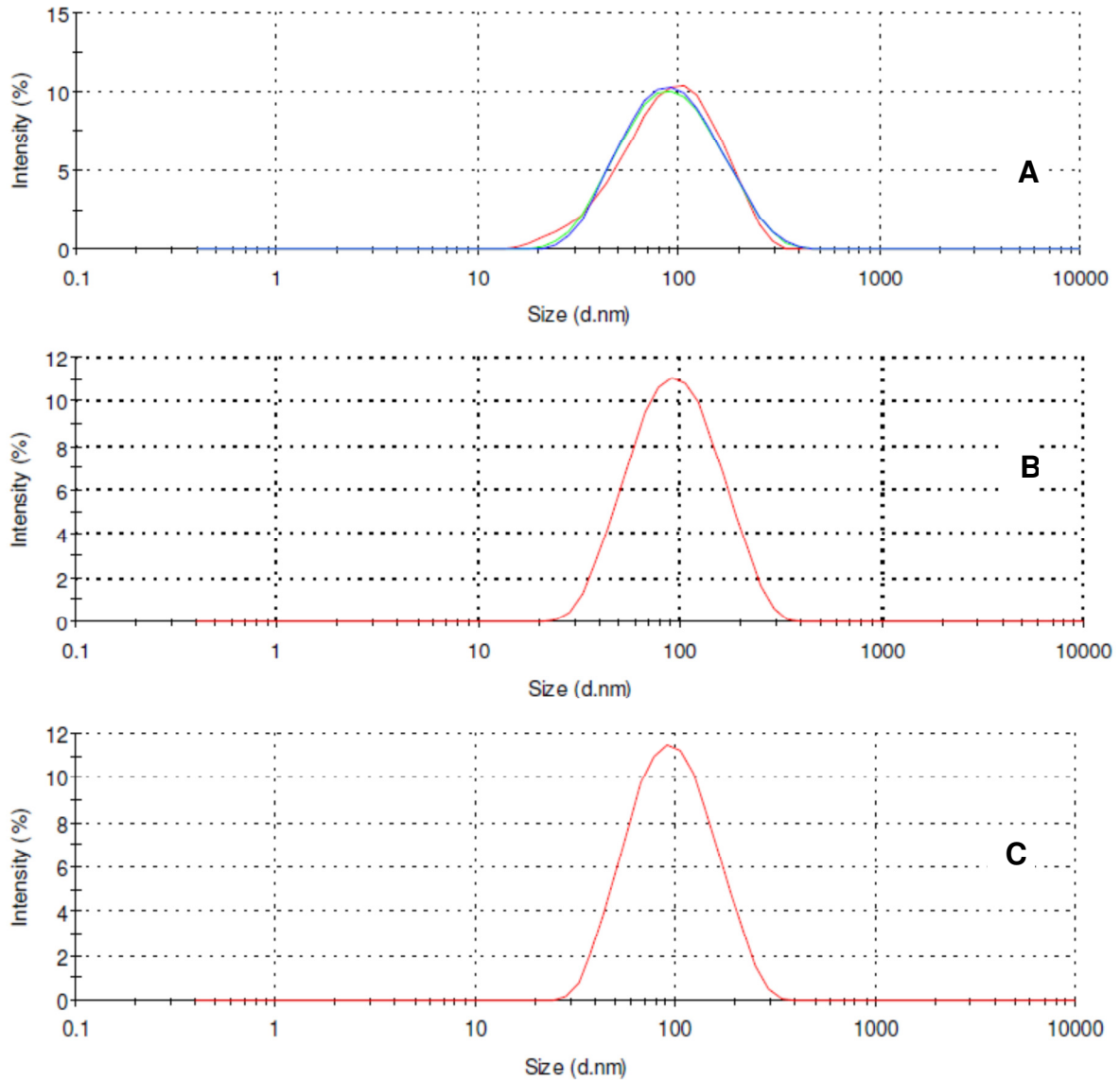


**Figure 6.14. Size distribution by intensity of various RiminoPLUS formulations with a Lipiodol: S<sub>mix</sub> ratio of 4:6**  
**A - S<sub>mix</sub> of DSPE PEG 2000: PC (97:3); B - S<sub>mix</sub> of DSPE PEG 2000: PC (94:6); C - S<sub>mix</sub> of DSPE PEG 2000: PC (91:9)**

## 6.5. Discussion and conclusion

Phospholipids were first conjugated to PEG in 1984 when Sears [133] coupled carboxy-PEG and pure soy phosphatidylethanolamine via an amide linkage. Subsequently, lecithin and PEG modified phospholipids have become the most commonly used emulsifiers for parenteral application [119] and are widely used in various registered pharmaceutical dosage forms. Although other hydrophilic polymeric blocks and mixes thereof could be used as efficient steric barriers provided that they are biocompatible, PEG still remains the hydrophilic block of choice used to form the corona of many particulate drug delivery systems.

Interest in nanotechnology and its biomedical application, particularly with respect to intelligent dosage form design, has exploded in recent years. [134] NDDS assembled with biocompatible high molecular weight lipopolymeric amphiphiles offer the advantage of direct access to the blood stream, rapid onset of action and improved targeting.

NDDS are a platform in which drugs can be targeted to specific sites through surface functionalization with targeting moieties and specific disassembly responses (triggers). DSPE PEG 2000 with folate or specific antibody conjugation on the distal portion of the hydrophilic block have been synthesised and are commercially available. Therefore, both Riminocelles and RiminoPLUS could be “upgraded” to include active targeting mechanisms with ease.

### *Riminocelles™*

The experimental approach used to optimise the binary system (Riminocelles) was very effective at achieving the desired objective with minimal resource expenditure. For all the pilot studies, only 60 mg of  $S_{mix}$  was required. This drug delivery system was optimised with respect to composition to obtain the desired particle characteristics thought pre-requisite for exploitation of the EPR effect of solid tumours.

The use of DSPE PEG 2000 and PC proved to be an efficient means of solubilising the poorly water soluble drugs, PTX and B663. The thin film hydration and filter method was reproducible, at various scales of synthesis (2 ml - 100 ml) to produce particles of reproducible size and encapsulation efficacy. This preparation method could foreseeably be scaled up to provide enough Riminocelle for clinical studies if required.

The fluctuation in B663 encapsulation efficacy as a function of amphiphile concentration is thought to be due to different conformations of aggregate structures that form at different points along an isothermic binary (lipid-water) phase diagram influencing the degree of solubility. [135, 136]

Through proportionally mixing replicate preparations, the inherent variability of encapsulation (~10% standard deviation) was used to prepare the final sterile formulation of 1 mg/ml PTX and 2.5 mg/ml B663 (with a controlled ratio) for *in vivo* toxicity, efficacy and pharmacokinetic studies. Such clinically relevant concentrations of PTX were solubilised at a low amphiphile concentration of 35 mg/ml. This methodology would require stricter standardisation, adhering to GMP in preparation for clinical trials.

Previous studies using D- $\alpha$ -tocopheryl polyethylene glycol 1000 succinate (TPGS) as a co-surfactant with DSPE PEG 2000 (in a 1:1 molar ratio) have reported that 3 - 5 mg/ml of PTX have been attained but at amphiphile concentrations in excess 100 mg/ml. [106]

Gao *et al.* [100] reported a PTX incorporation of 1.5 wt. % into DSPE PEG 2000 micelles. Gao *et al.* [77] reported a PTX incorporation of 3 wt. % into DSPE PEG/PC (1:4) mixed immunomicelles (with surface conjugated 2C5 MAb). In this study, a PTX incorporation of 2.86 wt. % together with 7.14 wt. % B663 in mixed lipopolymeric micelles was attained.

*In vitro* release studies under sink conditions suggests that the novel NDDS retains sufficient drug for effective drug delivery following the dilution experienced after IV



administration. It should however be stressed that this study did not attempt to model the *in vivo*, protein rich, plasma environment. Further studies with such lipopolymeric micelles should be evaluated for drug release in the presence of plasma proteins to mimic the *in vivo* environment.

Riminoelles loaded with PTX and B663 were independently observed (by Charles River Laboratories - Chapter 7) to be stable (without precipitation) and suitable for intravenous injection for periods in excess of 6 months when stored at 2 - 8 °C.

In summary, the ready-to-inject, sterile Riminoelles nanoparticulate co-formulation possesses good particle characteristics including: physical size, electrostatic stability, CMC and stable drug retention, which collectively suggest suitability for passive tumour targeting after IV administration.

The novel feature of this NDDS in comparison to currently used PTX formulations (Taxol and Abraxane) is the combined use of B663 as a chemosensitizing agent. The use of a FRDC encapsulated within NDDS is expected to offer greater efficacy against a wider range a drug resistant solid tumours and to reduce systemic toxicity.

#### *RiminoPLUS™*

The inner core of the nanoemulsion used for the manufacture of the RiminoPLUS formulation is composed of Lipiodol that has proven X-ray imaging capabilities and has been shown to solubilise diverse chemotherapeutics. It is thought that once released at the tumour site, drug saturated Lipiodol will remain within the tumour interstitium (and potentially increase intracellular concentrations) for prolonged periods [56], facilitating maximum neoplastic cell kill while facilitating diagnostic CT imaging.

The solubility of the B663 and B4125 in Lipiodol (7 mg/ml and 4 mg/ml respectively) being well below that of PTX (solubility ~10 mg/ml) is not conducive to attain the synergistic combination ratios identified *in vitro* as the drug ratio at

maximal encapsulation would be at levels where antagonistic effects are observed (Chapter 5). A possible solution may be to make use of alternative iodinated oils that have greater solubility for these Riminophenazines.

B663-loaded, kinetically metastable nano-sized (~100 nm) emulsions suitable for parenteral administration were successfully assembled with the aid of pseudoternary phase diagrams by ultrasonication at the water rich region (90% water) of the ternary phase diagram. Further dilution to 99% water prior to size determination using DLS was intended to plausibly match the dilution effect experienced after IV injection. The particle size attained is thought perfect for passive tumour accumulation after either IV or intra-arterial injection.

This nanoemulsion system was only stable for a short period of ~1 week. As many nanoemulsion systems do not possess long-term storage stability [117] this was not deemed to be a failed formulation. This nanoemulsion could still be of clinical utility and additional co-surfactants such as Polysorbate 80 could be used to improve the shelf life, as has been reported. [137]

The approach employed in preparing the nanoemulsion was simple and employed a minimum scale of material (10 µl Lipiodol). Future endeavours will benefit from the use of the created Excel spreadsheet that facilitates quick calculation of titration volumes in 10% increments. The advantage of the aqueous titration method is that the entire ternary phase diagram (for a particular Oil,  $S_{mix}$  combination) can be “mapped” using only 9 samples and that both microemulsion (formed spontaneously) and nanoemulsions (requiring energy input) can be identified.

## 7. *In vivo* models of experimental toxicity and oncology

### 7.1. Introduction

Paclitaxel (PTX),  $C_{47}H_{51}NO_{14}$  (molecular weight of 853.9), is a diterpenoid derived from *Taxus brevifolia*. PTX is a potent antineoplastic drug that has demonstrated significant antitumour activity against a wide variety of malignancies particularly ovarian, breast and non-small cell lung cancer. PTX is a cytotoxin active against dividing cells as it is a mitotic inhibitor that promotes the formation of highly stable microtubules that resist depolymerization, preventing cell division and arresting the cell cycle at the G<sub>2</sub>/M phase. [138].

PTX is highly hydrophobic and its intravenous administration is consequently dependent upon a suitable vehicle. Currently PTX is formulated as Taxol® (Bristol-Myers Squibb) within Cremophor EL® (polyethoxylated castor oil) and EtOH (1:1, v/v) to 6 mg/ml. Typically, Taxol will be further diluted with saline to a PTX concentration of 1 mg/ml prior to IV administration. This castor oil based vehicle is thought to be responsible for the hypersensitivity reactions encountered in many patients necessitating pre-treatment with antihistamines (diphenhydramine or cimetidine) and/or a glucocorticoid (dexamethasone). Non target toxicity includes haematological effects (neutropenia), peripheral neuropathy and transient myalgia. [139]

Due to the high occurrence of hypersensitivity reactions and the acquired resistance, many new formulations of paclitaxel are currently in various phases development all around the world. Although many of these formulations (Abraxane, LEP-ETU, Genexol-PM, PGG-PTX, Nanotax and NK105) have successfully eliminated the need for cremophor, they have done little to overcome the problem of Pgp mediated drug resistance. None of these formulations have included a synergistic drug partner to attempt to add cytotoxic potency for a greater range of cancers.

Riminocelles is a sterile co-formulation of an *in vitro* optimized synergistic combination of PTX and B663 prepared in a mixture of DSPE PEG 2000 and lecithin intended to be suitable for parenteral injection. Riminocelles is a nanoparticulate delivery system that has been designed to circumvent resistance and passively accumulate in solid tumour tissue after IV injection.

Prior to first in human clinical trials it is prudent to first evaluate the expected safety and efficacy of the investigational product in animal models in a way that conforms to international best practice and ethics. The contemporary view of pre-clinical toxicity is that one need only determine the specific information deemed pertinent prior to initiating a particular clinical trial. A unique pre-clinical development plan should be devised for each anticancer pharmaceutical considering all available data.

The primary goals of pre-clinical toxicity testing of anticancer drug products are to: identify safe phase 1 clinical trial starting dosages; identify potential organ toxicities and their reversibility; assist in the design of human dosing regimens and escalation schemes. [85, 140] The aim is to gain clinically relevant (predictive) data that can be used to justify (and support) human studies.

Considering the targeting nature (by design) and intent behind the investigational pharmaceutical under development (Riminocelles) - a healthy tumour-free mouse model cannot serve to assess what a true limiting dosage level would be, i.e. a severely toxic dose  $STD_{10}$  (MTD) as recommended by the FDA [84] and ICH [82]. There is no real scientific justification for toxicity testing of cancer-specific therapies in non-tumour-bearing animals. [141]

Accordingly, in an acute toxicokinetic study the goal was not to identify a MTD but rather to obtain important toxicokinetic information regarding the functioning and safety of the drug loaded NDDS. The primary aim of the toxicokinetic study was to assess the true *in vivo* stability of the NDDS and too evaluate the risk of novel toxicities brought about through changes in PTX distribution. As the targeting and efficacy of the NDDS was expected to be an improvement on existing PTX administration protocols, doses of PTX were limited to no higher than currently

used clinical dosages. As such, for acute toxicokinetic studies a single dose of 10 mg/kg PTX as determined to be safe by Gustafson *et al.*, 2005 [142] was used.

Apart from demonstrating safety (in rodent and non-rodent species) through acute and repeat dose toxicity studies as required by international regulatory authorities, a major goal (upon which future studies and financial investment hinge) is to establish the efficacy of the drug product using well-reasoned animal tumour models that are reflective and predictive of the human condition. This provides an opportunity to evaluate different doses and dosing schedules prior to initiating human trials so as to speed the establishment of clinically effective doses in phase I trials.

To ensure safety, it is required that both rodent and non-rodent animals are dosed using a clinically representative regime. Numerous tumour models for the evaluation of drugs have been developed ranging from chemically induced, syngeneic, transgenic and xenografts. Transplantation of human neoplastic cell cultures (xenografts) into immunodeficient athymic (nude) mice is frequently used in pre-clinical studies to evaluate the activity of potential anticancer agents. Subcutaneous implant models are most often employed because of the ease of inoculation and subsequent serial tumour measurement. [143] The use of human xenografts has become the “gold standard” in anticancer drug development and this technique is recommended by regulatory agencies. [144]

Nude mice implanted with the drug resistant HCT-15 colon adenocarcinoma cell line as a model of Pgp mediated MDR cancer, was used to investigate the efficacy and toxicity of two different Riminocelles and Taxol treatment schedules and compared to an untreated control group.

## 7.2. Materials

### Animals

Twelve female BALB/c mice were used for the acute toxicity experiments conducted at the University of Pretoria, Biomedical Research Centre (UPBRC).

Forty female homogenous nude (Crl: Nu-Foxn1<sup>nu</sup>) mice were used in the outsourced Charles River Laboratory (CRL) studies.

### Drugs and formulations

PTX was obtained from Sigma Aldrich (UPBRC) or from Hauser Pharmaceutical Services (CRL) as an off white powder and stored at -20<sup>o</sup>, protected from light.

Taxol® (paclitaxel - 99.8% was obtained from Hauser Pharmaceutical Services as an off white powder and stored at -20<sup>o</sup>, protected from light. Taxol was prepared fresh for each treatment by first dissolving in absolute ethanol, sonicating briefly, adding an equal volume of Cremophor to make a 6 mg/ml solution. Prior to administration it was diluted with saline to produce a clear and colourless 1mg/ml PTX solution.

PTX-Riminocelles™, (PTX [1 mg/ml] and B663 [2.5 mg/ml]) was prepared in the Department of Pharmacology and shipped via DHL (solution 9 packaging) at -20 °C to CRL (Ann Arbor, Michigan, USA) as 40 x 1 ml vials.

## 7.3. Methodology

### 7.3.1. Pilot safety and acute *in vivo* toxicokinetic assessment of Riminocelles

*Experimental procedures and schedule:*

Animals were acclimatized to conditions for a week prior to experimentation. They were individually ear-tagged and fed standard rodent food and water *ad libitum*.

On Day 1 of the pilot safety study the animals were weighed facilitating the calculation of bolus injection volume for each specific mouse:

$$\text{Mouse weight (kg)} \times 10 \text{ mg/kg} / 1 \text{ mg/ml} = X \text{ (ml)}$$

Riminocelles and Taxol were injected IV into the topically anaesthetised tail veins of 6 mice each at a PTX concentration of 10 mg/kg using a 30-gauge needle over ~1 min using a 1 ml Braun syringe. After injection the animals were observed for clinical evidence of toxicity and tolerance.

On day 7, three mice were randomly taken from each of the two groups. Terminal blood samples were drawn under isoflurane anaesthetization, (into heparin blood tubes) by cardiac puncture using pre-heparinised 1 ml needles for toxicity marker profiling. Organs (liver, spleen, kidney, adipose tissue) were collected, weighed and stored at -70°C for possible later drug level quantitation.

On day 8 and 9, the pharmacokinetic study was performed as outlined in Appendix C. Briefly, 5 mice (each) were injected with Riminocelles and Taxol for each time period (30 min, 1, 3, 6 and 24 hr hour). At termination sufficient blood was collected to facilitate both toxicity marker profiling and LC-MS/MS determination (Chapter 8). Five control mice were treated with saline and euthanized after 24 h facilitating comparative toxicity marker profiling and serving as a source of blank matrix samples.

On day 14 the remaining 3 mice in each group were terminated and blood drawn.

Through using this protocol, animal numbers were reduced and plasma toxicity biomarker profiles were attained at 1, 7 and 14 days post administration for both Taxol and Riminocelles.

### **7.3.2. Toxicity marker profiling**

Blood analysis was carried out immediately after collection at the Clinical Pathology Laboratories, Faculty of Veterinary Sciences, University of Pretoria.

The following tests were performed:

Haematological analysis - Haematocrit, haemoglobin concentration, total erythrocyte and leukocyte blood cell counts.

Kidney function markers - Blood urea nitrogen and blood creatinine.

Liver marker enzymes - Alanine aminotransferase (ALT), Aspartate aminotransferase (AST), Gamma-glutamyl transpeptidase (GGT).

### **7.3.3. Efficacy assessment**

The purpose of the proposed *in vivo* efficacy studies was to assess the anticancer effectiveness of the novel Riminocelle formulation in comparison to that of Taxol at an equivalent PTX doses using two schedules (Table 7.1.) versus an untreated using a model of Pgp mediated MDR.

Through outsourcing to a GLP facility (Charles River Laboratories) such a study also serves as the required GLP repeat-dose (mimicking the proposed clinical regime) as stipulated by ICH M3R2.



**Table 7.1. Study design**

Group	# Animals	Compound	Route	Schedule	Treatment days	PTX dose (mg/kg/inj.)
1	8	Untreated control	NA	NA	NA	NA
2	8	Taxol	IV	Q7dx4	Day 7, 14, 21, 28	10 mg/kg
3	8	Riminocelles	IV	Q7dx4	Day 7, 14, 15, 28	10 mg/kg
4	8	Taxol	IV	Q1dx7	Day 7-14	10 mg/kg
5	8	Riminocelles	IV	Q1dx7	Day 7-14	10 mg/kg

## Procedures

### *Mice and Husbandry*

Female mice (Crl:NU-Foxn1nu) of age 8-9 weeks were obtained from Charles River Laboratories. The mice were allowed to acclimate for 5 days. The mice were fed standard irradiated rodent food and water *ad libitum*. The mice were housed in static cages with sterile bedding inside clean rooms that provide HEPA filtered air into the barrier environment at 100 complete air changes per hour. The environment was controlled to a temperature range of 21 ± 2°C and a humidity range of 30-70%. All treatments, body weight determinations, and tumour measurements were carried out in these sterile conditions.

All mice were observed for clinical signs at least once daily. Mice with tumours in excess of 1000mg or with ulcerated tumours were euthanized, as were those found in obvious distress or in a moribund condition.

### *Cell Preparation and implantation*

HCT-15 human colon adenocarcinoma cells were cultured using RPMI 1640 supplemented with 10% non-heat inactivated fetal bovine serum, 1% (1M HEPES), 1% sodium pyruvate, in 5% CO<sub>2</sub> and 95% air humidified atmosphere at 37 °C. The HCT-15 cells were detached from the flasks using 0.25% trypsin/2.21mM EDTA in HBSS per each flask. The HCT-15 cells were collected through centrifugation at 300 *g* for 8 minutes at 4 °C. The cell pellets were suspending in complete media. The viability of the HCT-15 cell suspension was determined using trypan blue exclusion with a haemocytometer both before and after the inoculation period. Prior to implantation the cells were resuspended in 50% serum-free RPMI media and 50% Matrigel® to obtain a cell concentration of 5x10<sup>6</sup> cells/200 µl injection per mouse.

Test mice were implanted subcutaneously high in the right axilla (just under arm) on Day 0 using a 27-gauge needle and a 1 ml syringe. The cell suspension was maintained on wet ice to minimize loss of viability and inverted frequently to maintain a uniform cell suspension during the inoculation procedure.

### *Treatment*

Considering that a subcutaneous tumour is only definitely palpable at >100 mg. [145] Treatment was to begin once the tumours reach 100-200 mg (target 150 mg). [146] Animals were weight matched and assigned to respective groups such that the mean tumour burden in each group was within 10% of the overall mean. Before dosing, each animal was weighed and an appropriate dose volume of the respective [1 mg/ml] PTX formulations (Riminocelles and Taxol) was calculated via the following formulae: Mouse weight (kg) x 10 (mg/kg) / 1 mg/ml = X (ml). Slow injections into the tail vein typically lasted 1min. Appropriate precautions for normal IV chemotherapeutic administration were taken.

### *Tumour measurements and Efficacy endpoints*

Tumour measurements were recorded three times weekly. Tumour burden (mg) was estimated from calliper measurements by the formula for the volume of a prolate ellipsoid assuming unit density as [147, 148]:

$$\text{Tumour volume (mm}^3\text{)} = (\text{width}^2 \times \text{length (mm)}) \times 0.5$$

(Specific gravity assumed to be 1 g/cm<sup>3</sup> therefore mm<sup>3</sup> = mg)

Tumour Growth Delay (T - C value) was used to quantify efficacy where C is the median time in days required for a particular tumour to reach a predetermined mass and T is the median time required for the treatment group to reach the same predetermined evaluation size. Tumour Growth Delay was measured at a tumour weight of 750 mg.

Tumour-Cell-Kill was used as a secondary efficacy endpoint. The log<sub>10</sub> Tumour-Cell-Kill was calculated from the formula:

$$\text{Log}_{10} \text{ tumour cell kill total (gross)} = [\text{T} - \text{C value in days} / 3.32 (T_d)]$$

Where  $T_d$  is the tumour-volume doubling time (in days) estimated from the least squares best-fit straight line from a log-linear growth plot of the control group whilst in exponential growth, 200-800 mg range. [146, 147] The value 3.32 is derived from the number of doublings required for a cell population to increase 1 log<sub>10</sub> unit. [148]

For a treatment duration of between 5 and 20 days a Gross Log<sub>10</sub> tumour cell kill of >0.7 is required before a treatment is considered as active and a value of >2 would be required to produce tumour regressions in most models. [149]

Tumour growth inhibition values (%T/C) were determined every second day through comparison of the median tumour burden (mass) for each group relative to the untreated control. The Drug Evaluation Branch of the Division of Cancer Treatment, National Cancer Institute (NCI) considers a T/C ≤ 42% as significant

antitumour activity. A value <10% is considered highly active and justifies a clinical trial. [149]

#### *Assessment of Side Effects (GLP repeat dose toxicity assessment)*

Mouse body weights were recorded three times weekly. Treatment-related weight loss in excess of 20% was considered unacceptable and the animals were to have been euthanized. A dosage level was considered as tolerated if treatment-related weight loss (during and two weeks after treatment) is <20% and mortality during this period in the absence of potentially lethal tumour burdens is  $\leq 10\%$ . All mice were observed for nadir weight loss and weight loss return.

Upon death or euthanasia, all mice underwent necropsy to provide a general assessment of potential cause of death and perhaps identify target organs of toxicity. The presence or absence of any tumour metastases was also noted.

#### **7.3.4. Ethical considerations and committee approval**

All studies complied with the ethical approval given for project number H10-09 (University of Pretoria, AUCC) - Appendix A.

All animal studies were designed following the philosophy of the 3 R's (Reduce, Refine, Replace). Humane endpoints as stipulated by the SA National Standards (SANS 10386:2008) were followed. The veterinarian in charge had full authority to terminate any animal or the entire study in the event that any of the animals were deemed to be suffering.

All procedures carried out abroad were conducted in compliance with all the laws, regulations and guidelines of the National Institutes of Health (NIH) and with the approval of Discovery and Imaging Services, Ann Arbor's (DIS-AA) Animal Care and Use Committee.

### 7.3.5. Statistical analysis

Appropriate statistical comparisons were performed to determine whether the difference between various groups was statistically significant. A  $P < 0.05$  was considered significant.

Concerning the efficacy assessment, the median times to evaluation size (750mg) for all study groups were first analysed by application of the log rank (Kaplan-Meier) test to determine if any significant differences existed between groups. Upon identification that significant differences existed, multiple comparisons were performed to identify the groups that differ from one another.

One-way ANOVA was used to compare the weight differences of the various treatment and control group. For specific time points, Dunnett's multiple comparison (with control) post tests were used to identify statistically significant treatment-related weight loss.

Statistical significance was determined using Microsoft Excel analysis tools and GraphPad (Version 5).

## 7.4. Results

### 7.4.1. Acute toxicokinetics

All injections were well tolerated during the first 5 minutes post administration and subsequent observation points. Furthermore, the Riminocelle formulation was locally well tolerated at the injection site.

The animals in each group were monitored 3 times a day and weighed every second day for latent effects up to 14 days (Figure 7.1.). There is no statistically significant difference between the comparative weights on day 0 and day 14 for each respective treatment group. A slight trend can be seen in the second week for the Riminocelles group to increase in weight and the Taxol group to lose weight.

Poor weight matching and triaging into groups at the start of study could explain the observed difference in weight-time profiles between Riminocelles and Taxol. No clinical signs of toxicity were evident throughout the observation period.

Terminal blood samples drawn from 3 mice after 24 h in the pharmacokinetic study and from 3 mice after 7 days and 14 days post administration were assessed for plasma markers of toxicity and found to be within the normal range (Table 7.2.). The presence of GGT in the plasma of the Taxol treated group is noteworthy. On occasion, insufficient blood was collected to facilitate replicate measures of certain markers.

All carcasses within this initial pilot study underwent gross necropsy examination. No obvious lesions could be identified in either of the treatment groups. Macroscopic evaluation could not confirm specific or consistent organ pathology and therefore histopathology was not deemed prudent. Of mention is the yellow discoloration of body fat that is prominent even 14 days after acute administration of Riminocelles.

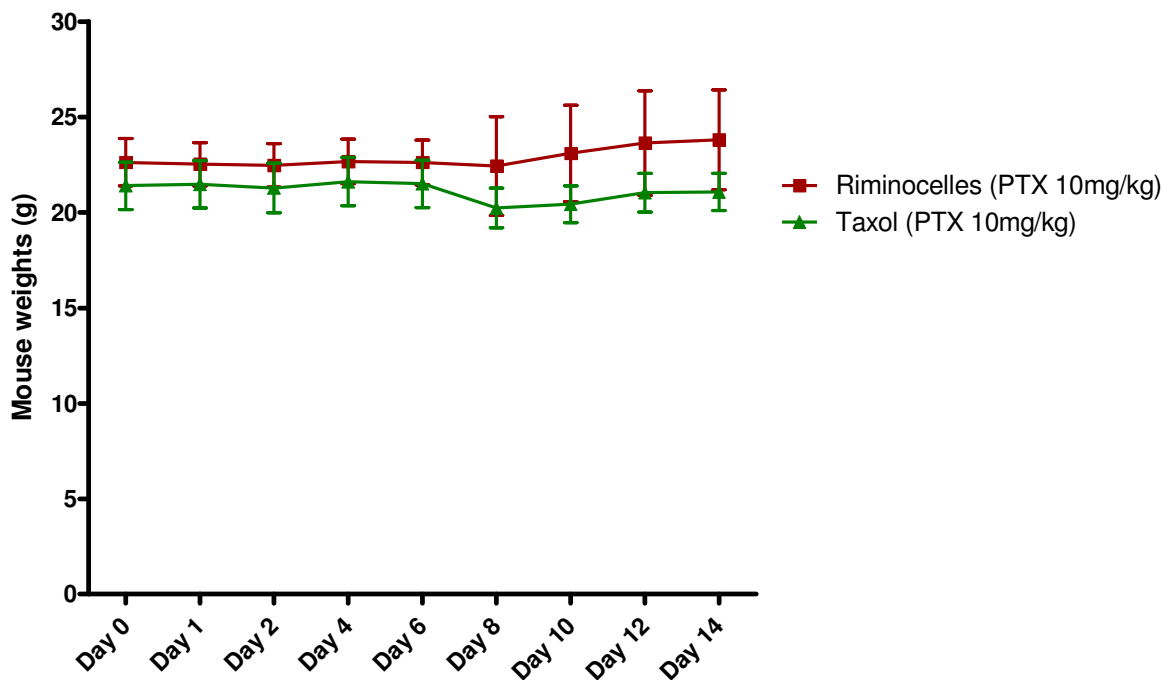


Figure 7.1. Weight changes after acute IV injection of Riminocelles and Taxol

**Table 7.2. Plasma toxicity biomarkers 1, 7 and 14 days after acute IV injection of Riminocelles and Taxol at a PTX dose of 1 mg/ml (n = 3)**

	Riminocelles						Taxol					
	Day 1		Day 7		Day 14		Day 1		Day 7		Day 14	
	Mean	SD	Mean	SD	Mean	SD	Mean	SD	Mean	SD	Mean	SD
<b>Clinical chemistry</b>												
ALT (IU/l)	31.2	5.1	26.3	2.5	22.0	*	28.6	2.7	33.3	18.2	26.7	6.4
AST (IU/l)	89.2	10.8	92.7	28.7	71.0	*	113.4	32.0	127.7	16.4	97.3	12.1
GGT (IU/l)	0.0	0.0	0.0	0.0	0.0	*	2.2	2.2	3.0	2.0	3.3	2.5
Urea (mM)	6.2	1.0	4.6	0.3	5.9	*	8.0	1.1	5.8	1.3	5.8	0.8
Creatinine (µM)	<18	0.0	<18	0.0	<18	*	<18	0.0	<18	0.0	<18	0.0
<b>Haematology</b>												
Hb (g/l)	135.8	3.3	148.5	3.5	134.0	18.4	138.8	4.7	131.3	10.6	135.3	3.8
RCC (x10 <sup>12</sup> /l)	8.6	0.3	9.8	0.2	8.5	1.1	8.8	0.3	8.7	0.4	8.4	0.4
HT (l/l)	0.4	0.0	0.5	0.0	0.4	0.1	0.4	0.0	0.4	0.0	0.4	0.0
MCV (fl)	48.0	1.1	46.8	0.4	46.5	1.3	47.0	0.8	47.2	4.2	48.2	1.7
MCH (g/dl)	15.7	0.3	15.2	0.0	15.8	0.0	15.7	0.1	15.1	1.6	16.1	0.6
MCHC (g/dl)	32.8	0.2	32.5	0.2	34.0	0.8	33.3	0.6	32.0	0.7	33.4	0.4
WCC(x10 <sup>9</sup> /l)	5.3	0.5	7.1	2.1	6.0	0.4	4.1	1.1	9.4	5.1	5.2	0.5
Neutrophils (x10 <sup>9</sup> /l)	1.4	0.3	1.9	0.2	1.5	0.9	1.0	0.6	2.9	3.6	1.2	0.3
Lymphocytes (x10 <sup>9</sup> /l)	3.7	0.4	4.9	1.7	4.2	0.3	2.9	1.5	5.2	1.6	3.7	0.3
Monocytes (x10 <sup>9</sup> /l)	0.1	0.1	0.3	0.1	0.2	0.1	0.1	0.1	1.0	1.2	0.3	0.2
Eosinophils (x10 <sup>9</sup> /l)	0.1	0.2	0.0	0.1	0.0	0.0	0.1	0.1	0.2	0.0	0.1	0.1
Basophils (x10 <sup>9</sup> /l)	0.0	0.0	0.0	0.0	0.0	0.0	0.0	0.0	0.1	0.1	0.0	0.0

\* Due to the low volume of blood drawn, replicate measure could not be attained

#### **7.4.2. GLP repeat dose toxicity**

A GLP repeat dose toxicity assessment of Riminocelles and Taxol was performed as part of the efficacy study. An equivalent PTX dose of 10 mg/kg for Riminocelles and Taxol was evaluated using two proposed dosing schedules of once a day (repeat for 7 days or unacceptable toxicity) and once a week repeat until progression or toxicity. Weight changes in tumour bearing mice were observed as an indicator of drug toxicity every second day until the end of the study (Figure 7.2.). Percent body weight loss at nadir and day of nadir were recorded (Table 7.3.).

Treatment began on day 7 when the mean tumour burden was 160 mg (range, 151-168 mg). The mean group body weight was well matched at the initiation of therapy (range, 22.5-23.2 g).

Statistical analysis of the percent body weight changes on day 14 revealed a statistically significant difference ( $P < 0.05$ ) between the control group and the Taxol (QDx7) group using one-way analysis of variance (ANOVA) with Dunnett's multiple comparison post-test (Figure 7.3.). Regardless, as these weight changes were minimal  $< 20\%$ , at this dosage both treatment regimens are considered well tolerated.



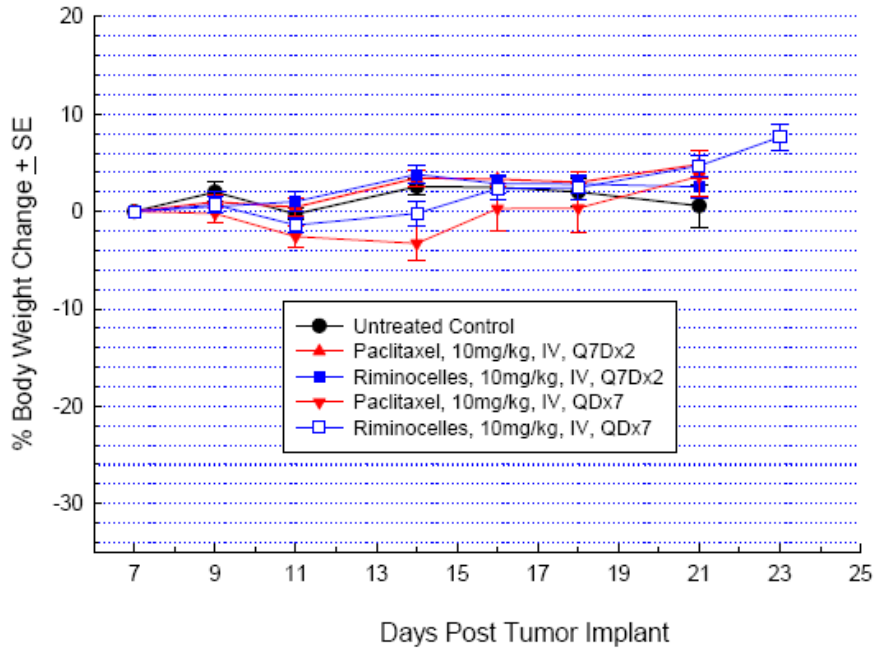


Figure 7.2. Percent body weight change for the respective groups for the duration of the study. Treatment began on day 7

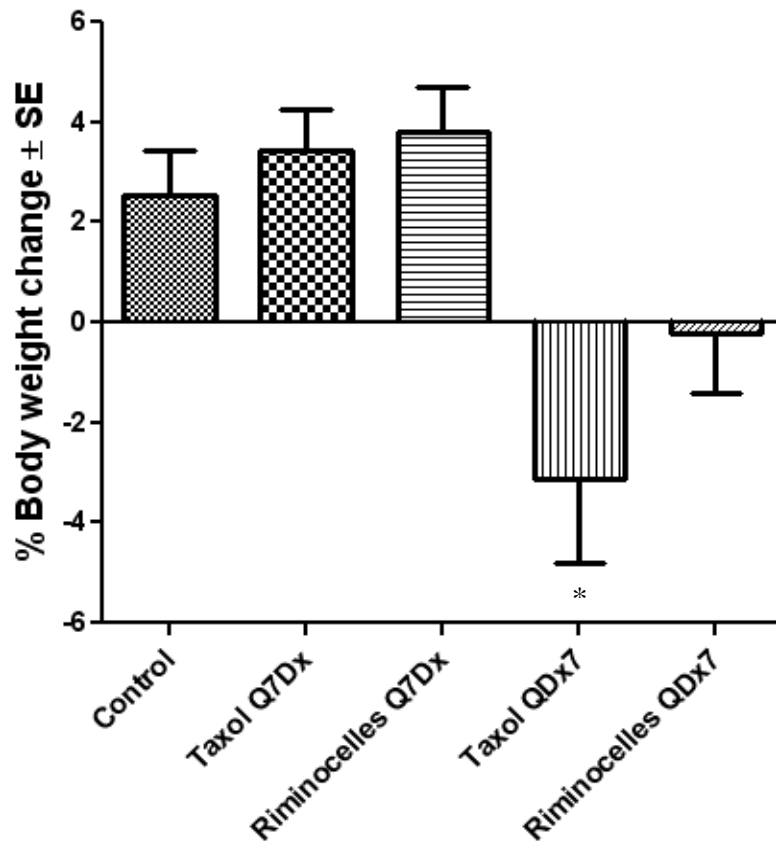


Figure 7.3. Percent body weight change on day 14 after dosing tumour bearing mice with Riminocelles and Taxol (10 mg/kg PTX).  $n = 8$ . One way ANOVA with Dunnett's multiple comparison post-test. \*  $P < 0.05$

### 7.4.3. Efficacy assessment

The control group reached a tumour evaluation size (750 mg) after 16 days and were all terminated due to tumour burden >1 g on day 22.

The activity of two different schedules of Taxol and Riminocelles against HCT-15 human xenografts is represented by the median tumour burden over time (Figure 7.4.), as this is the manner prescribed by the NCI for tumour-mass information. [149] It is immediately apparent that Riminocelles out performed Taxol. The log rank statistic for the survival curves was greater than would be expected by chance, that is to say there is a statically significant difference between the curves with a P value <0.001. A multiple comparison post-test was used to isolate the groups that differ from others. Treatment with Riminocelles at 10mg/kg following a schedule of QDx7 or Q7Dx4 produced statistically significant growth delays (T-C) of 3.2 and 2.7 days respectively at an evaluation size of 750 mg whilst treatment with Taxol did not result in any significant tumour growth delay (Table 7.3.). The tumour volume doubling time ( $T_d$ ) was determined to be 4.2 days and is within the historical range of the model. Tumour cell log kill (gross) is reported in Table 7.3. Treatment with Riminocelles following a schedule of QDx7 achieved the greatest tumour cell log kill value of 0.23.

Percent T/C values are shown in Figure 7.5. from the day treatment started to day 22 when the mice in the control group were terminated. The best %T/C was 54% produced by Riminocelles following a daily schedule after 4 days of treatment (day 11).

Previous calculations have considered only the median tumour burden of the groups. In Figure 7.6. the fate of individual mice is considered. In the Riminocelles group following a daily treatment schedule a greater proportion of the mice survive for longer. Treatment with Taxol was observed not to increase the time for tumour burden to reach >1 g.

Treatment with Riminocelles was well tolerated when administered IV. There were no clinical signs of toxicity or effect on vital organ function and necropsy findings

were limited to what appeared to be mild jaundice and yellow staining of the abdominal fat (Figure 7.7 and 7.8.) that can be attributed to riminophenazine disposition.

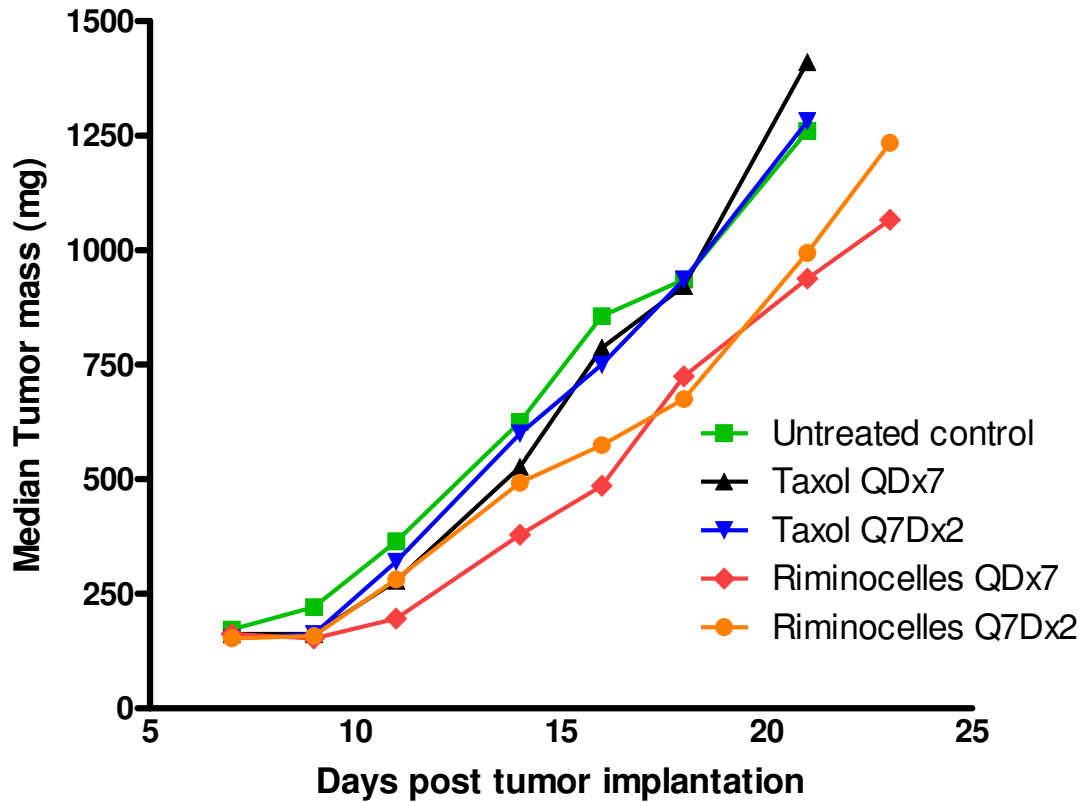


**Figure 7.4. Median tumour burden-time profile of HCT-15 subcutaneous xenografted human tumours in nude mice. Mice were treated with 10 mg/kg PTX as either Riminocelles or Taxol following two different schedules. Tumour growth delay measurements were determined at a size of 750 mg**

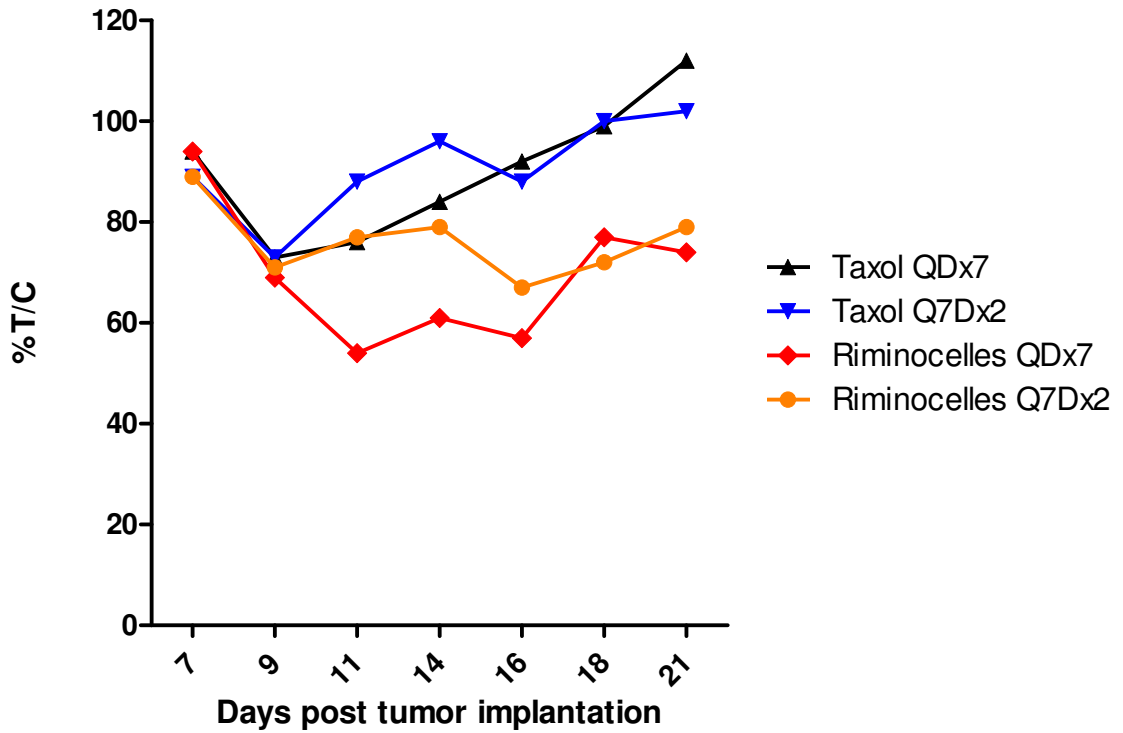


Figure 7.5. Tumour growth inhibition relative to untreated control over time expressed as % T/C

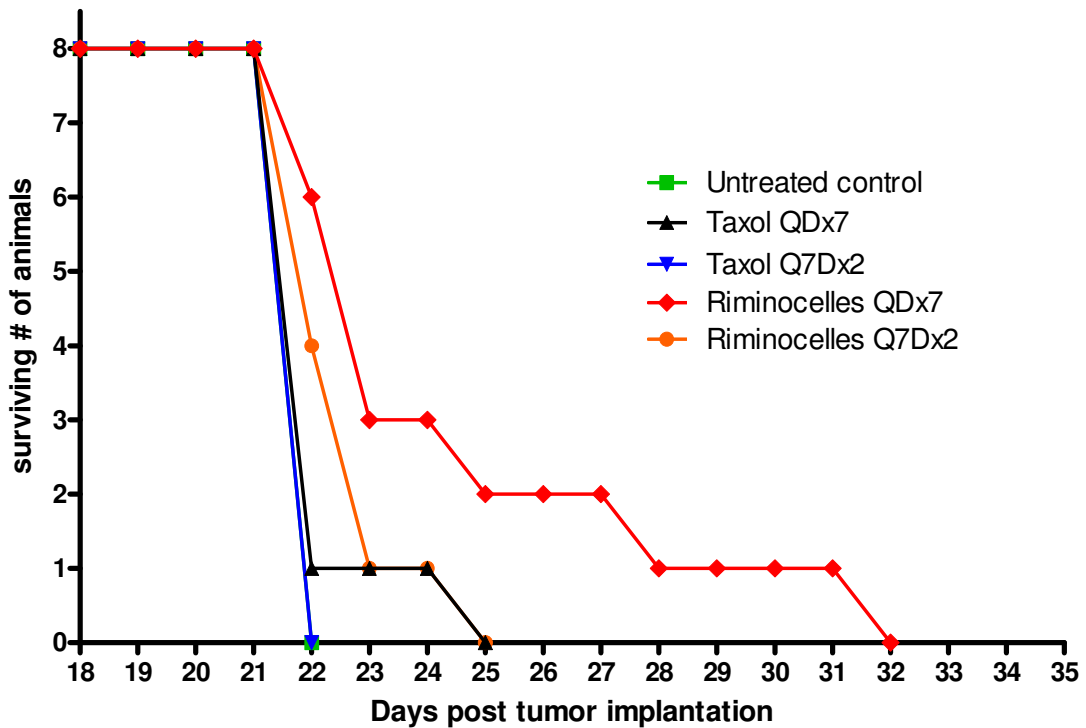


Figure 7.6. Time to tumour burden of 1000 mg for individual mice. The survival of Taxol treated mice (Q7Dx2) was no different to the untreated control

Table 7.3. Summary: Safety and efficacy of Riminocelles in comparison with Taxol

Treatment	Dose <sup>a</sup> (PTX) <sup>b</sup> (B663)	Schedule	Route	% Body wt. loss at nadir (day of nadir)	Rx related (day of nadir)	Tumour growth delay (day of nadir)	Tumour cell log kill (day of nadir)
Control	10 mg/kg <sup>a</sup>	NA	IV	0.4 (11)	0/8	NA	NA
Taxol	10 mg/kg <sup>a</sup>	QDx7	IV	3.5* (14)	0/8	0.5	0.04
Taxol	10 mg/kg <sup>a</sup>	Q7Dx2	IV	+	0/8	0.6	0.04
Riminocelles	10 mg/kg <sup>a</sup>	QDx7	IV	1.3 (11)	0/8	3.2*	0.23
Riminocelles	25 mg/kg <sup>b</sup>						
Riminocelles	10 mg/kg <sup>a</sup>	Q7Dx2	IV	+	0/8	2.7*	0.19
Riminocelles	25 mg/kg <sup>b</sup>						

+ Weight increases

\* P<0.05



**Figure 7.7. Mild “jaundice appearance” that occurred after Riminocelle administration reminiscent of characteristic clofazimine skin discoloration**

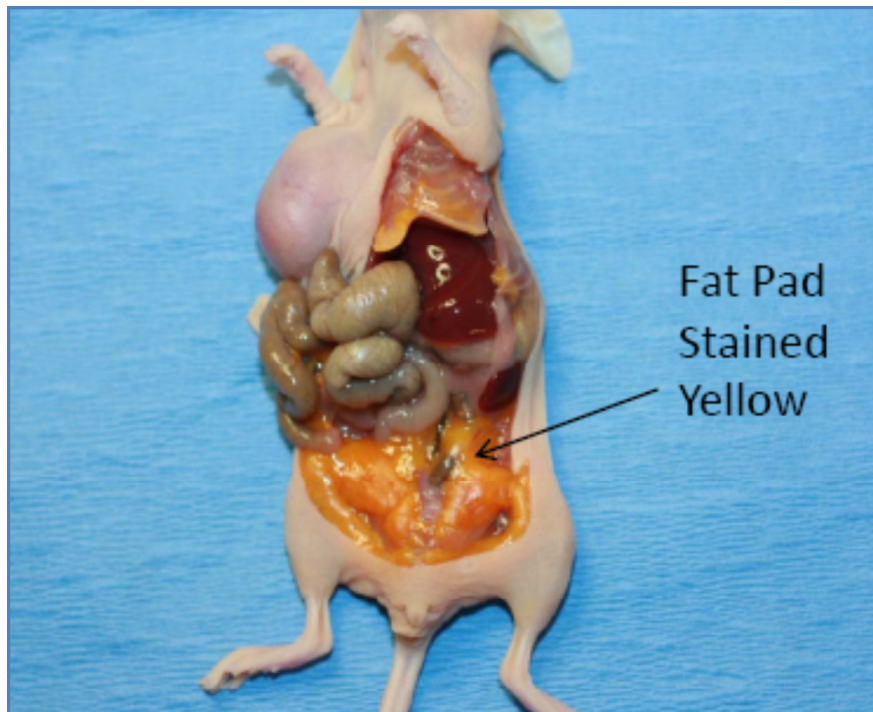


**Figure 7.8. Necropsy revealed yellow/orange stained fat tissue due to clofazimine disposition after Riminocelle administration**

## 7.5. Discussion and conclusion

The practicality of conducting pre-clinical studies using animal models must be weighed against what specific research questions have been raised and the information that can be gained. Ultimately, the value of any model lies in its ability to be predictive of the human scenario.

After demonstrating the IV suitability, local tolerability and lack of toxicity produced by Riminocelles in acute toxicity studies using normal healthy mice, the efficacy of Riminocelles was compared to Taxol at an equivalent PTX concentration of 10 mg/kg using highly drug resistant HCT-15 human colon adenocarcinoma cell cultures xenografted subcutaneously in nude mice. This study was performed as a proof of concept using a cancer cell model that demonstrates Pgp mediated MDR.

This study was designed so as to directly compare Riminocelles to that of the commercial formulation, Taxol. Crudely, the effect shown compared to Taxol can then be used as a reference to allow comparison with numerous other re-formulations that have already been or remain to be developed and evaluated *in vivo* with a parallel Taxol treatment group.

In terms of efficacy endpoints: the tumour cell kill values and the % T/C values attained for Riminocelles (while far superior to that attained for Taxol) are below that advocated by the NCI as indicating substantial activity warranting the initiation of clinical trials. Although Riminocelles statistically ( $P < 0.05$ ) outperformed Taxol in terms of efficacy, in this particular model of intrinsic Pgp expression, a PTX dose of 10 mg/kg was not sufficiently potent and the colon adenocarcinoma tumours still progressed rapidly.

Time to a maximum tumour burden of 1 g for individual mice promisingly revealed more mice in the Riminocelles treatment group to survive for longer compared to the Taxol treated groups. One mouse in particular (representing 12.5% of the population) following a daily treatment schedule survived for an additional 7 days compared to the Taxol group again highlighting the superiority of the novel co-



formulation. A shortcoming of this study was that it was not powered to distinguish whether the advantage gained is due to the fixed ratio drug combination or as result of the nanoparticulate delivery vehicle. To this end, future experimental designs could foreseeable include an additional group where clofazimine is administered via oral gavage in addition to Taxol.

In addition, future studies should make use of cancer types for which PTX is clinically indicated such as ovarian, breast and lung xenografts. The ICH S9 guideline [82] clearly stipulates that it is not a requirement to use the proposed clinical cancer type in pre-clinical studies. In clinical trials, all unresectable and refractory cancer patients could be potential volunteers.

In terms of safety: As prescribed by ICH M3R2, Riminocelles has been tested in a GLP compliant repeat dose toxicity study using a clinically representative dosage form. The lack of significant weight changes and the absence of acute toxicity biomarkers indicate that the dose of Riminocelles can be substantially increased (contrary to Taxol that incurred significant weight loss when administered daily). Future pre-clinical efficacy studies should be aimed at investigating a range of doses so as to determine the MTD of the co-formulation remembering that a tumour model is required to accurately assess the toxicity of cytotoxic drug products that by design are meant to distribute specifically to solid tumour tissue.

As the oral LD<sub>50</sub> for B663 in normal mice is >4 g/kg [31] it is reasonable to assume that the dose of B663 could be increased several fold without incurring toxicity. The current encapsulation efficacies achieved within Riminocelles would seemingly limit the B663 dose considering the maximum acute IV dosing volume that can be given safely to a mouse (<400 µl). Should volume restrictions and encapsulation efficacy impede dose increase, oral supplementation with B663 could be considered. The discoloration of adipose tissue and skin is an expected and reversible feature of B663 administration and should not be misinterpreted as jaundice nor as a dose limiting adverse effect. Specific distribution to and retention by fat tissue of B663 for sustained periods is a clear indicator that specific targeting to the tumour (in the most part) has not been achieved.



Before suggesting an appropriate starting dose for first in man studies, all the available pre-clinical data, particularly the pharmacokinetic data should be considered (chapter 8). Currently Taxol is being used clinically at several dosages and schedules with the optimal regimen not yet being clear. [138] The most common regimens (following appropriate premedication) are IV administration of 135 or 175 mg/m<sup>2</sup> over 3-24 h every three weeks. Shorter dosing intervals have typically been met with greater adverse effects presumable due to the cremophor vehicle. [135] It this study it has been demonstrated *in vivo* that novel cremophor-free vehicles could conceivable allow for a re-evaluation of the optimal PTX dosing schedule allowing for a greater cumulative dose to be administered in a shorter period of time (once daily for a week, or longer - if tolerated).

A repeat dose toxicity study in a second species (non-rodent) animal model is required prior to initiating clinical studies, as stipulated by ICH M3R2. [88] Such a repeat dose study will allow for a clinical study of the same duration to be initiated. Should a measurable benefit be seen in human cancer patients there would be no justification to stop treatment. [88] Strategically, such a repeat dose study in non-rodent animals mimicking the proposed clinical schedule is to be conducted last, only after rodent efficacy, toxicity and pharmacokinetic data has been scrutinised and progression justified.

In summation, the Riminocelles system was shown to be safe and efficacious in a human xenograft model of Pgp mediated drug resistant cancer cells. Riminocelles exhibits less toxicity and greater efficacy than Taxol. This study serves as a proof of concept, demonstrating that B663 combination with PTX is rational and can be used with benefit against Pgp expressing cancers.

This study is in support of previous clinical studies evaluating the anticancer activity of B663 [33, 34] The value of including B663 (even if administered orally as Lamprene) within taxane and additional combination chemotherapeutic regimens (doxorubicin) is definitive and should be considered by clinicians as a salvage route when faced with refractory cancer.

## 8. Development and application of an optimised and validated LC-MS/MS method

### 8.1. Introduction

LC with tandem MS/MS detection is a powerful technique that affords the quantitation of low picogram (on-column) amounts of several compounds in parallel. It is considered the method of choice for quantitation of compounds within diverse biological matrices. [150] LC-MS/MS detection in multiple reaction monitoring (MRM) mode gives the appearance of perfect selectivity because only the specific transitions of the analytes of interest are monitored (Q1>Q3). Viewing such an extracted ion chromatogram may give one the false sense that sample clean-up is not required; however co-eluting, undetected matrix components may suppress or enhance the ion intensity of analytes and thereby have a detrimental effect on the accuracy and precision of an assay. [151] It is therefore of importance to routinely evaluate the effect of the sample matrix on assay validity. Excipients, particularly surfactants used in drug formulation may themselves be a source of these matrix effects.

Pre-clinical development of drugs requires that a reliable bioanalytical method be available with sufficient sensitivity to quantitate drug concentrations within small samples facilitating pharmacokinetic studies in mice. In addition, the same analytical method may serve to determine compound stability at various storage conditions as well as to quantitate drug loading within various dosage forms.

Linearity, accuracy and precision, recovery as well as matrix effects were investigated as validation parameters. Matrix effects from several tissue samples were investigated quantitatively through comparison of the calibration standard slopes and mean peak areas (at equivalent nominal concentrations) of matrix matched and solvent based standard sets. Initial method development was supported by post-column, constant analyte infusion experiments that were used to qualitatively observe the matrix effects on individual analytes.

The objective was to develop a general sample clean-up method applicable to diverse sample matrices and to quantitate both PTX and B663 using a simple, rapid and validated LC-MS/MS method. This method was applied to the biopharmaceutical analysis of Riminocelles and Taxol so as to assess the influence of formulation upon the disposition of PTX.

## 8.2. Materials

Deionised water (~18M $\Omega$ ) was produced from the municipal water supply after processing by an ELGA purification unit (ELGA, Wycombe, UK). Ammonium hydroxide solution was purchased from Merck (Darmstadt, Germany). Mass spectrometry grade methanol (MeOH) and formic acid (HCO<sub>2</sub>H) were purchased from Fluka Analytical (Buchs, Switzerland). Methyl *tert* butyl ether (MtBE) was purchased from Sigma Aldrich (St Louis, MO, USA).

Paclitaxel (PTX) and its internal standard Docetaxel (DTX) were purchase from Sigma Aldrich (St Louis, MO, USA). Clofazimine (B663) was supplied by Dr J.F. O' Sullivan, (Laboratories of the Medical Research Council of Ireland, Trinity College, Dublin, Republic of Ireland).

DSPE PEG 2000 and LIPOID S 75-3 samples were generously provided by Lipoid GmbH (Ludwigshafen, Germany) and were used to co-formulate PTX and B663 within mixed lipopolymeric micelles (Riminocelles) at a final concentration of 1 mg/ml and 2.5 mg/ml respectively. Concentrated Taxol 6 mg/ml was prepared in house with 50:50 (v/v) Cremophor EL: ethanol. Prior to administration, Taxol was diluted to 1 mg/ml with sterile saline 0.9% (w/v).

## 8.3. Methodology

### 8.3.1. Stock solutions, calibration standards, quality control and recovery samples

Numerous 0.5 mg/ml stock solutions of the individual analytes (PTX and B663) and 0.2 mg/ml stock solutions of the internal standard (DTX) were prepared in MeOH. The solutions were aliquoted and stored in microreaction vials at -20°C.

Working solutions of each analyte were separately prepared on each day of experimentation from stock solutions to 5000 ng/ml before the two analytes were mixed in equal volumes and further diluted with MeOH to produce a concentration of 1250 ng/ml each for both analytes. Further working solutions were prepared through appropriate serial dilution into six clean tubes.

These six working solutions were diluted 4:1 with 1000 ng/ml DTX to prepare appropriate volumes of the following final (analyte equivalent) MeOH calibration standards: 1.95, 7.81, 31.25, 125, 500, 1000 ng/ml (all with a final constant DTX concentration of 200 ng/ml).

Matrix matched calibration standards for each tissue (liver, kidney, fat, spleen and plasma) were prepared by reconstituting (with the aid of sonication) dried drug naïve control tissue sample extracts within 500 µl of the various calibration solutions.

Three independent quality control (QC<sub>100</sub>) samples of 100 ng/ml in MeOH were prepared on each day of experimentation. In addition, recovery samples (10, 250 and 500 ng in extraction solvent (final volume in vial 500 µl, therefore 20, 500 and 1000 ng/ml) were spiked into each of the blank tissue matrices (from drug naïve control mice) prior to extraction and comparing recovered analyte concentration versus expected analyte concentration and reported as a percent recovery.

Each day of analysis therefore included: triplicate runs of newly prepared blank standards; triplicate runs of matrix matched standards; triplicate quality control

(QC<sub>100</sub>) runs and triplicate runs of three recovery samples from each of the respective matrices at three nominal concentrations (20, 500, 1000 ng/ml) spanning the calibration range.

Replicate sets of known concentrations were run before and after the analysis of the unknown samples thereby allowing the assessment of analyte stability over the time required for sample processing.

### **8.3.2. Sample preparation**

Liquid-liquid extraction with MtBE was used for mouse plasma sample preparation. In brief, 50 µl of each plasma sample was aliquoted into a clean 2 ml microcentrifuge tube. For recovery samples, known amounts of analytes (in MeOH) were spiked pre-extraction into control (drug naïve) plasma to facilitate recovery assessment. Half a millilitre of MtBE was added and the mixture thoroughly vortex mixed, then centrifuged (Heraeus Instruments, Megafuge 1.0R) at 15 000 x *g* for 10 min at 10 °C and finally placed in -70 °C to freeze the aqueous layer. The upper, fluid ether layer was decanted into clean microcentrifuge tubes. This procedure was repeated thrice, each time pooling the organic layer that was subsequently dried using a Centrivap vacuum centrifuge concentrator with cold trap (Labconco) and reconstituted with the aid of sonication bath in 400 µl MeOH (with or without standards depending on whether the sample was an unknown or a matrix matched standard) and 100 µl IS solution.

Concerning different mouse tissues, representative sections (target 20 mg, range 15-25 mg) were accurately weighed into clean microcentrifuge tubes. After adding 1 ml of a 95% MeOH in 1% HCO<sub>2</sub>H solution (with addition of analyte spikes for recovery samples), the mixtures were homogenized using an ultrasonicator (Biologics, Inc. Model 3000) with a power output of ~ 150 watts at 20 kHz (80% pulse - to ensure that the samples did not overheat) for 2 min using a stepped titanium micro tip (3.81 mm diameter). The samples were centrifuged at 15 000 x *g* for 10 min at 10 °C, the supernatant was carefully removed, transferred to new tubes and dried in a Centrivap vacuum centrifuge to approximately 200 µl before

being diluted 1:3 with 1% HCO<sub>2</sub>H in water to ensure full analyte ionization and loaded onto a SPE cartridge (BondElut Plexa 60 mg, 1 ml) that had been sequentially conditioned and equilibrated with 1 ml of MeOH and H<sub>2</sub>O respectively. The cartridges were washed with 1 ml of 40% MeOH before the analytes were eluted with 95% MeOH in 1% HCO<sub>2</sub>H followed by a 50 µl MeOH slug to clean the frit. Similar to the plasma procedure the cleaned extracts were dried using a Centrivap vacuum centrifuge concentrator and reconstituted in 400 µl MeOH and 100 µl IS solution. Thereafter all samples were transferred to clean, clear 2 ml vials with snap caps (Chromacol, Trumbull, USA) before injection of 10 µl into the LC-MS/MS system for analysis.

Various matrix blanks from different tissue taken from drug naïve control mice were likewise processed to facilitate qualitative evaluation of matrix effects over the course of the chromatographic run through post column, direct infusion experiments. Through such means, zones of matrix interferences with the chromatographic run were identified.

### **8.3.3. Chromatographic conditions**

An Agilent 1100 series HPLC consisting of a binary pump, vacuum degasser and an autosampler was used. Baseline chromatographic separation was achieved with an Apollo C18 (150 mm x 4.6 mm), 5 µm column protected by a C18 Security Guard cartridge. As isocratic mobile phase of 95% MeOH in 0.1% HCO<sub>2</sub>H (pH adjusted with ammonia hydroxide to 3.5) was used at a flow rate of 1 ml/min and column temperature of 40 °C. The total run time was 5 min.

### **8.3.4. Mass spectrometric conditions**

An AB Sciex 4000 QTrap mass spectrometer (Applied Biosystems/ MDS Sciex) with a Turbo “V” electrospray ionization (ESI) source was operated in positive ion mode using Multiple Reaction Monitoring (MRM).

Compound dependent ionization parameters were quantitatively optimized for each drug (in mobile phase) through direct injection into the ESI source using a Harvard syringe pump at a constant flow rate of 10 $\mu$ l/min.

Compound independent parameters that remained constant were as follows: Curtain gas, 25 psi; Ion spray voltage, 5500 V; Ion source temperature, 450 °C; Ion source gas 1, 35 psi; Ion source gas 2, 40 psi; Collision gas, medium; Entrance potential, 10 V.; Collision cell exit potential, 12 V.

All modules of the complete LC-MS/MS system were centrally operated by Analyst software, version 1.5.2 (Applied Biosystems/MDS Sciex) facilitating data acquisition and processing.

### 8.3.5. Validation procedures

Validation of the bioassay was performed with due consideration to FDA guidelines for Bioanalytical Methods Validation [152].

Linearity was assessed in various sets of MeOH and various matrix matched standards over the concentration range of 1.95-1000 ng/ml. Intra-day precision and accuracy were determined for both MeOH standards and for each specific tissue matrix by analysing replicates of three nominal concentrations (1.95, 31.25 and 500 ng/ml). Inter-day precision and accuracy was determined for three nominal concentrations in MeOH on 5 separate days. Percent coefficient of variance (% CV) was used as the measure of precision. The percent accuracy (% Accuracy) was determined by comparison of the measured concentration with known nominal concentration. Deviations greater than  $\pm 15\%$  away from the expected nominal concentration indicate unacceptable accuracy and precision.

Extraction recovery (%) of the two analytes was assessed at three levels (20, 500, 1000 ng/ml) in triplicate by spiking blank matrix prior to sample processing and expressing recovery as mean percentage  $\pm$  SD of the expected concentration.



Matrix effects were evaluated in three ways: firstly the slope of calibration curves for a particular matrix were compared with the slope of a blank matrix (solvent) calibration curve and expressed as the slope factor; secondly through determination of percentage matrix effect (% ME) by comparing the mean peak area of matrix matched standards with the peak area of blank matrix standards at various nominal concentrations; thirdly, matrix effects were qualitatively observed through direct post-column infusion of the analytes whilst injecting relevant reconstituted drug naïve (blank matrix) extracts using the LC autosampler.

### 8.3.6. Application in pharmacokinetic study

The optimized LC-MS/MS analytical method was used to assess the pharmacokinetics and tissue distribution of the novel co-formulation in parallel with an equivalent PTX dose (10 mg/kg) of Taxol. Fifty five female BALB/c mice were acclimatized to laboratory setting for a week prior to experimentation. The animals were fed standard rodent feed and water *ad libitum*. Prior to experimentation, mice were randomly assigned to eleven cages of five mice each. The two PTX formulations were administered to five mice at each time point (30 min, 1, 3, 6 and 24 h). Before IV administration of the formulation via the lateral tail vein, each animal was weighed and an appropriate dose calculated. Precise timing of when the dose was given and when the animal was euthanised was documented in study monitoring sheets. Saline was administered to 5 mice who were euthanised after 24 h serving as the source of blank drug naïve matrix.

At euthanasia, blood samples were drawn via cardiac puncture from isoflurane anaesthetized mice into heparin treated paediatric blood collection tubes. Blood samples (~500 µl) were immediately centrifuged, plasma harvested, appropriately labelled with group, time and dose and stored at -70°C. Organs (liver, spleen, kidney and adipose tissue) were dissected out, labelled and stored at -70°C until analysed.



This study complied with the SANS 10386:2008 guidelines for research animals with ethical approval given by the Animal Use and Care Committee (AUCC) of the University of Pretoria (Project # H10-09).

The study schedule followed is summarised in Appendix C.

## 8.4. Results and discussion

### 8.4.1. Chromatography and Mass spectrometry

Infusion based quantitative optimization experiments were conducted to achieve the greatest possible signal. Optimized MRM transition parameters for each of the compounds attained in positive ion mode are presented in Table 8.1.

Baseline chromatographic separation of the two analytes was achieved using a simple isocratic mobile phase in 5 min. Due to the similarity in structure, the internal standard, DTX and PTX were shown to co-elute with a retention time (RT) of 1.76 min. The isocratic method favouring a fast run time (without the necessity of column re-equilibration) was seen as favourable over achieving resolution between the taxanes having different molecular masses. No fragment cross talk (Q3) was evident between the co-eluting taxane (PTX and DTX) fragments due to the different characteristic fragment ions selected. A MRM dwell time of 50 ms allowed for sufficient data points to be acquired across the respective ~30 second peak widths of PTX and DTX without any loss in sensitivity.

B663 eluted with a retention time of 3.61 min. A representative MRM chromatogram is shown in Figure 8.1. Numerous studies have reported MS detection of PTX. This is the first study using MS for the detection of B663.

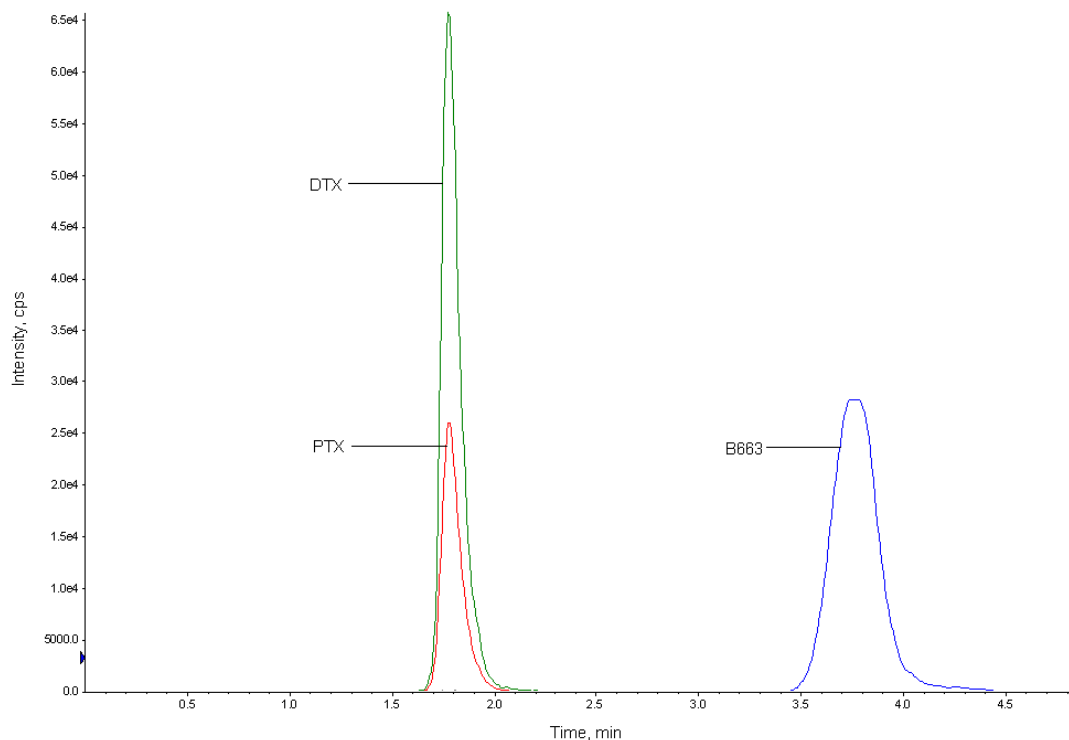


**Figure 8.1. Representative Extracted Ion Chromatogram (XIC) of paclitaxel (PTX), docetaxel (DTX) and clofazimine (B663). Mobile phase: 95% MeOH in 0.1% HCO<sub>2</sub>H (pH 3.5 with ammonium hydroxide). Green - DTX; Red - PTX; Blue - B663**

**Table 8.1. Quantitatively optimised MRM transitions determined for the analytes and IS after direct infusion into the ESI source**

<b>Compound</b>	<b>MRM transition (m/z)</b>	<b>DP (V)</b>	<b>CE (V)</b>	<b>CXP</b>
<b>Paclitaxel</b>	854.3 > 569.4	51	17	8
<b>Clofazimine</b>	474.0 > 431.1	76	51	12
<b>Docetaxel</b>	808.3 > 527.2	46	15	4

#### 8.4.2. Assay validation parameters

Specificity was determined using blank matrix of drug naïve mice where no peaks were detected using the specified MRM transitions. A standard curve for PTX was established by plotting concentration versus the ratio of the peak area of PTX to that of chemically similar DTX (IS) to increase the accuracy and precision of the assay by corrected for small amounts of variation including matrix effects. The calibration curve for B663 used external standardization alone considering the large peak area and matrix elution zone differences between B663 and DTX.

A reproducible linear relationship between concentration and detector response was observed for both analytes over the concentration range of 1.95-1000 ng/ml with average correlation coefficients being above 0.99 for most sample matrices using a weighting factor of  $1/x^2$  due to the use of serial dilution sequence. The linear equations describing the calibration curves in various matrices are shown in Table 8.2. The LOQs were established as being the lowest points of the standard curves, i.e. 1.95 ng/ml as the variability in quantitation was less than  $\pm 15\%$ .

Results of intra-day and inter-day accuracy and precision of the assay in MeOH are shown in Table 8.3. Both the accuracy and the precision on any of the given 5 days for the selected standards and independent quality control (QC<sub>100</sub>) samples were within the defined  $\pm 15\%$  acceptance criteria. The results of assay performance for each respective matrix are shown in Table 8.4. In nearly all cases the precision of the assay declined with decreasing concentrations. Selected nominal standard concentrations of analysis were within 15% reflecting the suitability of assay.

Recovery using liquid-liquid extraction with MtBE was found to extract  $100.93\% \pm 15.79$  of PTX and  $103.65\% \pm 4.95$  of B663 from plasma at a spiked concentration of 100 ng/ml. Ultrasonic extraction of various tissue sections into an acidic buffer followed by C18 SPE (following a generic method) was shown to effectively extract and efficiently clean-up the analytes of interest (Table 8.5). Generally, the extraction efficacy was found to be concentration-independent regardless of the

matrix. The variability and in certain cases low extraction yield (B663) attained by using a generic sample preparation protocol for all tissues attests to the diversity each respective tissue matrix.

This slope of the lines of the respective matrix calibration standards was compared to the slope constructed for solvent calibrators to produce a slope factor designating the overall extent of the matrix effect over the entire calibration range (Table 8.2). The effect of matrix was largely mitigated through adequate sample preparation as shown through post-column, constant infusion experiments and did not greatly influence the assay outcomes (Figure 8.2). Both B663 and PTX were shown to have similar matrix effect-time profiles (degree of suppression) suggesting the presence of easily ionizable compounds from tissue matrix competing successfully for charge in the ESI source (Figure 8.2.A).

**Table 8.2. Mean standard calibration lines of paclitaxel (PTX) and clofazimine (B663) in blank solvent and various matrices comparing the slope as an expression of matrix interference over the full calibration range**

Compound	Calibration range	Equation	Weighting factor	R	Slope factor
		<b>MeOH</b>			
<b>Paclitaxel</b>	1.95-1000 ng/ml	$y=2.34X + 0.0255$	$1/x^2$	0.99	1
<b>Clofazimine</b>	1.95-1000 ng/ml	$y=1.41 \times 10^4 X + 2.12 \times 10^4$	$1/x^2$	0.99	1
		<b>Plasma</b>			
<b>Paclitaxel</b>	1.95-1000 ng/ml	$y=2.63X + 0.00128$	$1/x^2$	0.99	1.12
<b>Clofazimine</b>	1.95-1000 ng/ml	$y=1.53 \times 10^4 X + 9.44 \times 10^4$	$1/x^2$	0.99	1.09
		<b>Liver</b>			
<b>Paclitaxel</b>	1.95-1000 ng/ml	$y=4.44X + 0.0023$	$1/x^2$	0.99	1.90
<b>Clofazimine</b>	1.95-1000 ng/ml	$y=2.61 \times 10^4 X + 3.59 \times 10^4$	$1/x^2$	0.99	1.85
		<b>Spleen</b>			
<b>Paclitaxel</b>	1.95-1000 ng/ml	$y=2.42X + 0.00675$	$1/x^2$	0.99	1.03
<b>Clofazimine</b>	1.95-1000 ng/ml	$y=2.77 \times 10^4 X + 5.1 \times 10^4$	$1/x^2$	0.97	1.96
		<b>Kidney</b>			
<b>Paclitaxel</b>	1.95-1000 ng/ml	$y=2.27X + 0.00493$	$1/x^2$	0.99	0.97
<b>Clofazimine</b>	1.95-1000 ng/ml	$y=2.9 \times 10^4 X + 4.47 \times 10^4$	$1/x^2$	0.98	2.06
		<b>Fat</b>			
<b>Paclitaxel</b>	1.95-1000 ng/ml	$y=2.42X + 0.00675$	$1/x^2$	0.99	1.03
<b>Clofazimine</b>	1.95-1000 ng/ml	$y=2.28 \times 10^4 X + 2.1 \times 10^4$	$1/x^2$	0.99	1.62

**Table 8.3. Inter- (n = 3) and intra- (n = 5) day precision and accuracy of the analytes in MeOH and QC of the assay**

Nominal [ ] (ng/ml)	<u>PTX</u>			<u>B663</u>		
	Calculated mean (ng/ml)	% CV	% Accuracy	Calculated mean (ng/ml)	% CV	% Accuracy
<b>Intra-day</b>						
1.95	1.86	9.14	97.83	1.83	8.75	96.54
31.25	33.37	2.04	106.62	34.39	1.46	109.89
500	462.95	12.30	92.60	457.19	5.13	91.44
QC <sub>100</sub>	106.67	4.30	106.67	114.00	1.10	114.00
<b>Inter-day</b>						
1.95	1.89	13.18	96.67	1.82	19.75	93.48
31.25	29.13	13.06	93.07	29.72	14.32	94.96
500	427.64	5.08	85.53	493.76	14.52	98.75
QC <sub>100</sub>	96.75	10.96	96.75	90.45	6.09	90.45

**Table 8.4. Performance of the assay and matrix effects. Intraday accuracy and precision (n = 3) of analytes at various nominal concentrations from plasma and various tissues**

Nominal [ ] (ng/ml)	<u>PTX</u>				<u>B663</u>			
	Calculated mean (ng/ml)	% CV	% Accuracy	% ME*	Calculated mean (ng/ml)	% CV	% Accuracy	% ME
<b>Liver</b>								
1.95	1.95	6.55	99.88	90.60	1.91	11.53	97.93	114.10
31.25	32.39	5.25	103.47	38.50	34.91	3.95	111.55	86.93
500	488.42	3.26	97.68	46.10	463.87	3.05	92.77	91.00
<b>Spleen</b>								
1.95	1.96	4.66	100.10	65.60	1.89	15.60	96.97	140.50
31.25	31.20	6.18	99.68	61.10	34.17	14.70	104.62	105.80
500	501.57	3.34	100.31	65.60	474.14	13.70	94.83	109.20
<b>Kidney</b>								
1.95	1.93	14.65	99.12	48.90	1.83	8.90	94.02	132.70
31.25	30.30	2.71	96.79	43.70	34.85	10.70	111.34	112.40
500	509.26	3.77	101.85	49.00	455.98	8.47	91.20	110.00
<b>Fat</b>								
1.95	1.97	14.22	101.28	56.60	1.92	12.98	98.41	88.00
31.25	32.05	4.17	102.39	59.30	34.55	14.00	110.38	86.24
500	482.82	3.82	96.56	64.10	472.81	12.69	94.56	89.70
<b>Plasma</b>								
1.95	1.94	1.60	99.30	69.46	1.85	10.36	94.89	134.34
31.25	33.88	1.55	108.25	85.15	31.51	3.54	100.66	98.4
500	477.43	1.32	95.49	96.34	493.81	4.98	98.76	107.38

\* % ME = percentage change due to matrix effects

**Table 8.5. Recovery (extraction efficacy %  $\pm$ SD) of paclitaxel and clofazimine form various tissue matrices, (n=3)**

Nominal [ ] (ng/ml)	Liver		Kidney		Spleen		Fat	
	PTX	B663	PTX	B663	PTX	B663	PTX	B663
<b>20</b>	97.6 $\pm$ 22.4	33.5 $\pm$ 1.4	86.2 $\pm$ 2.6	59.5 $\pm$ 7.8	98.7 $\pm$ 8.5	95.8 $\pm$ 17	75.3 $\pm$ 2.6	60.4 $\pm$ 11.5
<b>500</b>	104.5 $\pm$ 2	45.2 $\pm$ 20.9	93.3 $\pm$ 3.9	60 $\pm$ 7.6	89.1 $\pm$ 1.5	47.8 $\pm$ 7.5	80.9 $\pm$ 3.5	65 $\pm$ 12.5
<b>1000</b>	102 $\pm$ 6	42 $\pm$ 9.2	92.4 $\pm$ 3.9	52.4 $\pm$ 6	91.6 $\pm$ 7.2	60.5 $\pm$ 7.6	69 $\pm$ 1.8	50.1 $\pm$ 14.4



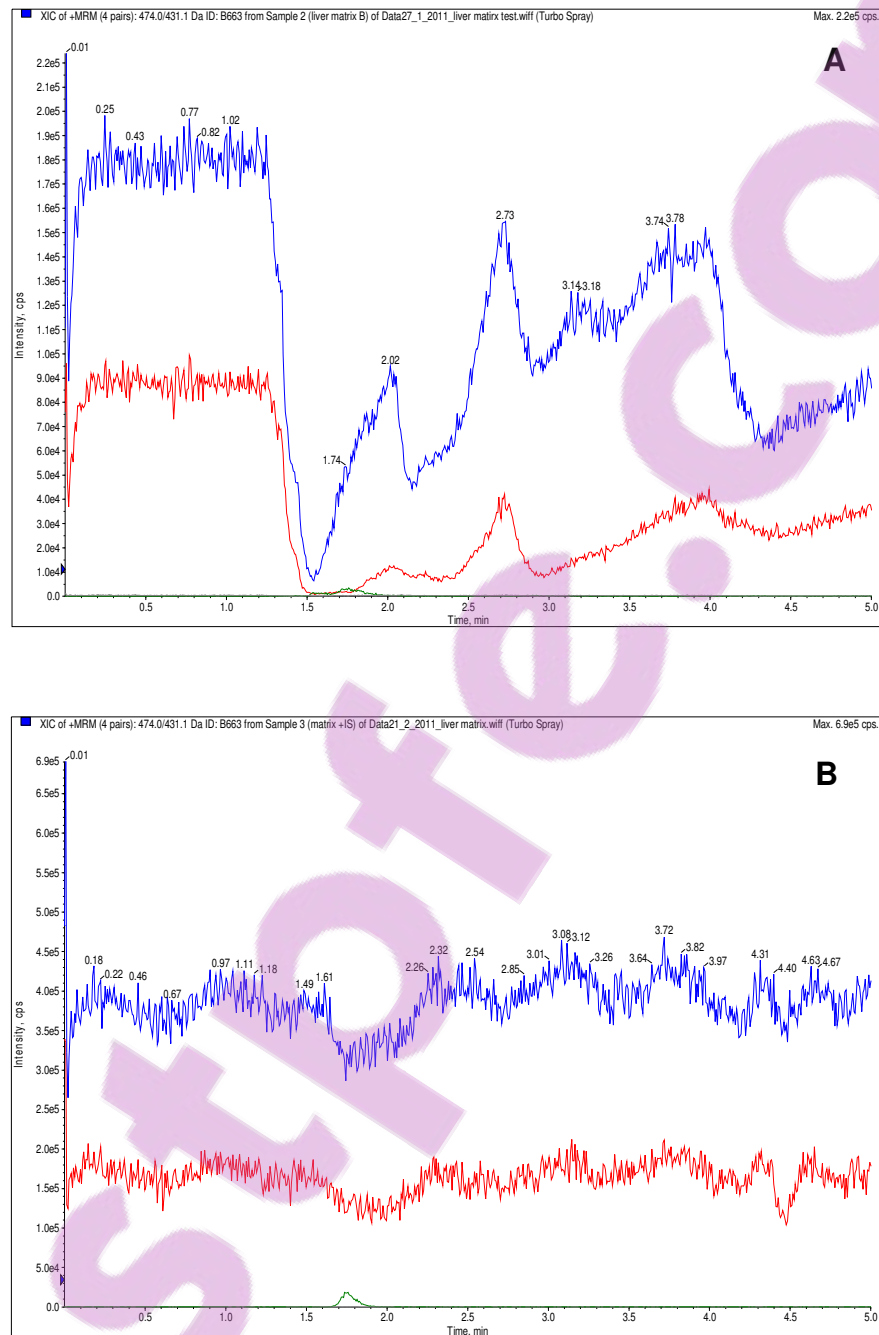


**Figure 8.2. Qualitative matrix monitoring: Direct post-column infusion of an analyte mixture into the ESI source at constant flow rate whilst separating a blank tissue extract (Liver matrix) by the LC-MS/MS method. Red - PTX; Blue - B663**

**A) Prior to SPE B) After SPE clean up.**

### 8.4.3. Method application

Despite the low recoveries attained for B663 from various tissue matrices using the generic extraction and SPE sample preparation procedures, the simple isocratic method proved robust and validation parameters suggested the suitability of the method to reproducibly quantitate the analytes accurately from diverse matrices. The developed and optimized sample clean up and LC-MS/MS methods were applied to assess the pharmacokinetics and tissue disposition of the PTX-B663 nanoparticulate co-formulation (Riminocelles) in comparison to Taxol at an equivalent PTX dose of 10 mg/kg.

Statistically significant differences ( $P < 0.05$ ) were found for the PTX concentration (between the two formulations) within plasma after 30 min and 1 hr. (Figure 8.3.) and within the liver after 30 min (Figure 8.3.) indicating that the micellar nanoparticulate delivery system appears to accumulate preferentially within the liver. This same effect has been reported for paclitaxel-loaded gelatine nanoparticles [150]. The highest concentration of PTX for both formulations was found in the liver which is to be expected and in general a similar tissue disposition time profile was shown for fat, kidney and spleen independent of which formulation was administered (Figure 8.3.). After initial distribution primarily to the liver, B663 was seen to slowly re-enter the plasma compartment reaching a  $C_{max}$  at 3 h and to ultimately accumulate in (and stain) fat tissue for prolonged periods as is a well-established characteristic of B663. [154]

Of importance is that the tissue concentration-time profiles demonstrate that the *in vitro* optimized fixed ratio (PTX:B663) is not maintained in circulation for longer than the first 30 min. This is suggestive of rapid micelle dissociation due to *in vivo* thermodynamic instability owing to the abundant presence of plasma proteins, especially albumin [155]. This lack of micelle integrity has a direct impact on the efficacy of the developed nanoparticulate co-formulation. The specified (*in vitro* optimised) synergistic FRDC is not maintained *in vivo* nor are the drugs (now free) selectively delivered to the tumour site.

The success of ratio dependent synergistic drug interactions is dependent upon the development of delivery systems that are stable after intravenous administration and that avoid immune recognition permitting prolonged systemic circulation facilitating passive tumour accumulation. Without such delivery systems the full potential of synergistic FRDC cannot be realised and clinically utilized against disseminated cancer.

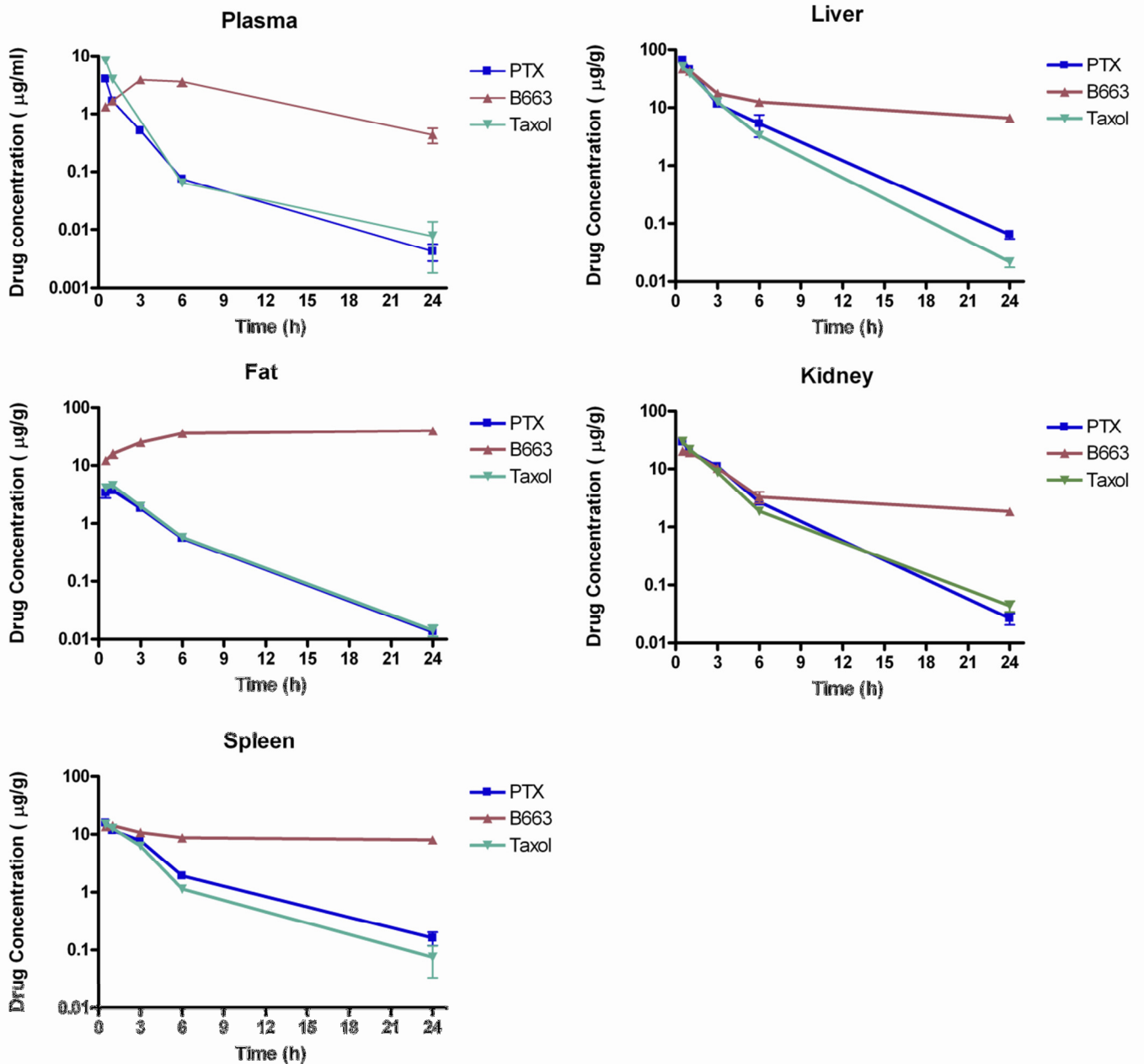


Figure 8.3. Plasma and various tissue concentration time profiles after an IV bolus administration of Taxol (10 mg/kg PTX) and a novel co-formulation (10 mg/kg PTX and 25 mg/kg B663)

## 8.5. Conclusion

In conclusion, an optimized and validated LC-MS/MS method has been developed for the quantitation of paclitaxel and clofazimine from diverse tissue sources. Good linearity with  $r > 0.99$  was attained over a concentration range of 1.95 ng/ml - 1000 ng/ml. The sensitivity of this method is demonstrated by the fact that only 50  $\mu$ l of mouse plasma and 20 mg of tissue were required for analysis. The LOQ of the method was established as 1.95 ng/ml for both PTX and B663. Acceptable recoveries and mitigation of matrix effects through sample clean up suggests that this method is suitable for a wide range of applications. The method could be successfully applied in a pharmacokinetic study of a novel nanoparticulate co-formulation of PTX and B663 following IV administration.

The large differential change of the ratio of PTX to B663 in various tissue types is thought indicative of micelle disassembly due to the *in vivo* thermodynamic instability of lipopolymeric micelles constructed from DSPE-PEG 2000 and lecithin. The pharmacokinetics and tissue disposition of PTX was very similar for both Taxol and Riminocelles. Although Riminocelles did not positively alter (control) the pharmacokinetics of PTX, Riminocelles is a well-tolerated, Cremophor-free IV formulation and will therefore avoid the need for premedication clinically to prevent the allergic reactions associated with this excipient.

The results of this study are in strong support of improving the *in vivo* integrity of such simple lipopolymeric micelles so as to maintain the optimised fixed-ratio of the drugs and support tumour targeting.

## 9. Final discussion and conclusions

In 2008, cancer accounted for 13% of all deaths. [1] As medical and chemical science improves, so too should the prognosis and cure rate for these patients. Metastasis is largely responsible for cancer deaths - approximately 30% of patients have clinically detectable metastasis at the time of diagnosis. [156] Therefore therapeutic interventions have to be systemic in nature in order to tackle cancer dissemination. One of the major reasons for the relatively poor prognosis of cancer is resistance to existing treatments and therefore developing agents that are active against MDR cancer cells is a primary objective of contemporary oncology R&D.

With focused efforts worldwide, our understanding of the genotypic and phenotypic biochemical differences between neoplastic and normal cells is increasing. There is therefore much hope that through further research and better understanding, small molecule drugs or biologicals that are “perfectly” selective for a particular cancer can be designed or discovered and utilized to elicit true cures.

The worldwide anticancer market in 2009 was a reputed 50 billion US\$. [157] It is not then surprising that big pharma spends in excess of 25% of its R&D budget on the development of such products. [158] In this time of industry “crisis” and worldwide economic challenges, the pharma industry is following and relying upon a strategy of rational target design to achieve success and return on investment. [159]

Rational drug design involves first identifying a receptor target. Good targets would be critically involved with cell growth or survival and would ideally be highly specific to cancer cells. After a target receptor has been identified: computer modelling, combinatorial chemistry and HTS are tools that can be used to identify structurally complementary small-molecules (ligands) for further pre-clinical development (formulation and *in vivo* proof). In addition, humanized MAbs can be genetically engineered with hybridoma technology to specifically target a unique cancer cell antigen of choice, targeting immune responses and directing active delivery of cytotoxins after encapsulation within NDDS. [160]

There should be very good reason behind pursuing a particular TPP and not just random screening. Drug development is costly, even in the academic environment. The industry needs return on research investment to be sustainable. Studies should have a strong translational emphasis and should attempt to bring a product (with benefit) to the patient. Targeting cancer with increasing precision (controlled delivery) through intelligent drug and dosage form design is required to minimize the risk of late stage drug attrition (Figure 9.1.) NDDS development could support the safety and efficacy of practically all new drugs and should therefore be investigated and their assembly optimised. Collaboration between polymer, pharmaceutical and medical science is key to develop and move innovative products along the development path, from the laboratory to the bedside.

Studies in early phases (pre-clinical) should naturally be designed to collect as much relevant scientific information as is possible at the lowest cost, so that decisions pertaining to drug development progression (down the critical path) can be informed. Pre-clinical studies provide more of an opportunity to experiment than do clinical trials in humans. The limitations of pre-clinical (*in vitro* and *in vivo*) models should always be kept in mind. Pertinent and specific questions as to the safety, efficacy and proper functioning of the TPP, considering the shortcomings of the model used, should be asked and answered to reduce failures in later, more expensive development phases.

With respect to the highly morbid and heterogeneous nature (multiple mutations) of cancer, oncological drugs are going to continue to be used in poly-chemotherapeutic regimens, so as to target several action sites (receptors) simultaneously, increasing response and avoiding the development of acquired resistance (extraneous pro cell-survival mechanisms - a hallmark of cancer cells). New chemical entities with novel, potent mechanisms of action and intelligent formulations comprising functional excipients that are affordable to all patients are required.

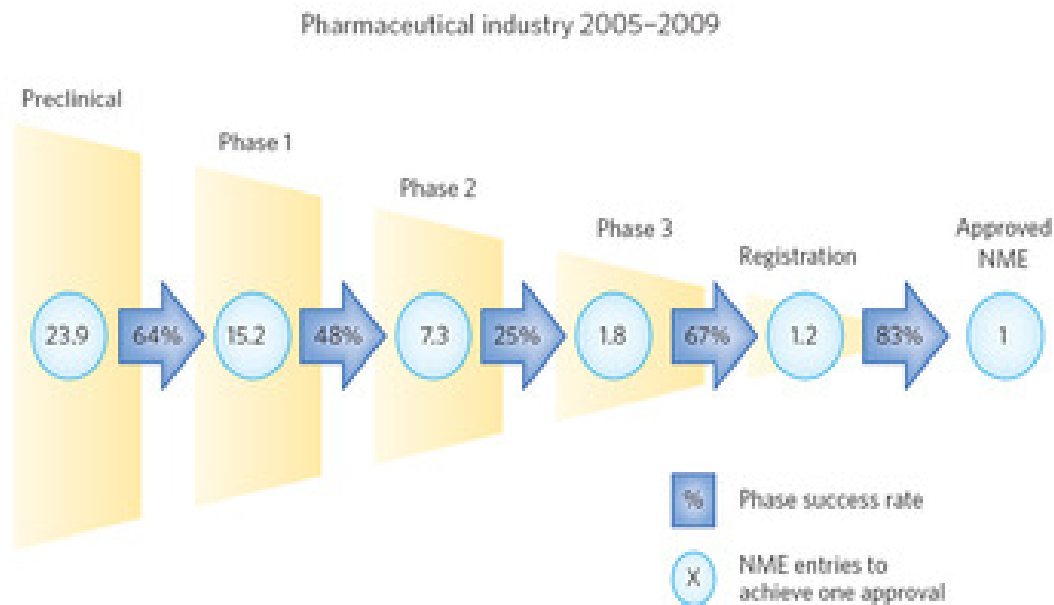


**Figure 9.1. Success rate of Pharmaceutical R&D [156]**  
(Used with permission)

Potent pharmacodynamics does not necessarily imply efficient pharmacokinetics nor make formulation any easier for a particular drug. The key to achieving better therapeutic responses may lie in utilizing already available (off patent) drugs more effectively (in combination) rather than in developing new drugs. [45] Many innovative approaches have been used towards more selectively delivering cytotoxic drugs to tumorous tissue, thus increasing the drug dose (at tumour site) and reducing systemic exposure.

As has been investigated in this study, a pragmatic approach to improve therapeutic responses without the discovery or design of novel drugs is to rationally combine registered drugs with complimentary action in fixed-ratios to obtain maximal synergy. As numerous drug combinations are possible, *in vitro* studies are the only ethical means of optimizing synergistic effects, prior to *in vivo* studies where the enhanced efficacy effects and safety profile can be confirmed.



To fully realize the potential of synergistic FRDC, the specified drug ratio must be maintained *in vivo* and delivered (targeted) to the tumour tissue. NDDS represent an effective way to selectively deliver multiple drugs to the tumour site in specified synergistic combination ratios. The integrity of the delivery system *in vivo* as reflected by maintenance of the loaded drug-drug ratio as well as by prolonged systemic circulation is pre-requisite in order to attain effective passive tumour targeting.

It was hypothesized that through using synergistic drug combinations selectively delivered through targeting NDDS, specificity for cancer can be improved both pharmacodynamically and pharmacokinetically over currently used chemotherapeutics.

To restate (*Pre-clinical development plan, page 27*), the long term aims of this study were to:

Phase 1. Identify the lead synergistic FRDC *in vitro*

Phase 2. Assemble and characterize a novel NDDS that (co)-encapsulates the optimised FRDC

Phase 3. Evaluate the *in vivo* safety, efficacy and pharmacokinetic functionality of the FRDC-NDDS

In this study, the *in vitro* combination potential of three commonly used SC in combination with Rimiophenazines was assessed. Rimiophenazines were shown *in vitro* to act in quantifiable synergy with ETOP, PTX and VIN. Any of these three Pgp substrates that are now off patent can stand to benefit greatly from re-formulation in combination with either B663 or its more hydrophilic TMP derivative B4125. In addition, B663 at non-toxic concentrations was shown to improve the activity of DOX using a MRP expressing neoplastic cell culture, thus validating the label of – broad-spectrum resistance circumventor.

In terms of re-positioning Rimiophenazines as anticancer drugs: after *in vitro* studies the already registered Rimiophenazine, clofazimine (B663) was combined

with the widely used SC, PTX for further pre-clinical development (formulation and *in vivo* experiments).

Using the thin film hydration method, PTX and B663 were successfully and stably encapsulated at a synergistic molar ratio of 1:4.5 (PTX:B663) within a mixed lipopolymeric micellular system called Riminocelles™. As Riminocelles was shown to be of a good particle size for passive tumour accumulation (~ 200 nm) and possessed adequate electrostatic stability, the formulation was evaluated using *in vivo* models of experimental toxicity and oncology.

An acute toxicokinetic study (14 day observation period) and a 21 day GLP repeat dose toxicity study in mice has shown PTX-Riminocelles to be well tolerated and non-toxic at clinically used PTX dosages in contrast to the current formulation Taxol, that incurred statistically significant ( $P < 0.5$ ) weight loss after 14 days.

HCT-15 cells are particularly drug resistant human colorectal adenocarcinoma, for which surgery is the primary modality with curative intent and PTX (a substrate of Pgp) would not be a front line drug. This intrinsic Pgp expression model was used first for *in vitro* confirmatory studies before conducting GLP repeat dose toxicity and efficacy studies in nude mice implanted subcutaneously as a proof of concept of improved efficacy.

The FRDC (1:5, PTX:B663) of Riminocelles showed a 72% improvement *in vitro* ( $IC_{50}$  value) and clearly a superior benefit using *in vivo* models of experimental oncology with 12.5% of the QDx7 Riminocelles treatment group surviving 31.3% longer than both the untreated control group and the Q7Dx2 Taxol treatment group. The most outstanding result of this study was that at an equivalent PTX dose, Riminocelles was statistically ( $P < 0.05$ ) more efficacious and less toxic than Taxol in a relevant Pgp drug resistant model. This illustrates the benefit of the drug combination and serves to suggest that PTX-Riminocelles could be used with benefit in patients with refractory ovarian, breast or lung cancers who may traditionally be treated with Taxol.

Although *in vitro* drug retention studies under simulated sink conditions demonstrated adequate drug retention within the delivery system over time, the pharmacokinetic study conducted in healthy mice served to unveil the shortcomings of the delivery system *in vivo*. The results attained (particularly the initial lack of control over the drug ratio between PTX and B663 in plasma within the first 30 min) and supported by recent thermodynamic revelations in literature, [155] indicate that although Riminocelles (simple DSPE PEG 2000 micelles) can endure huge dilution, their integrity is not maintained long in plasma due to rapid adsorption onto the highly abundant albumin which possess strong affinity for the hydrophobic acyl chains of phospholipids. [155]

*In vivo*, the amphiphiles (DSPE-PEG and PC) making up Riminocelles would exist in a dynamic equilibrium in either micellar, monomeric or albumin bound states (Figure 9.2). Due to the prevalence of albumin in plasma and insufficient forces maintaining aggregation, equilibrium strongly favours the albumin bound state and micelle break up would therefore occur rapidly, in contrast to what has been previously thought and reported [101, 102, 103, 108, 109]. This discrepancy and erroneous consensus about DSPE-PEG based micelle stability (lasting for more than a decade) has been explained by targeting that occurs quickly prior to micelle disassemble [155].

Taking all the collected data together, the efficacy and the pharmacokinetic study results indicate that passive tumour accumulation was not satisfactorily achieved and that the greater anticancer effect (relative to Taxol) observed is due to the drug combination rather than due to enhanced tumour delivery. For this reason (*Stage III. Checkpoint, page. 28*), further repeat dose toxicity studies in a second (non-rodent) animal species in preparation for clinical trials is not warranted without first making improvements to the Riminocelles formulation with special attention to the *in vivo* stability and establishing efficacy in additional experimental (PTX relevant) models of drug resistant cancer. Future micelle development using lipopolymers should therefore include an *in vitro* assessment of stability in plasma or albumin rich solutions.

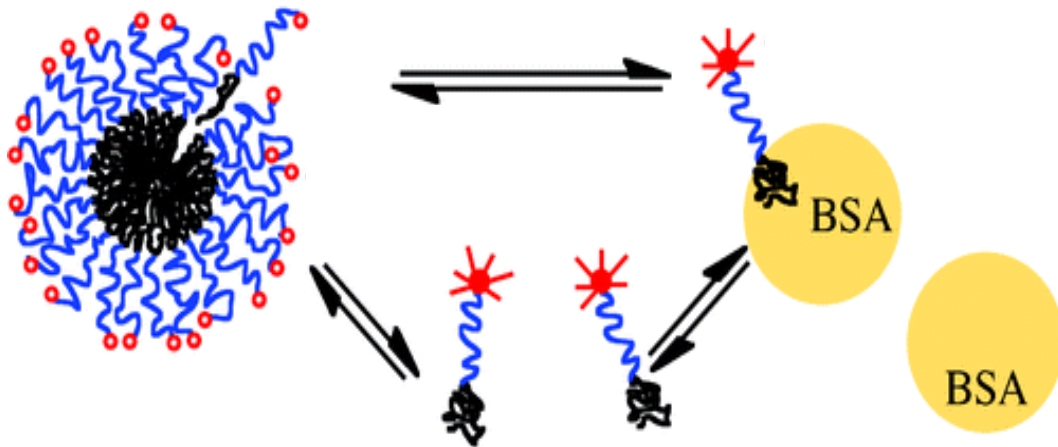


**Figure 9.2. Thermodynamic instability of DSPE PEG micelles in the presence of bovine serum albumin (BSA). [155]  
(Used with permission)**

Although the developed Riminocelle formulation did not function as desired *in vivo* (i.e. passively target cancer); it must be stressed at this stage that all the components, including the two drugs and the mixture of surfactants used to assemble Riminocelles are already approved and registered individually for medicinal use and therefore, in principal accelerated development and clinical usage is feasible particularly considering that Riminocelles has been shown to outperform Taxol in terms of both efficacy and safety in a mouse study.

A second NDDS, a nanoemulsion formulation called RiminoPLUS™ imaging was successfully developed that entraps Lipiodol contrast agent at its core and is thus thought to enable CT imaging capabilities after passive tumour accumulation following either loco-regional (intra-arterial) or IV administration. The aqueous titration method, aided by ternary phase diagrams (made simple through the application of an Excel spreadsheet) was used in conjunction with the input of ultrasonic energy at predetermined points to assemble monodisperse

nanoemulsions of ~100 nm in diameter. Although not taken further into *in vivo* studies due to poor zeta potential and stability of only a week (therefore not a finished product), further studies are warranted to evaluate the *in vivo* imaging ability of this system. The simplified protocol using automated titration calculations following the respective tie lines of a ternary phase diagram will be useful for the design of future such systems.

Prior to additional *in vivo* investigations, the activation barrier for desorption (disassembly of NDDS) needs to be increased to provide the required stability for prolonged systemic circulation thus fulfilling the passive targeting prerequisite. [155] Future possible improvements to the formulations may include: the use of exogenous polymeric amphiphiles for which albumin has no affinity [161]; covalent cross-linking of the outer corona with PEG [67, 68] although this may impede release at the target site; strengthening the hydrophobic forces holding the micelles together by the addition of cholesterol whose structuring effect has been shown to reduce albumin induced disassembly [128]; inclusion of a interwoven polymeric/protein scaffold to provide increased hydrophobic, electrostatic and steric stability as well as target recognition as in the case of lipoproteins, that have evolved over millennia as an effective way to transport and selectively distribute lipid substances and hydrophobic compounds throughout the body. It is therefore not surprising that lipoproteins have been reconstituted to deliver drugs. [162] Future NDDS will greatly benefit from adding targeting ligands (selective for cancer specific receptors).

To date, only a few nanoparticulate formulations, e.g. Doxil (Liposomal DOX) and Abraxane (Albumin bound PTX) have successfully entered the market as nanoparticulate re-formulations of standard chemotherapeutics. The pharmaceutical development of many novel PTX nanoparticulate re-formulations with improved *in vivo* safety and efficacy performance have stalled after the initial pre-clinical studies or in early clinical trial phases (e.g. LEP-ETU, Genexol-PM, PGG-PTX, Nanotax and NK105). These novel investigational products, that like Riminocelles, provide verifiable benefit over Taxol are confronted with a translational challenge and the question – why is Taxol still used clinically to treat

patients when new and improved, cremophor-free formulations exist? The challenge is therefore to develop a significantly better drug that is more affordable so as to compete in the market. The development of FRDC formulations (in particular combinations of already approved drugs with synergistic interactions and broad action against diverse resistance mechanisms) represents substantial improvement justifying further development and its use over that of Taxol.

To proceed to clinical trials, a competitive advantage would need to be offered to the extent that the product will not be eclipsed by another new product entering the market. The need to avoid an expensive exercise in redundancy must be considered. It would therefore be prudent to provide evidence of the proper functioning (selective delivery) of the delivery system and superior efficacy in diverse models of experimental oncology. Only then can the expense of a second species repeat dose toxicity test and clinical trials in humans be scientifically justified

The results of this study serve to highlight the great potential of *in vitro* optimized synergistic FRDC against MDR cancer. Lipopolymeric micelles are an effective way to formulate multiple hydrophobic drugs for intravenous administration and present a means by which disseminated cancer could be targeted; provided that the delivery system possess the prerequisite *in vivo* stability and surface attributes.

Therefore, future recommendations are that improved NDDS with greater *in vivo* stability and functionality should be developed using advanced bio-polymeric materials and that the synergistic FRDC concept should be expanded upon to include several different drugs and combinations thereof that possess proprietary value. Novel binary (micelles) and ternary (nanoemulsions) NDDS could be developed using the methods outlined in this study. The emphasis of future projects should be further stressed on translating the research into clinical applications. Through applying the FRDC-NDDS concept with more refinement, improved drug products comprising synergistic combinations of pre-registered drugs could be developed quickly to the benefit of patients.



## References

- [1] World Health Organization (WHO). [cited 2007/3/27]. Available from: [www.who.int/cancer](http://www.who.int/cancer).
- [2] Stevens A, Lowe J. Pathology. 2<sup>nd</sup> edition. St. Louis: Mosby; 2000. p. 79-104.
- [3] Bosch F. The contributions of Paul Ehrlich to pharmacology: a tribute on the occasion of the centenary of his Nobel Prize. *Pharmacology*. 2008; 82(3):171-9.
- [4] Chiu GN, Wong MY, Ling LU, Shaikh IM, Tan KB, Chaudhury A, Tan BJ. Lipid-based nanoparticulate systems for the delivery of anti-cancer drug cocktails: Implications on pharmacokinetics and drug toxicities. *Curr Drug Metab*. 2009;10(8):861-74.
- [5] Verheul HMW, Pinedo HM. Clinical implications of drug resistance. In: Pinedo HM, Giaccone G. (Eds.). *Drug resistance in the treatment of cancer*. Cambridge University press; 1998.
- [6] Goldie JH. Drug resistance in cancer: A perspective. *Cancer Metastasis Rev*. 2001; 20: 63-8.
- [7] Szakacs G, Paterson JK, Ludwig JA, Booth-Genthe C, Gottesman MM. Targeting multidrug resistance in cancer. *Nat Rev*. 2006; 5: 219- 234.
- [8] van de Vrie W, Marquet RL, Stoter G, De Bruijn EA, Eggermont MM. *In vivo* model systems in P-glycoprotein-mediated multidrug resistance. *Crit Rev Clin Lab Sci*. 1998; 35(1): 1-57.
- [9] Ford JM. Experimental reversal of P-glycoprotein-mediated multidrug resistance by pharmacological chemosensitizers. *Eur J Cancer*. 1996; 32A(6): 991-1001.
- [10] Avendano C, Menendez JC. Inhibitors of multidrug resistance to antitumour agents (MDR). *Curr Med Chem*. 2002; 9: 159-193.
- [11] Robert J, Jarry C. Multidrug resistance reversal agents. *J Med Chem*. 2003; 46(23): 4805-4817.
- [12] Gitler MS, Monks A, Sausville EA. Preclinical models for determining efficacy of drug combinations: mapping the road to the clinic. *Mol Cancer Ther*. 2003; 2: 929-932.
- [13] Ramsay EC, Dos Santos N, Dragowska WH, Laskin JJ, Bally MB. The formulation of lipid-based nanotechnologies for the delivery of fixed dose anticancer drug combinations. *Curr Drug Deliv*. 2005; 2: 341-351.

- [14] Decker S, Sausville EA. Preclinical modelling of combination treatments: fantasy or requirement? *Ann NY Acad Sci.* 2005; 1059: 61-9.
- [15] Frei E, Elias A, Wheeler C, Richardson P, Hryniuk W. The relationship between high-dose treatment and combination chemotherapy: the concept of summation dose intensity. *Clin Cancer Res.* 1998; 4: 2027-2037.
- [16] Zoli W, Ricotti L, Tesei A, Barzanti F, Amadori D. In vitro models for a rational design of chemotherapy combinations in human tumours. *Crit Rev Oncol Hematol.* 2001; 37: 69-82.
- [17] Mayer LD, Harasym TO, Tardi PG, Harasym NL, Shew CR, Johnstone SA. Ratiometric dosing of anticancer drug combinations: Controlling drug ratios after systemic administration regulates therapeutic activity in tumour-bearing mice. *Mol Cancer Ther.* 2006; 5(7): 1854-1863.
- [18] Mayer LD, Janoff AS. Optimizing combination chemotherapy by controlling drug ratios. *Mol Interv.* 2007; 7(4): 216-223.
- [19] Reddy VM, O'Sullivan JF, Gangadharam RJ. Antimycobacterial activities of riminophenazines. *J Antimicrob Chemother.* 1999; 43: 615-623.
- [20] O'Connor R, O'Sullivan JF, O'Kennedy R. The pharmacology, metabolism and chemistry of clofazimine. *Drug Metab Rev.* 1995; 27 (4): 591-614.
- [21] Morrison NE, Marley GM. Clofazimine binding studies with Deoxyribonucleic acid. *Int J Lepr.* 1975; 44(4): 475- 481.
- [22] Barry VC, Belton JG, Conalty ML, Denneny JM, Edward DW, *et al.* A new series of phenazines (rimino-compounds) with high antituberculosis activity. *Nat.* 1957; 4568: 1013-5.
- [23] Arbiser JL, Moschella SL. Clofazimine: A review of its medicinal uses and mechanisms of action. *J Am Acad Dermatol.* 1995; 32: 241-7.
- [24] Holdiness MR. Clinical pharmacokinetics of Clofazimine. *Clin Pharmacokinet.* 1989; 16: 74-85.
- [25] Van Rensburg CEJ, Anderson R, O'Sullivan JF. Riminophenazine compounds: pharmacology and antineoplastic. *Crit Rev Oncol Hematol.* 1997; 25: 55-67.
- [26] Van Rensburg CEJ, Van Staden AM, Anderson R. The Riminophenazine agents Clofazimine and B669 inhibit the proliferation of cancer cell lines in vitro by phospholipase A2-mediated oxidative and nonoxidative mechanism. *Cancer Res.* 1993; 53: 318-323.



- [27] Van Rensburg CEJ, Theron AJ, Chasen M. The riminophenazine agents clofazimine and B669 inhibit the proliferation of intrinsically multidrug resistant carcinoma cell lines. *Oncol Rep.* 1996; 3: 103-6.
- [28] Van Rensburg CEJ, Anderson R, Myer MS, Joone GK, O'Sullivan JF. The riminopheanzine agents clofazimine agents clofazimine and B669 reverse acquired multidrug resistance in a human lung cancer cell line. *Cancer Lett.* 2004; 85: 59-63.
- [29] Myer MS, Van Rensburg CEJ. Chemosensitizing interactions of clofazimine and B669 with human K562 erythroleukaemia cells with varying levels of expression of P-glycoprotein. *Cancer Lett.* 1996; 99: 73-8.
- [30] Van Rensburg C, Durandt C, Garlinski P, O'Sullivan J. Evaluation of the antineoplastic activities of the riminopheanzine agents clofazimine and B669 in tumour bearing rats and mice. *Int J Oncol.* 1993; 3: 1011-3.
- [31] Sri-Pathmanathan R, Plumb J, Fearon K. Clofazimine alters the energy metabolism and inhibits the growth rate of a human lung-cancer cell line *in vitro* and *in vivo*. *Int J Cancer.* 1994; 56: 900-5.
- [32] Pourgholami M, Lu Y, Wang L, Stephens R, Morris D. Regression of Novikoff rat hepatocellular carcinoma following loco-regional administration of a novel formulation of clofazimine in lipiodol. *Cancer Lett.* 2004; 207: 37-47.
- [33] Ruff P, Chasen M, Long J, Van Rensburg C. A phase II study of clofazimine in unresectable and metastatic hepatocellular carcinoma. *Ann Oncol.* 1998. 9:217-9.
- [34] Falkson C, Falkson G. A phase II evaluation of clofazimine plus doxorubicin in advanced, unresectable primary hepatocellular carcinoma. *Oncology.* 1999; 57: 232-5.
- [35] Forner A, Hessheimer AJ, Real MI, Bruix J. Treatment of hepatocellular carcinoma. *Crit Rev Oncol Hematol.* 2006; 60 (2): 89-98.
- [36] Van Niekerk E, Sullivan JF, Joone GK, van Rensburg CEJ. Tetramethylpiperidine-substituted phenazines inhibit the proliferation of intrinsically resistant carcinoma cell lines. *Invest New Drugs.* 2001; 199: 211-7.
- [37] Van Rensburg CEJ, Joone GK, O'Sullivan JF. Clofazimine and B4121 sensitize an intrinsically resistant human colon cancer cell line to P-glycoprotein substrates. *Oncol Rep.* 2000; 7: 193-5.
- [38] Van Rensburg CEJ, Joone GK, O'Sullivan JF. Tetramethylpiperidine-substitution increases the antitumour activity of the riminophenazines for an acquired multidrug-resistant cell line. *Anticancer Drug Des.* 2000; 15(4): 303-6.

- [39] Rhodes PM, Wilkie D. Antimitochondrial activity of Lamprene in *Saccharomyce cerevisiae*. *Biochem Pharmacol.* 1973; 22: 1047-1056.
- [40] Klopp CT, Alford TC, Bateman J. Fractional intraarterial cancer chemotherapy with methyl-bis-amine hydrochloride. *Ann Surg.* 1950; 132: 811-832.
- [41] Collins JM. Pharmacologic rationale for regional drug delivery. *J Clinical Oncol.* 1984; 2(5): 498-504.
- [42] Davidson T, Wallace J, Carnochan P. The rabbit as an experimental model for regional chemotherapy 1. Intra-arterial hindlimb infusion. *Lab Anim.* 1986; 20: 343-6.
- [43] Ensminger WD, Gyves JW. Regional chemotherapy of neoplastic disease. *Pharmac Ther.* 1983; 21: 277-293.
- [44] Eckman WW, Patlak CS, Fenstermacher JD. A critical evaluation of principles governing the advantages of intraarterial infusions. *J Pharmacokinet Biopharm.* 1974; 2: 257-285.
- [45] Aigner KR. Intra-arterial infusion: Overview and novel approaches. *Sem Surg Oncol.* 1998; 14: 248-253.
- [46] Muller H, Hilger R. Curative and palliative aspects of regional chemotherapy in combination with surgery. *Support Care Cancer.* 2003; 11: 1-10.
- [47] Brigger I, Duberner C, Couvreur P. Nanoparticles in cancer therapy and diagnosis. *Adv Drug Deliv Rev.* 2002; 5: 631-651.
- [48] Maeda H, Fang J, Inutsuka T, Kitamoto Y. Vascular permeability enhancement in solid tumour: various factors, mechanisms involved and its implications. *Int Immunopharmacol.* 2003; 3: 319-328.
- [49] Khaled G. Enhanced permeability and retention of macromolecular drugs in solid tumours: A royal gate for targeted anticancer nanomedicines. *J Drug Target.* 2007; 15(7-8): 457-464.
- [50] Torchilin VP. Drug targeting. *Eur J Pharma Sci.* 2000; 11 (Suppl. 2): S81-S91.
- [51] Iyer AK, Khaled G, Fang J, Maeda H. Exploiting the enhanced permeability and retention effect for tumour targeting. *Drug Discov Today.* 2006; 11 (17/18): 812-8.
- [52] Hoarau D, Delmas P, David S, Roux E, Leroux J. Novel long-circulating lipid nanocapsules. *Pharm Res.* 2004; 21(10): 1783-9.

- [53] Kommareddy S, Shenoy DB, Amiji MM. Long circulating polymeric nanoparticles for drug and gene delivery to tumours. In: Amiji MM (Eds.) Nanotechnology for cancer therapy. New York: CRC press; 2007. p 231-242
- [54] Durand-Fontanier S, Simon A, Luc Duroux J, Descottes B, Delage C. Lipiodol Ultra-Fluid: An antitumour agent-in vitro study. *Anticancer Res.* 1999; 19: 4357-4361.
- [55] Hind RE, Loizidou M, Fleming J, Batty V, Birch S, Taylor I. Biodistribution of lipiodol following hepatic arterial injection. *Eur J Sur Oncol.* 1992; 18: 162-167.
- [56] Konno T, Maeda H, Iwai K, Maki S, Tashiro S, Uchida M, *et al.* Selective targeting of Anti-cancer Drug and simultaneous image enhancement in solid tumours by arterially administered lipid contrast medium. *Cancer.* 1984; 54: 2367-2374.
- [57] Konno T. Targeting cancer chemotherapeutics agents by use of Lipiodol contrast medium. *Cancer.* 1990; 66: 1897-1903
- [58] Novell JR, Parnhoo SP, Dawson K, Dick R, Kelleher SM. Targeted therapy for recurrent breast carcinoma with regional 'Lipiodol'/epirubicin infusion. *Lancet.* 1990; 336: 1383.
- [59] Ozono S, Okajima E, Hirao Y, Babaya K, Komada S, Matsuki H, *et al.* Transcatheter arterial embolization of vesical artery in the treatment of invasive bladder cancer. *Eur Urol.* 1988; 15(3-4): .176-9.
- [60] Konno T. Targeting chemotherapy for hepatoma: arterial administration of anticancer drugs dissolved in lipiodol. *Eur J Cancer.* 1992; 28 (2/3): 403-9.
- [61] Taniguchi H, Takahashi T, Yamaguchi T, Sawai K. Intraarterial infusion chemotherapy for metastatic liver tumours using multiple anticancer agents suspended in a lipid contrast medium. *Cancer.* 1989; 64(10): 2001-6.
- [62] Lee I, Park YT, Roh K, Chung H, Ick CK, Seo YJ. Stable paclitaxel formulations in oily contrast medium. *J Control Release.* 2005; 102: 415-425.
- [63] Seto H, Tsuji S, Watanabe N, Futatsuya R, Nomura K, Maeda M. Biodistribution of intravenously injected [<sup>131</sup>I] Lipiodol in rats. *Radiot Med.* 1992; 10(5): 196-8.
- [64] Boucher E, Garin E, Guylligomarch A, Boudjema K, Raoul JL. Intra-arterial injection of iodine -131- labelled Lipiodol for treatment of Hepatocellular carcinoma. *Radiother Oncol.* 2007; 82(1): 76-82.

- [65] Chou FI, Fang KC, Chung C, Lui WY, Chi CW, Liu RS, *et al.* Lipiodol uptake and retention by human hepatoma cells. *Nucl. Med. Biol.* 1995; 22(3): 379-386.
- [66] de Baere T, Denys A, Briquet R, Chevallier P, Dufaux J, Roche A. Modification of arterial and portal hemodynamics after injection of iodized oils and different emulsions of iodized oils in the hepatic artery. An experimental study. *J Vasc Inter Radiol.* 1998; 9(2): 305-310.
- [67] Bae KH, Lee Y, Park TG. Oil-encapsulating PEO-PPO-PEO/PEG shell cross-linked nanocapsules for target-specific delivery of paclitaxel. *Biomacromolecules.* 2007; 8(2): 650-6.
- [68] Ho Kong W, Lee WJ, Cui ZY, Bae KH, Park TG, *et al.* Nanoparticulate carrier containing water-insoluble iodinated oil as a multifunctional contrast agent for computer tomography imaging. *Biomaterials.* 2007; 28: 5555-5561.
- [69] Jang SH, Wientjes MG, Lu D, Au J. Drug delivery and transport to solid tumours. *Pharm Research.* 2003; 20(9): 1337-1350.
- [70] Davignon JP, Slack JA, Beijnen J, Vezin R, Schoemaker TJ. EORTC/CRC/NCI Guidelines for the formulation of investigational cytotoxic drugs. *Eur J Cancer Clin Oncol.* 1988; 24(9): 1535-8.
- [71] Beijnen JH, Flora KP, Halbery GW, Henrar REC, Slack JA. CRC/EORTC/NCI Joint formulation working party: experiences in the formulation of investigational drugs. *Br J Cancer.* 1995; 72: 210-8.
- [72] Neervannan S. Preclinical formulations for discovery and toxicology: physicochemical challenges. *Expert Opin Drug Metab Toxicol.* 2006; 2(5): 715-731.
- [73] Langer R. Drug delivery and targeting. *Nature.* 1998; 392 (6679 Suppl): 5-10.
- [74] Lee Y, Zocharski PD, Samas B. An intravenous formulation decision tree for discovery compound formulation development. *Int J Pharm.* 2003; 253: 111-9.
- [75] Crowley PJ, Martini LG. Formulation design: new drugs from old. *Drug Discov Today: Ther Strateg.* 2004; 1(4): 537-542
- [76] Sutton D, Nasongkla N, Blanco E, Gao J. Functionalized micellar systems for cancer targeted drug delivery. *Pharm Res.* 2007; 24(6): 1029-1046.
- [77] Gao Z, Lukyanov AN, Chakilam AR, Torchilin VP. PEG-PE/Phosphatidylcholine mixed immunomicelles specifically deliver encapsulated Taxol to tumour cells of different origin and promote their efficient killing. *J Drug target.* 2003; 11(2): 87-92.

- [78] Letchford K, Burt H. A review of the formation and classification of amphiphilic block copolymer nanoparticulate structures: micelles, nanospheres, nanocapsules and polymersomes. *Eur J Pharm Biopharm.* 2007; 65: 259-269.
- [79] Le Garrec D, Ranger M, Leroux JC. Micelles in anticancer drug delivery. *Am J Drug Deliv.* 2004; 2(1): 15-42.
- [80] Sezgin Z, Yuksel N, Baykara T. Preparation and characterization of polymeric micelles for solubilization of poorly soluble anticancer drugs. *Eur J Pharm Biopharm.* 2006; 64: 261-8.
- [81] Tomaszewski JE. Preclinical pharmacology and toxicology of antineoplastic drugs. The NCI perspective [presentation on the internet]. c2010 [cited 2010/6/1]. Available from: [www.venkatrao.net/files/2491458.ppt](http://www.venkatrao.net/files/2491458.ppt).
- [82] ICH S9. ICH harmonised tripartite guideline. Nonclinical evaluation for anticancer pharmaceuticals. 2009. Available from: <http://www.ich.org/cache/compo/502-272-1.html#S9>
- [83] ICH Final Business Plan, S9: Pre-clinical guideline on oncology therapeutic development. 2007. Available from: <http://www.ich.org/cache/compo/502-272-1.html#S9>
- [84] DeGeorge JJ, Ahn C, Andrews P, Brower M, Giorgio D, Goheer MA, *et al.* Regulatory considerations for preclinical development of anticancer drugs. *Cancer Chemother Pharmacol.* 1998; 41: 173-185.
- [85] EMEA, CPMP/SWP/997/96. Note for guidance on the pre-clinical evaluation of anticancer medicinal products. July 1998.
- [86] Nakae D, Onodera H, Fueki O, Urano T, Komiyama N, Sagami F, *et al.* Points to consider on the non-clinical safety evaluation of anticancer drugs. *J Toxicol Sci.* 2008; 33(2), 123-126.
- [87] ICH Final Concept Paper, S9: Pre-clinical guideline on oncology therapeutic development. 2007. Available from: <http://www.ich.org/cache/compo/502-272-1.html#S9>
- [88] ICH M3 (R2). ICH harmonised tripartite guideline. Guidance on nonclinical safety studies for the conduct of human clinical trials and marketing authorization for pharmaceuticals. 2008. Available from: <http://www.ich.org/cache/compo/502-272-1.html#M3>

[89] CDER, Guidance for industry: Target product profile - A strategic development and process tool, 2007. Available from: <http://www.fda.gov/downloads/Drugs/GuidanceComplianceRegulatoryInformation/Guidances/ucm080593.pdf>

[90] Competitive drug development. Drug development strategy [homepage on the internet]. c2009 [cited 2007/27/8]. Available from: [http://www.cddconsulting.com/services\\_01.htm](http://www.cddconsulting.com/services_01.htm)

[91] Sadrieh N, Miller TJ. Nanotechnology: Regulatory perspective for drug development in cancer therapeutics. Amiji M.M. (Eds.). In: Nanotechnology for cancer therapy. New York: CRC press; 2007

[92] Ramsay EC, Dos Santos N, Dragowska WH, Laskin JJ, Bally MB. The formulation of lipid-based nanotechnologies for the delivery of fixed dose anticancer drug combinations. *Curr Drug Deliv*. 2005; 2: 341-351.

[93] Tallarida RJ, Stone DJ, Raffa RB. Efficient designs for studying synergistic drug combinations. *Life Sci*. 1997; 61(26): 417-425.

[94] Chou TC. Theoretical basis, experimental design and computerised simulation of synergism and antagonism in drug combination studies. *Pharmacol Rev*. 2006; 58: 621-681.

[95] Decker S, Sausville EA. Preclinical modelling of combination treatments: fantasy or requirement? *Ann NY Acad Sci*. 2005; 1059: 61-9.

[96] Mossmann T. Rapid colorimetric assay for cellular growth and survival: application to proliferation and cytotoxicity assays. *J Immunol Methods*. 1983; 65, 55-63.

[97] Macpherson I, Cassidy J. Challenges in combinatorial oncology studies. *Pharm Med*. 2008; 22(2): 85-97.

[98] Ali MJ, Navalitloha Y, Vavra MW, Kang E, Itskovich AC, *et al*. Isolation of drug delivery from drug effect: problems of optimizing drug delivery parameters. *Neuro-Oncol*. 2006; 8: 109-118.

[99] Lee RJ. Liposomal delivery as a mechanism to enhance synergism between anticancer drugs. *Mol Cancer Ther*. 2006; 5(7): 1639-40.

[100] Gao Z, Lukyanov AN, Singhal A, Torchilin VP. Diacyllipid-polymer micelles as nanocarriers for poorly soluble anticancer drugs. *Nano Lett*. 2002; 2(9): 979-982.



[101] Trubetskoy VS, Torchilin VP. Use of polyethylene-lipid conjugates as long circulating carriers for delivery of therapeutic and diagnostic agents. *Adv Drug Deliv Rev.* 1995; 16: 311-320.

[102] Lukynov AN, Torchilin VP. Micelles from lipid derivatives of water-soluble systems for poorly soluble drugs. *Adv Drug Deliv Rev.* 2004; 56: 1273-1289.

[103] Torchilin VP. Lipid-core micelles for targeted drug delivery. *Curr Drug Delivery.* 2005; 2: 319-327.

[104] Krishnadas A, Rubenstein I, Onyukel H. Sterically stabilized phospholipid mixed micelles: in vitro evaluation as a novel carrier for water-insoluble drugs. *Pharm Research.* 2003; 20(2): 297-302.

[105] Wang J, Mongayt D, Torchilin VP. Polymeric micelles for delivery of poorly soluble drugs: Preparation and anticancer activity in vitro of paclitaxel incorporated into mixed micelles based on poly(ethylene glycol)-lipid conjugate and positively charged lipids. *J DrugTarget.* 2005; 13(1), 73-80.

[106] Dabholkar RD, Sawant RM, Mongayt DA, Devarajan PV, Torchilin VP. Polyethylene glycol-phosphatidylethanolamine conjugate (PEG-PE)-based mixed micelles: Some properties, loading with paclitaxel, and modulation of P-glycoprotein-mediated efflux. *Int J Pharm.* 2006; 315: 148-157.

[107] Tang N, Du G, Wang N, Liu C, Hang H, Liang W. Improving penetration in tumours with nanoassemblies of phospholipids and doxorubicin. *J Natl Cancer Inst.* 2007; 99(13): 1004-15

[108] Lukyanov AN, Gao Z, Mazzola L, Torchilin V. Polyethylene glycol-diacyl lipid micelles demonstrate increased accumulation in subcutaneous tumours in mice. *Pharm Res.* 2002; 19(10): 1424-9.

[109] Lukyanov AN, Gao Z, Torchilin VP. Micelles from polyethylene glycol / phosphatidylethanolamine conjugates for tumour drug delivery. *J Control Release.* 2003; 91: 99-102.

[110] Alkan-Onyukel H, Ramakrishnan S, Chai H, Pezzuto JM. A mixed micellar formulation suitable for the parenteral administration of Taxol. *Pharm Res.* 1994; 11(2): 206-212.

[111] Hickey S, Lawrence MJ, Hagan SA, Buckin V. Analysis of the phase diagram and microstructural transitions in phospholipid microemulsion systems using high-resolution ultrasonic spectroscopy. *Langmuir.* 2006; 22: 5575- 5583.

[112] Chen M. Lipid excipients and delivery systems for pharmaceutical development: A regulatory perspective. *Adv Drug Deliv Rev.* 2008; 60: 768-777.

- [113] Pey CM, Maestro A, Sole I, Gonzalez C, Solans C, Gutierrez JM. Optimization of nano-emulsions prepared by low energy emulsification methods at constant temperature using a factorial design study. *Colloids Surf A: Physicochem Eng Aspects*. 2006; 288: 144-150.
- [114] Fernandez P, Andre V, Rieger J, Kuhnle A. Nano-emulsion formation by emulsion phase inversion. *Colloids Surf A: Physicochem Eng Aspects*. 2004; 251: 53-8.
- [115] Sadurni N, Solans C, Azemar N, Carcia-Celma MJ. Studies on the formation of O/W nano-emulsions, by low-energy emulsification methods, suitable for pharmaceutical applications. *Eur J Pharm Sci*. 2005; 26: 438-445.
- [116] Bouchemal K, Briancon S, Perrier E, Fessi H. Nano-emulsion formulation using spontaneous emulsification: solvent, oil and surfactant optimisation. *Int J Pharm*. 2004; 280: 241-251.
- [117] Lawrence MJ, Warisnoicharoen W. Recent advances in microemulsions as drug delivery vehicles. In: Torchilin V.P. (Eds.). *Nanoparticulates as drug carriers*. London: Imperial College Press; 2006. p 125- 172
- [118] Capek I. Degradation of kinetically-stable o/w emulsions. *Adv Colloid Interface Sci*. 2004; 107: 125-155.
- [119] Izquierdo P, Feng J, Esquena J, Tadros TF, Dederen JC, Garcia MJ. The influence of surfactant mixing ratio on nano-emulsion formation by the pit method. *J Colloid Interface Sci*. 2005; 285: 388-394.
- [120] Tiwari SB, Amiji MM. Nanoemulsion formulations for tumour-targeted delivery. In: Amiji M.M (Eds.). *Nanotechnology for cancer therapy*. New York: CRC press; 2007. p 723-740.
- [121] Torchilin VP. PEG-based micelles as carriers of contrast agents for different imaging modalities. *Adv Drug Deliv Rev*. 2002; 54: 235-252.
- [122] Dominguez A, Fernandez A, Gonzalez N, Iglesias E, Montenegro L. Determination of critical micelle concentration of some surfactants by three techniques. *J Chem Educ*. 1997; 74(10): 1227-1231.
- [123] Cho YC, Lee J, Lee SC, Huh KM, Park K. Hydrotropic agents for the study of in vitro paclitaxel release from polymeric micelles. *J Control Release*. 2004; 97: 249-257.
- [124] Zetasizer nano series manual. Records and reports – viewing the results [cited 2010/6/3]. Available from: [www.biophysics.bioc.cam.ac.uk/files/zetasizer\\_nano\\_user\\_man0317-1.1.pdf](http://www.biophysics.bioc.cam.ac.uk/files/zetasizer_nano_user_man0317-1.1.pdf)



- [125] Ashok B, Arleth L, Hjelm RP, Rubenstein I, Onyukel H. In vitro characterization of PEGylated phospholipid micelles for improved drug solubilisation: Effects of PEG chain length and PC incorporation. *J Pharma Sci.* 2004; 93(10), 2476-2487.
- [126] Mu L, Chrastina A, Levchenko T, Torchillin VP. Micelles from poly(ethylene glycol)-phosphatidylethanolamine conjugates (Peg-Pe) as pharmaceutical nanocarriers for poorly soluble camptothecin. *J Biomed Nanotech.* 2005; 1(2): 190-195.
- [127] Sezgin Z, Yuksel N, Baykara T. Preparation and characterization of polymeric micelles for solubilization of poorly soluble anticancer drugs. *Eur J Pharm Biopharm.* 2006; 64: 261-8.
- [128] Vakil R, Kwon GS. Effect of cholesterol on the release of amphotericin B from PEG-Phospholipid micelles. *Mol Pharm.* 2007; 5(1), 98-104.
- [129] Sandsröm MC, Johansson E, Edwards K. Influence of preparation path on the formation of discs and threadlike micelles in DSPE-PEG2000/lipid systems. *Biophys Chem.* 2008; 132: 97-103.
- [130] Montes-Burgos I, Walczyk D, Hole P, Smith J, Lynch I, Dawson K. Characterisation of nanoparticle size and state prior to nanotoxicological studies. *J Nanopart Res.* 2010; 12: 47-53.
- [131] Wang J, Mongayt DA, Lukyanov AN, Levchenko TS, Torchilin VP. Preparation and in vitro synergistic anticancer effect of vitamin K3 and 1,8-diazabicyclo[5,4,0]undec-7-ene in poly(ethylene glycol)-diacyllipid micelles. *Int J Pharma.* 2004; 272: 129-135.
- [132] Malvern instruments, Technical note. Dynamic light scattering: An introduction in 30minutes. [cited 2010/4/13]. Available from: [http://www.malvern.com/malvern/kbase.nsf/allbyno/KB000792/\\$file/MRK656-01\\_An\\_Introduction\\_to\\_DLS.pdf](http://www.malvern.com/malvern/kbase.nsf/allbyno/KB000792/$file/MRK656-01_An_Introduction_to_DLS.pdf).
- [133] Sear BD. Synthetic phospholipid compounds. US patent 4,426,330. 1984.
- [134] Lacko AG, Nair M, Mcconathy WJ. Lipoprotein nanoparticles as delivery vehicles for anti-cancer agents. In: Amiji M.M. (EDS). *Nanotechnology for cancer therapy.* New York: CRC Press; 2007. p 777-786.
- [135] Luzzati V, Husson F. The structure of the liquid -crystalline phases of lipid-water systems. *J Cell Biol.* 1962; 12: 207-219.

- [136] Bedu-Addo FK, Huang L. Interaction of PEG-phospholipid conjugates with phospholipid: implications in liposomal delivery. *Adv Drug Deliv Rev.* 1995; 16: 235-247.
- [137] Lundberg BB, Mortimer BC, Redgrave TG. Submicron lipid emulsions containing amphiphatic polyethylene glycol for use as drug carriers with prolonged circulation time. *Int J Pharma.* 1996; 134: 119-127.
- [138] Rowinsky EK, Tolcher AW. Microtubule-targeting drugs. In: Perry M.C.(Eds). *Chemotherapy source book.* 3<sup>rd</sup> edition. Lippincott Williams and Wilkins; 2001.
- [139] Weiss RB, Donehower RC, Wiernik PH, Ohnuma T, Gralla RJ, Trump DL, *et al.* Hypersensitivity reactions from Taxol, *J Clin Oncol.* 1990; 8: 1263-1268.
- [140] Newell DR, Silvester J, McDowell C, Burtles S. The cancer research UK experience of pre-clinical toxicology studies required to support early clinical trials with novel cancer therapies. *Eur J Cancer.* 2004; 40: 899-906.
- [141] Double J. Toxicity testing in the development of anticancer drugs. *The Lancet Oncol.* 2002; 3: 438-9.
- [142] Gustafson DL, Merz AL, Long ME. Pharmacokinetics of combined doxorubicin and Paclitaxel in mice. *Cancer lett.* 2005; 220: 161-9.
- [143] Jacob D, Davis J, Fand. Xenografted tumour models in mice for cancer research, a technical review. *Gene Ther Mol Biol.* 2004; 8: 213-219.
- [144] Fieberg H, Burger AM. Human tumour xenografts and explants. In: Teicher BA (Eds.) *Tumour models in cancer research.* New Jersey: Humana Press; 2002. p 113-140.
- [145] Osieka R, Thomas CB. Human colon cancer xenografts in nude mice models from experimental chemotherapy. In: Houchens D, Ovejera A. (Eds.). *Proceedings of the symposium on the use of athymic (nude) mice in cancer research.* New York: Gustav Fischer; 1977.
- [146] Plowman J, Dykes D, Hollingshead M, Simpson-Herren L, Alley M. Human tumour xenograft models in NCI drug development. In: Teicher BA (Eds). *Anticancer drug development guide.* New Jersey: Humana Press; 1997. p 101-126.
- [147] Corbett T, Valeriote F, LoRusso P, Polin L, Panchapor C, Pugh S, *et al.* *In vivo* methods for screening and preclinical testing. In: Teicher BA (Eds). *Anticancer drug development guide.* New Jersey: Humana Press; 1997. p .75-100.

- [148] Teicher BA. *In vivo* tumour response endpoints. In: Teicher BA (Eds.). Tumour models in cancer research. New Jersey: Humana Press; 2002. p 593-616.
- [149] Corbett T, Polin L, Roberts BJ, Lawson AJ, Leopold III WR, White K, *et al.* Transplantable syngeneic rodent tumours. In: Teicher BA (Eds.). Tumour models in cancer research. New Jersey: Humana Press; 2002. p 41-72.
- [150] Matuszewski BK, Constanzer ML, Chavez-Eng CM. Strategies for the assessment of matrix effect in quantitative bioanalytical methods based on HPLC-MS/MS. *Anal Chem.* 2003; 75: 3019-3030.
- [151] Van Eechhaut A, Lanckmans K, Sarre S, Smolders I, Michotte Y. Validation of bioanalytical LC-MS/MS assays: Evaluation of matrix effects. *J Chromatogr B.* 2009; 877: 2198-2207.
- [152] Food and Drug Administration, Guidelines for industry on Bioanalytical Method Validation, Federal Register. 2001: 66 (100): 28526.
- [153] Yeh TK, Lu Z, Weintjes MG, Au JL. Formulating paclitaxel in nanoparticles changes its disposition. *Pharma Res.* 2005; 22: 867-874.
- [154] Holdiness MR. Clinical pharmacokinetics of Clofazimine: A review. *Clin Pharmacokinet.* 1989; 16: 74-85.
- [155] Kastantin M, Missirlis D, Black M, Ananthanarayanan B, Peters D, Tirrell M. Thermodynamic and kinetic stability of DSPE-PEG(2000) micelles in the presence of bovine serum albumin. *J Phys Chem B.* 2010; 114: 12632-12640.
- [156] Menon K, Teicher BA. Metastasis models. In: Teicher B.A. (Eds.). Tumour models in cancer research. New Jersey: Humana Press; 2002.
- [157] Leading anticancer drugs: world market prospects 2011-2021. c2011 [cited 2011/5/4]. Available from: <http://www.visiongain.com/Report/578/Leading-Anti-Cancer-Drugs-World-Market-Prospects-2011-2021>.
- [158] Pharma projects. Pharma R&D annual review 2010. c2010 [cited 2011/5/4]. Available from: [http://www.pharmaprojects.com/therapy\\_analysis/annual-review-2010-therapies.htm](http://www.pharmaprojects.com/therapy_analysis/annual-review-2010-therapies.htm).
- [159] Bunnage MR. Getting pharmaceutical R&D back on target. *Nat Chem Biol.* 2011; 7(6): 335-9.
- [160] Targeted cancer therapeutics - National cancer institute. [cited 2011/9/19]. Available from: <http://www.cancer.gov/cancertopics/factsheet/therapy/targeted>.

[161] Li J, Owen SC, Shoichet MS. Stability of self-assembled polymeric micelles in serum. *Macromolecules*. 2011; 44: 6002-8.

[162] Ng KK, Lovell JF, Zheng G. Lipoprotein-inspired nanoparticles for cancer thermostics. *Acc Chem Res*. 2011; 44(10): 1105-1113.

[163] Van Rensburg CEJ, Joone G, Van Niekerk E, Anderson R. B4112, a novel tetramethylpiperidine-substituted phenazine that inhibits the proliferation of multidrug-resistant cancer cell lines. *Ann NY Acad Sci*. 1999; 886(1): 280-2.

[164] Van Rensburg CEJ, Anderson R, Joone G, Myer MS, O'Sullivan JF. Novel tetramethylpiperidine-substituted phenazine are potent inhibitors of P-glycoprotein activity in a multidrug resistant cancer cell line. *Anticancer Drugs*. 1997; 8: 708-715.

[165] Mulder A. [Unpublished, Honours project]. Department of Pharmacology, University of Pretoria; 2006.

[166] Medlen C, Anderson R, O'Sullivan JF. MDR resistance treatment and novel pharmaceutically active Riminophenazines. US Patent 5763443. June 9 1998.

## Appendix A. AUCC approval letters



UNIVERSITEIT VAN PRETORIA  
UNIVERSITY OF PRETORIA  
YUNIBESITHI YA PRETORIA

Ref: H010-09

31 March 2009

**ANIMAL USE AND CARE COMMITTEE**

Private Bag X04  
Onderstepoort  
0110

Tel: 012-529 8434  
Fax: 012-529 8300

Prof CE Medlen  
Department of Pharmacology  
Faculty of Health Sciences  
([ce@medlen@up.ac.za](mailto:ce@medlen@up.ac.za))

Dear Prof Medlen

**H010-09: The toxicity and anti-cancer activity of novel drugs developed by CANSA and BioPAD sponsored "Anti cancer drug development consortium"**

The application for ethical approval, dated 13 March 2009 was approved by the Animal Use and Care Committee at its meeting held on 30 March 2009.

Best regards

  
**Elmarie Mostert**  
**AUCC Coordinator**

Copy Dr E Avsar



UNIVERSITEIT VAN PRETORIA  
UNIVERSITY OF PRETORIA  
YUNIBESITHI YA PRETORIA

**ANIMAL USE AND CARE COMMITTEE**  
Private Bag X04  
0110 Onderstepoort

Tel +27 12 529 8434 / Fax +27 12 529 8300  
e-mail: [aucc@up.ac.za](mailto:aucc@up.ac.za)

Ref: H010-09 (Amendment 1)

03 June 2010

Prof CE Medlen / Dr D Cromarty  
Department of Pharmacology  
Faculty of Health Sciences  
( [connie.medlen@up.ac.za](mailto:connie.medlen@up.ac.za) / [duncan.cromarty@up.ac.za](mailto:duncan.cromarty@up.ac.za) )

Dear Prof Medlen

The title addition, "Efficacy evaluation of Riminocelles™ against MDR, HCT-15 colon adenocarcinoma xenografts in Balb/C nude mice use" to the original application **H010-09** "The toxicity and anticancer activity of novel drugs developed by the CANSA and BioPAD sponsored "Anti cancer drug development consortium" was approved by the AUCC

Best regards

**Elmarie Mostert**

**AUCC Coordinator**

Copy: D Koot

## Appendix B. Review of Riminophenazine QSAR

**Table 1. Increased sensitivity of various Riminophenazine derivatives using non-toxic doses of Vinblastine and Doxorubicin against two Pgp expressing cell lines. Adapted from: Medlen *et al.* (US Patent). [166]**

At non-toxic [ ]	Increased sensitivity (fold reduction in IC <sub>50</sub> value of Riminophenazine)			
	Vinblastine		Doxorubicin	
	Compound	K562/MMB	H69/LX4	K562/MMB
B4100	3.53	6.38	1.2	1.37
B4119	1.46	5.69	1.88	1.03
B4121	97.83	7.57	3.12	2.34
B4128	6.49	2.82	1.78	1.57
B4163	10.63	3.46	1.5	1.15
B4169	24.66	7.36	2.95	1.45
B4103	0.69	5.21	1.3	1.37
B4126	4.45	2.69	1.28	1.54
B4127	6.07	2.91	2.53	1.01
B4178	6.03	1.97	1.1	1.5
B3786	not tested	3.6	not tested	1.02
B3962	4.07	2.15	1.79	1.32
B4019	not tested	2.11	not tested	1.34
B4070	2.94	2.63	0.82	1.68
B4090	7.3	5.64	1.42	1.49
B4112	19.5	21.38	2.36	3.54
B4123	6.8	4.69	1.84	1.15
B4125	11.96	1.97	1.65	1.5
B4158	4.69	3.29	1.75	1.19
B4159	7.02	5.79	1.77	1.42
B4174	1.78	0.86	1.5	0.79
B4177	not tested	10.71	not tested	0.7
B663	5.92	6.72	1.67	1.9

**Table 2. Mean IC<sub>50</sub> value (µg/ml) for various Riminophenazines against various neoplastic and normal cell cultures**

Cell culture	B663	B4112	B4121	B4125	B3962	B4090	B4100	B4123	B4128	B4169	B3786	B4331	B4103	B4119	B4126	Reference
<i>Neoplastic</i>																
FaDu (human pharynx squamous carcinoma)	2															26
T24(human bladder carcinoma)	1															26
PLL/PRF/5 (PLC), (human Hepatocellular carcinoma)**	1.65	0.705	0.81	0.77	0.49		0.72		1.25				0.63	0.97	0.55	26, 27, 36, 163
WIL (human non-small cell lung cancer)**	4.8															31
HepG2 (human Hepatocellular carcinoma)**	1.3	0.5	0.8	0.6	0.3		0.6		0.8				0.4	0.4	0.5	27, 36, 163
HeLa (human cervical)	0.8	0.4	0.8	0.7	0.5		0.4		0.8				0.7	0.6	0.4	26, 27, 36
Mahlavu (human Hepatocellular carcinoma)**	1.5															27
CaCO2 (human colorectal)**	1.9	1.0	0.7	0.2	0.3		0.3		0.8				1.3	0.3	0.4	27, 36, 163
K562/MMB (human erythroleukaemia)*	0.23	0.18	2.25		0.29	0.20	0.34	0.33	0.38	2.86						163, 164
COLO320DM (human colorectal carcinoma)*	2.1	0.7	0.9	0.4	0.4		0.5		1.0				0.5	0.7	0.6	36, 163
HT-29 (human colorectal carcinoma)*	1.4	0.4	0.7	0.1	0.3		0.5		0.9				0.4	0.4	0.4	36, 163
WHO 3 (human oesophageal)	1.1	0.3	0.6	0.3	0.3		0.5		0.7				0.3	0.6	0.4	36, 163
Du145 (human prostate)		0.7														163
H69/LX4 (human small cell lung cancer)*	2.9	0.4	0.8		0.6		0.8				0.6	0.7				38
H69/P (human small cell lung cancer)	1.6	0.8	0.5	0.8	0.4		0.7		1.2				0.9	1.2	0.6	38
Novikoff (rat hepatocellular)**	2.3	0.8	0.9	0.8										0.8		165
Jurkat (human acute T cell leukaemia)	1.2	0.3	0.4	0.3										0.2		165
MCF7(human breast)	1.6	0.3	0.4	0.6										0.3		165
<b>Mean</b>	1.7	0.5	0.8	0.5	0.4	0.2	0.5	0.3	0.9	2.9	0.6	0.7	0.6	0.6	0.5	
<i>Normal</i>																
Vervet kidney cells	>4															26
Human Fibroblasts	5.0	1.1	1.0	1.7										0.6		26, 165
Fibro (MRC5)	>2.5	0.8	0.8	1.0	0.6		0.8		0.9				1.0	0.8	0.4	36
Resting human lymphocytes	1.8	0.7	0.9	0.8										0.5		165
Stimulated (PHA) lymphocytes	0.62	0.49	0.88	0.69										0.33		165
<b>Mean</b>	2.5	0.8	0.9	1.1	0.6		0.8		0.9				1.0	0.5	0.4	

\* Pgp expressing (classical resistance)

\*\* Intrinsic non-classical resistance



## Appendix C. Pharmacokinetic and tissue distribution study schedule

### Day 8 (Pharmacokinetic and tissue distribution study)

55 female mice are required for this experiment.

#### Groups and caging

1. PTX [10 mg/kg] Riminocelles™ to 25 mice (5 cages of 5), i.e. cage A1-A5.
2. PTX [10 mg/kg] Taxol® to 25 mice (5 cages of 5), i.e. cage B1-B5.
3. Administer saline (negative control) to 5 mice (1 cage of 5), i.e. cage C1.

#### Experiment schedule

Before IV dosing through the tail vein, each animal was weighed and an appropriate dose calculated. Precise timing of when the dose was given and when the animal was euthanised was documented in study monitoring sheets.

07h00	Administer [10 mg/kg] PTX-Riminocelles to A1 (6 hr group).
07h25	Administer [10 mg/kg] PTX-Taxol to B1 (6 hr group).
07h50	Administer [10 mg/kg] PTX-Riminocelles to A2 (3 hr group).
08h15	Administer [10 mg/kg] PTX-Taxol to B2 (3 hr group).
08h40	Administer [10 mg/kg] PTX-Riminocelles to A3 (30 min group).
09h10	Euthanise, collect terminal blood <sup>a</sup> and organ <sup>b</sup> samples from A3.
09h35	Administer [10 mg/kg] PTX-Taxol to B3 (30 min group).
10h05	Euthanise Sacrifice, collect terminal blood and organ samples from B3.
10h50	Euthanise, collect terminal blood and organ samples from A2.
11h15	Euthanise, collect terminal blood and organ samples from B2.
11h40	Administer [10 mg/kg] PTX-Riminocelles to A4 (24 hr group).
12h05	Administer [10 mg/kg] PTX-Taxol to B4 (24 hr group).
12h30	Administer negative control (saline) to C1 (24 hr group).
13h00	Euthanise, collect terminal blood and organ samples from A1.
13h25	Euthanise, collect terminal blood and organ samples from B1.
14h00	Administer [10 mg/kg] PTX-Riminocelles to A5 (1 hr group).
14h25	Administer [10 mg/kg] PTX-Taxol to B5 (1 hr group).
15h00	Euthanise, collect terminal blood and organ samples from A5.
15h25	Euthanise, collect terminal blood and organ samples from B5.

Next day

11h40 Euthanise, collect terminal blood and organ samples from A4.  
12h05 Euthanise, collect terminal blood and organ samples from B4.  
12h30 Euthanise, collect terminal blood and organ samples from C1

**<sup>a</sup>Heparinised blood samples are to be drawn via cardiac puncture from 5 (isoflurane anaesthetized) mice at 30 min, 1 hr, 3, 6 for drug level quantitation. At 24 h two blood samples are to be drawn for both toxicity marker profiling and drug quantitation.**

**<sup>b</sup>Organs (Liver, spleen, kidney, lungs and adipose tissue) are to be collected and weighed before being analysed for drug content via LC-MS/MS.**